AD-A187 235 DREDGING OPERATIONS TECHNICAL SUPPORT PROGRAM DESIGN AND MANAGEMENT OF DR..(U) ARMY ENGINEER WATERWAYS EXPERIMENT STATION VICKSBURG MS ENVIR.. 1/2

UNCLASSIFIED F D SHIELDS ET AL. JUN 87 WES/TR/D-87-2 F/G 13/2 NL

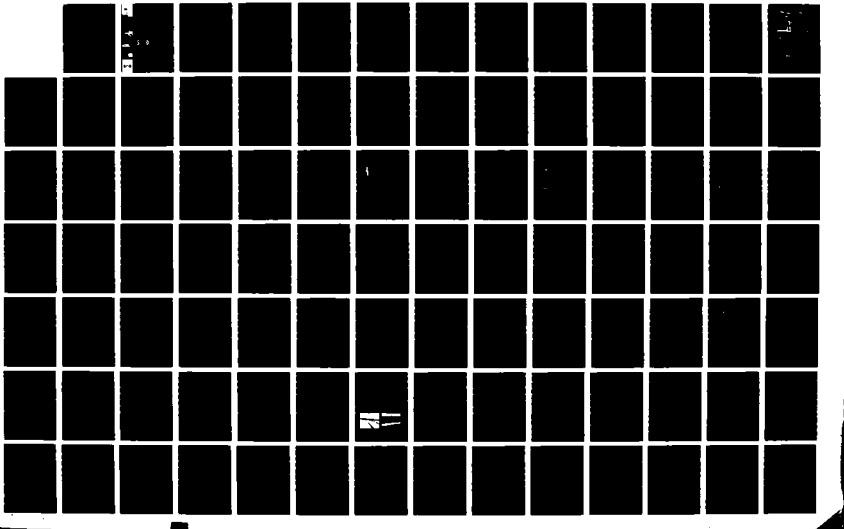

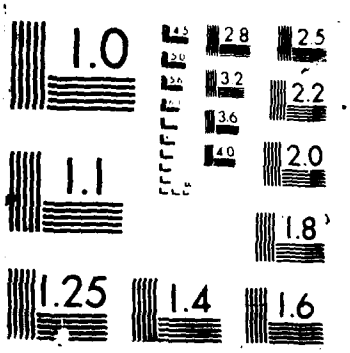
1.0
1.1
1.25
1.4
1.6
1.8
2.0
2.2
2.5
2.8
3.2
3.6
4.0

US Army Corps of Engineers

AD-A187 235

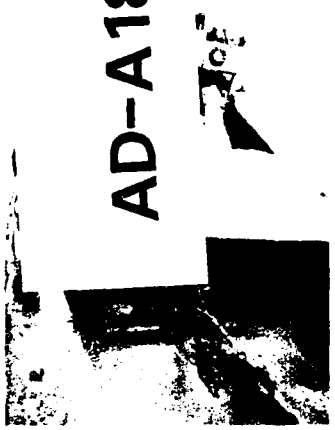

DREDGING OPERATIONS TECHNICAL SUPPORT PROGRAM

8

FILE COPY

TECHNICAL REPORT D-87-2

DESIGN AND MANAGEMENT OF DREDGED MATERIAL CONTAINMENT AREAS TO IMPROVE HYDRAULIC PERFORMANCE

by

F. Douglas Shields, Jr., Edward L. Thackston, Paul R. Schroeder

Environmental Laboratory

Donald P. Bach

Hydraulics Laboratory

DEPARTMENT OF THE ARMY
Waterways Experiment Station, Corps of Engineers
PO Box 631, Vicksburg, Mississippi 39180-0631

DTIC
ELECTE
OCT 2 1 1987
S D
or D

June 1987
Final Report

Approved For Public Release; Distribution Unlimited

Prepared for DEPARTMENT OF THE ARMY
US Army Corps of Engineers
Washington, DC 20314-1000

87 10 8 004

Destroy this report when no longer needed. Do not return it to the originator.

The findings in this report are not to be construed as an official Department of the Army position unless so designated by other authorized documents.

The contents of this report are not to be used for advertising, publication, or promotional purposes. Citation of trade names does not constitute an official endorsement or approval of the use of such commercial products.

The D-series of reports includes publications of the Environmental Effects of Dredging Programs:

Dredging Operations Technical Support

Long-Term Effects of Dredging Operations

Interagency Field Verification of Methodologies for Evaluating Dredged Material Disposal Alternatives (Field Verification Program)

Unclassified
SECURITY CLASSIFICATION OF THIS PAGE

REPORT DOCUMENTATION PAGE

Form Approved
OMB No 0704 0188
Exp Date Jun 30 1986

1a REPORT SECURITY CLASSIFICATION Unclassified	1b RESTRICTIVE MARKINGS
2a SECURITY CLASSIFICATION AUTHORITY	3 DISTRIBUTION / AVAILABILITY OF REPORT Approved for public release; distribution unlimited
2b DECLASSIFICATION / DOWNGRADING SCHEDULE	
4 PERFORMING ORGANIZATION REPORT NUMBER(S) Technical Report D-87-2	5 MONITORING ORGANIZATION REPORT NUMBER(S)
6a NAME OF PERFORMING ORGANIZATION USAEWES Environmental Laboratory 6b OFFICE SYMBOL (If applicable)	7a NAME OF MONITORING ORGANIZATION
6c ADDRESS (City, State, and ZIP Code) PO Box 631 Vicksburg, MS 39180-0631	7b ADDRESS (City, State, and ZIP Code)
8a NAME OF FUNDING / SPONSORING ORGANIZATION US Army Corps of Engineers 8b OFFICE SYMBOL (If applicable)	9 PROCUREMENT INSTRUMENT IDENTIFICATION NUMBER
8c ADDRESS (City, State, and ZIP Code) Washington, DC 20314-1000	10 SOURCE OF FUNDING NUMBERS PROGRAM ELEMENT NO / PROJECT NO / TASK NO / WORK UNIT ACCESSION NO

11 TITLE (Include Security Classification)
Design and Management of Dredged Material Containment Areas to Improve Hydraulic Performance

12 PERSONAL AUTHOR(S)
Shields, F. Douglas, Thackston, Edward L., Schroeder, Paul R., Bach, Donald P.

13a TYPE OF REPORT	13b TIME COVERED	14 DATE OF REPORT (Year, Month, Day)	15 PAGE COUNT
Final report	FROM ____ TO ____	June 1987	141

16 SUPPLEMENTARY NOTATION
Available from National Technical Information Service, 5235 Port Royal Road, Springfield, VA 22161.

17 COSATI CODES		
FIELD	GROUP	SUB GROUP

18 SUBJECT TERMS (Continue on reverse if necessary and identify by block number)
Confined disposal facility design
Dredged material
Dredged material disposal
Dredging
Hydraulic efficiency
(Continued)

19 ABSTRACT (Continue on reverse if necessary and identify by block number)

Dredged material is often disposed into diked containment areas (DMCAs). Typically, the dredged material is pumped into a containment area as a slurry that is 10- to 20-percent solids by weight. Water and solids separate in the containment area because of gravity sedimentation, and the clarified water is discharged over a weir and through a culvert to a receiving water body. The suspended solids concentration of DMCA effluent is inversely related to the residence time of water in the DMCA. The longer the water stays in the DMCA before it is discharged, the lower the effluent turbidity and suspended solids concentration will be. Residence time is therefore an important consideration in design of DMCAs.

Designers attempt to size DMCAs to provide adequate sediment storage and effluent quality at least cost. The currently recommended procedure for sizing DMCAs uses the

(Continued)

20 DISTRIBUTION / AVAILABILITY OF ABSTRACT	21 ABSTRACT SECURITY CLASSIFICATION
☒ UNCLASSIFIED/UNLIMITED ☐ SAME AS RPT ☐ DTIC USERS	Unclassified
22a NAME OF RESPONSIBLE INDIVIDUAL	22b TELEPHONE (Include Area Code) / 22c OFFICE SYMBOL

DD FORM 1473, 84 MAR

Unclassified

18. SUBJECT TERMS (Continued).

Modeling dredged material containment area	Settling
Residence time distribution	Tracer
Retention time	Upland containment
Sedimentation basin	

19. ABSTRACT (Continued).

estimated average residence time. Prior to this study, estimates of mean residence time were based on only a few observations of operating DMCAs. The mean residence time was simply estimated to be 0.44 times the ponded volume divided by the inflow rate.

This study presents observed residence time distribution data from some 12 DMCAs. These data were collected by injecting Rhodamine WT dye at the inflow point and monitoring dye concentration in the outflow. The resultant time-concentration curve is identical to the residence time distribution during the dye test. In addition, similar data for chlorine contact chambers, physical models, and waste stabilization ponds found in the literature are also examined.

A composite data set from all different sources showed a strong relationship between the ratio of mean residence time to theoretical residence time (theoretical residence time is equal to the pond volume divided by the average flow rate) and the pond length-width ratio. Baffles or spur dikes can be used to increase the effective length-to-width ratio of a given DMCA, thereby increasing the mean residence time without increasing the overall size. The relationship between mean residence time and length-width ratio was incorporated into the DMCA design procedure, and a process for selecting DMCA size, shape, and spur dike layout to achieve minimum cost resulted.

The utility of state-of-the-art mathematical hydrodynamic models for simulating flow through DMCAs is examined in Appendix A. It was found that the mathematical models are capable of reproducing the observed residence time distributions fairly well if model coefficients are arbitrarily adjusted to achieve best fit. However, better field data will be required to develop reliable a priori modeling capability. Although additional research based on higher quality field data is needed to provide more definitive information on DMCA residence time distribution, at this point it is apparent that in many cases DMCA economics could be improved by the use of baffles or spur dikes.

PREFACE

This study was conducted as part of the Dredging Operations Technical Support (DOTS) Program at the US Army Engineer Waterways Experiment Station (WES), Vicksburg, Miss. The DOTS Program is sponsored by the Office, Chief of Engineers, US Army, through the Dredging Division of the Water Resources Support Center, Fort Belvoir, Va. The DOTS is managed by the WES Environmental Laboratory (EL) through the Environmental Effects of Dredging Programs (EEDP). Dr. Robert Engler was Program Manager for the EEDP, and Mr. Thomas R. Patin was the DOTS Program Coordinator. Mr. David B. Mathis was the WRSC-D Technical Monitor during preparation and publication of this report.

This report was prepared between April 1985 and April 1986. Data analysis and preparation of the main body of the report were done by Mr. F. Douglas Shields, Jr., Dr. Edward L. Thackston, and Dr. Paul R. Schroeder of the Water Resources Engineering Group (WREG), Environmental Engineering Division (EED), EL. Technical support was provided by Mses. Cindy Cox, Kathy Smart, and Anita Zitta, all of the WREG. The DYECON computer program mentioned herein was written by Mr. Steve Pranger of the WREG, and Mr. Pranger assisted with use of the program for this study. Many helpful suggestions were made by Dr. Thomas Walski, also of the WREG. Dr. Walski and Dr. Michael R. Palermo, Chief, WREG, acted as technical reviewers for the draft report. WREG personnel worked under the direct supervision of Dr. Palermo and Mr. Clifford L. Truitt, Acting Chief, WREG, and under the general supervision of Dr. Raymond L. Montgomery, Chief, EED, and Dr. John Harrison, Chief, EL.

Field data used in this study were collected by WREG personnel and Brian J. Gallagher and Company, contractor. References cited herein may be consulted for the names of those involved. Wind data were obtained from the National Weather Service of the National Oceanic and Atmospheric Administration except as otherwise noted.

The study described in Appendix A was performed by Messrs. Donald P. Bach, William D. Martin, and Samuel B. Heltzel of the Estuarine Simulation Branch, Estuaries Division of the WES Hydraulics Laboratory (HL). Mr. Robert A. Boland, Jr., was Chief of the Estuarine Simulation Branch. General supervision was provided by Mr. William H. McAnally, Jr., Chief of the Estuaries Division, and by Messrs. H. B. Simmons and Frank A. Herrmann, Jr., who were Chiefs of the HL during the study period. Appendix B was prepared by

DTIC COPY INSPECTED 7

A-1

Dr. Schroeder of the WREG. This report was edited by Ms. Lee T. Byrne of the WES Information Products Division.

COL Allen F. Grum, USA, was the previous Director of WES. COL Dwayne G. Lee, CE, is the present Commander and Director. Dr. Robert W. Whalin is Technical Director.

This report should be cited as follows:

Shields, F. D, et al. 1987. "Design and Management of Dredged Material Containment Areas to Improve Hydraulic Performance," Technical Report D-87-2, US Army Engineer Waterways Experiment Station, Vicksburg, Miss.

CONTENTS

CONVERSION FACTORS, NON-SI (METRIC) UNITS OF MEASUREMENT

Non-SI units of measurement used in this report can be converted to SI (metric) units as follows:

Multiply	By	To Obtain
acres	4,046.873	square metres
acre-feet	1,233.489	cubic metres
cubic feet	0.02831685	cubic metres
cubic yards	0.7645549	cubic metres
degrees (angle)	0.01745329	radians
feet	0.3048	metres
gallons	3.785412	cubic decimetres
inches	2.54	centimetres
miles (US statute)	1.609347	kilometres
square feet	0.09290304	square metres
square yards	0.8361274	square metres
yards	0.9144	metres

DESIGN AND MANAGEMENT OF DREDGED MATERIAL CONTAINMENT AREAS TO IMPROVE HYDRAULIC PERFORMANCE

PART I: INTRODUCTION

Background

1. The US Army Corps of Engineers (CE) annually supervises the dredging of about 480 million yd^3* of sediment from the Nation's rivers and harbors (Francingues et al. 1985). Due to environmental, economic, or institutional reasons, a large quantity (though fractionally small) of this dredged material must be placed on land in diked dredged material containment areas (DMCAs). In DMCAs, solids in the dredged material are separated from water by sedimentation, and the resulting clarified water may be discharged back to the waterway. DMCAs typically have irregular shapes, range from 10 to 100 acres in area, and have ponded depths of 2 to 10 ft. Inflows to these areas are from dredge pipes and typically range from 5 to 30 cfs. Inflows tend to be unsteady and intermittent. Outlets from DMCAs are usually weirs with stop-log crests. The hydraulic performance of a DMCA is reflected by the frequency distribution of residence time for water passing through. The estimation of residence time is an important factor in the design of DMCAs.

2. Preliminary guidance for determining residence time was developed by Montgomery (1978) during the Dredged Material Research Program (DMRP). Refinement and validation of the procedures were conducted under the Disposal Operations Technical Support (DOTS) program. These efforts included field studies of residence time in a number of DMCAs. This report describes the results of the field studies and the development of refined techniques for estimating residence time of DMCAs. The effects of various design decisions and management techniques on residence time distributions are also explored.

---

* A table of factors for converting non-SI units of measurement to SI (metric) units is presented on page 4.

Use of Residence Time in Design of Containment Areas

3. Montgomery (1978) developed a design procedure for DMCAs for fine-grained dredged material. This work showed that design must be based on two general phenomena: (a) the settling characteristics of the dredged material and (b) the hydraulic characteristics (residence time distribution) of flow through the DMCA.

4. The settling characteristics of dredged material are a function of many variables and must be experimentally determined using laboratory procedures developed by Montgomery (1978) and extended by Palermo (1984). Whether the slurry undergoes flocculent settling (the manner clays normally settle in fresh water) or zone settling with a distinct interface (the manner sediments normally settle in salt water), the clarification (removal of suspended solids by settling) is a strong function of time. A typical set of curves describing flocculent settling of a slurry at different initial suspended solids concentrations as a function of time is shown in Figure 1. Obviously, the longer the residence time, the more solids are removed by settling.

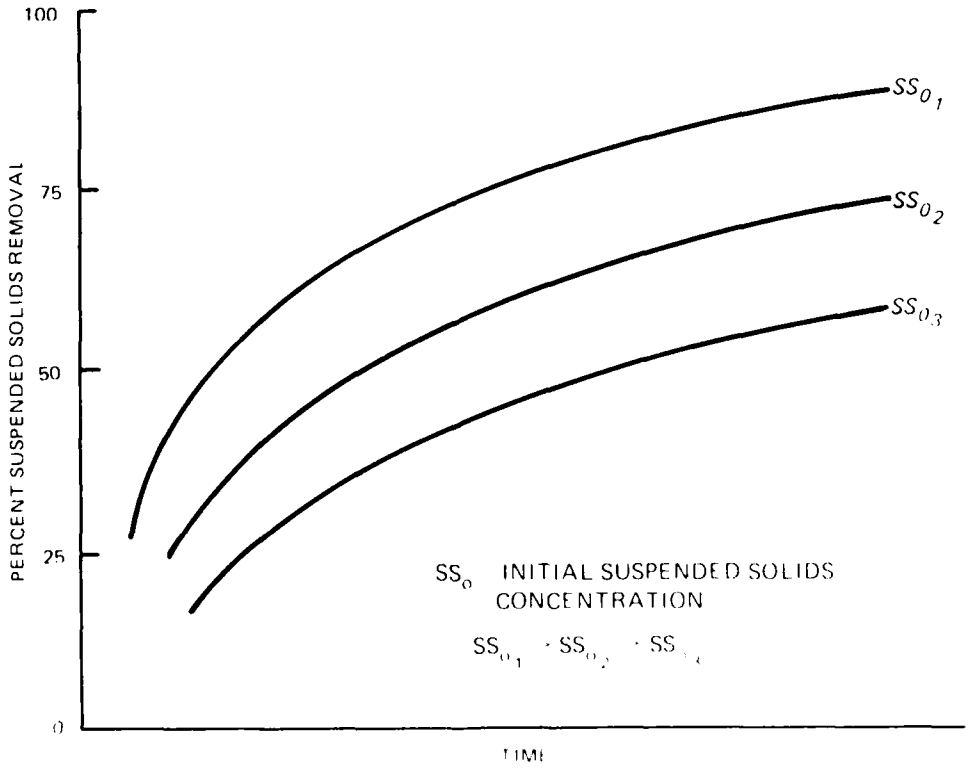

Figure 1. Removal of suspended solids with time

5. The ideal type of residence time distribution in a DMCA would be plug flow. Plug flow may be described as a situation in which each parcel of water entering the basin proceeds through the basin in exact order of entry, occupies the full cross section from top-to-bottom and side-to-side, undergoes no mixing or longitudinal dispersion, and exits the basin with a residence time equal to the theoretical residence time. The theoretical residence time is equal to the ponded volume divided by the average flow rate, $T = V/\bar{Q}$. Such an ideal regime is impossible to achieve in practice.

6. In practice, mixing and dispersion occur in the DMCA, causing some parcels of water to exit earlier than the theoretical residence time. There are also "dead zones," in which velocities toward the outlet are considerably less than average and eddy recirculation currents are set up, causing these areas not to function as fully involved flow paths (Figure 2). Thus, the effective flow volume is less than the total DMCA volume. Since the effective volume is less than the total volume, the mean residence time $\bar{t}$ is less than T.

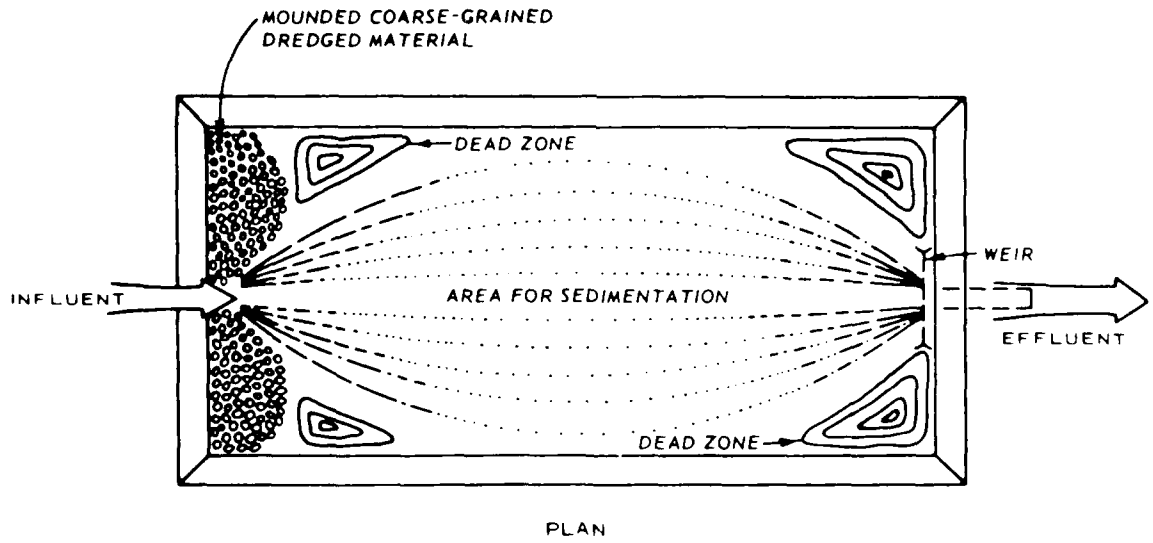

Figure 2. Typical DMCA showing dead zones and effective flow volume, from Montgomery (1978)

7. The mean residence time of a DMCA may be directly measured by instantaneously injecting a quantity of tracer dye at the inflow and monitoring dye concentration in the outflow (Figure 3). If the data are collected in discrete form, a set of time-concentration pairs results. Dye concentration data of this type were obtained in the field studies described in this report.

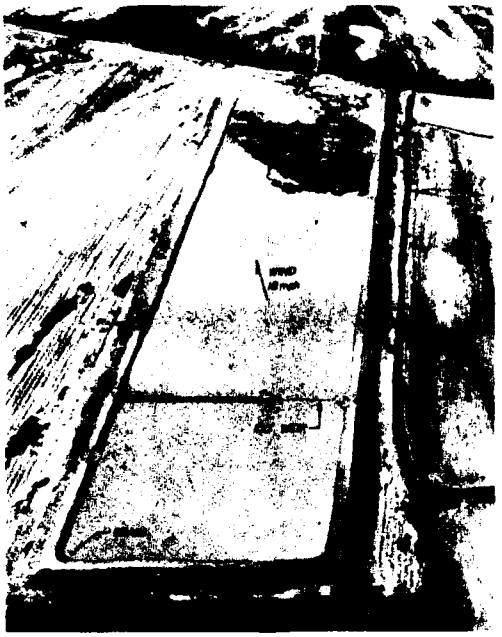

a. 30 min after start of test

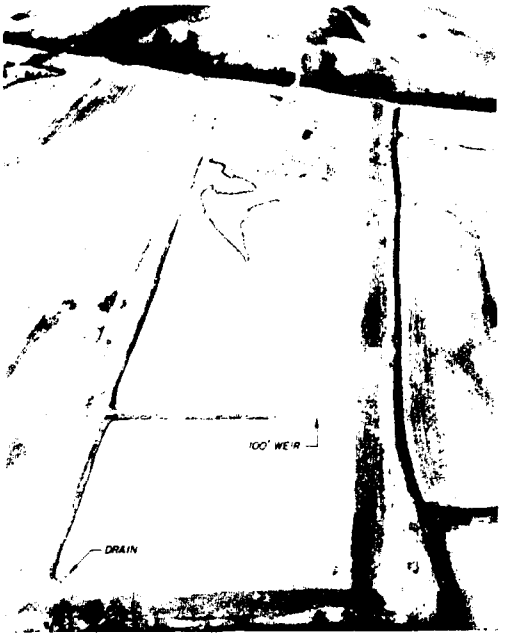

b. 1.0 hr after start of test

c. 1.5 hr after start of test

d. 2.0 hr after start of test

Figure 3. Surface plume from DMCA dye tracer test, from Montgomery (1978)

Mean residence time is determined as the centroid of the dye concentration curve (Figure 4) and can be computed by:

$$\bar{t} = \frac{\sum_{i=1}^{n-1} \bar{t}_i \, (\bar{C}_i - C_b) \, \Delta t_i q_i}{\sum_{i=1}^{n-1} (\bar{C}_i - C_b) \, \Delta t_i q_i} \qquad (1)$$

where

$\bar{t}_i = (t_{i+1} + t_i)/2$

C_i = concentration of tracer at time t_i

$\bar{C}_i = (C_{i+1} + C_i)/2$

C_b = background concentration of tracer

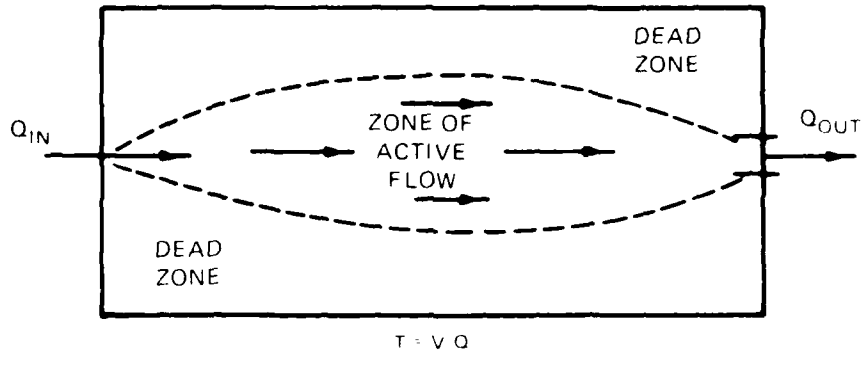

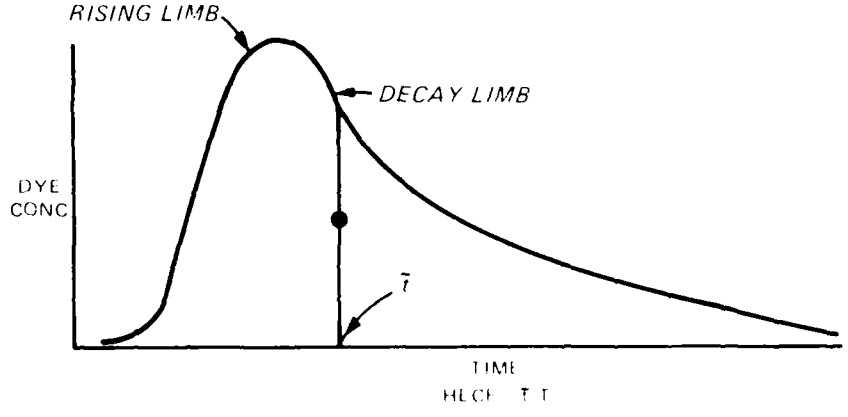

Figure 4. Conceptual illustration of theoretical and mean residence times in a dredged material containment area

$\Delta t_i = (t_{i+1} - t_i)$

q_i = effluent discharge rate during the i^{th} time interval.

The q_i factors may be omitted if flow rates are constant. Fluorescence readings may be substituted for fluorescent tracer dye concentration since fluorescence is approximately a linear function of dye concentration. The summation ideally should be continued until effluent dye concentration returns to the background level and remains there for several time increments.

8. The departure of residence time distribution from ideal is partially described by the hydraulic efficiency $\bar{t}/T$. The reciprocal of the hydraulic efficiency is called the hydraulic efficiency correction factor (HECF):

$$HECF = \frac{T}{\bar{t}} \tag{2}$$

Required DMCA size and hence cost to achieve a particular effluent quality are directly related to the HECF. The recommended DMCA design procedure requires that the theoretical residence time as determined by laboratory settling tests (or the DMCA ponded volume) necessary to achieve the desired effluent quality be multiplied by the HECF (Palermo, Montgomery, and Poindexter 1978; Palermo 1985). For sediment slurries exhibiting zone settling, the design procedure also requires that the minimum DMCA surface area needed for effective zone settling as determined by laboratory settling tests be multiplied by the HECF (Palermo, Montgomery, and Poindexter 1978). These procedures correct DMCA sizes determined from laboratory results for the nonideal settling conditions found in DMCAs.

9. Montgomery (1978) recommends assuming a hydraulic efficiency of 0.44 (and thus a HECF of 2.25) for situations in which site-specific information on the DMCA residence time distribution is unavailable. Montgomery's recommendation was the only available quantitative design guidance prior to publication of this report. The impact of using an assumed value of 0.44 for hydraulic efficiency when actual efficiencies range from 0.2 to 0.7 on DMCA sizing calculations is shown below:

Assumed $\bar{t}/T$	Assumed HECF	Actual $\bar{t}/T$	Actual HECF	Pond Volume* Required	Pond Volume* from Design
0.44	2.25	0.2	5.00	222	100
0.44	2.25	0.3	3.33	148	100
0.44	2.25	0.4	2.50	111	100
0.44	2.25	0.44	2.25	100	100
0.44	2.25	0.5	2.00	89	100
0.44	2.25	0.6	1.67	74	100
0.44	2.25	0.7	1.43	64	100

* Volumes are expressed in percentage of the volume required when the actual hydraulic efficiency is 0.44. For situations involving zone settling, identical numbers would apply to site surface area as well as ponded volume.

Using 0.44 for hydraulic efficiency can significantly increase DMCA size (and thus cost) if actual efficiency is greater than 0.44. On the other hand, using 0.44 might result in unacceptable effluent quality for situations in which efficiencies were less.

Purpose and Scope

10. The purpose of this report is to provide information to supplement the existing guidance by Montgomery (1978) for selection of HECFs for DMCA design. Part II of this report describes the relationship between DMCA flow patterns and residence time distribution. A short literature review is also included in Part II. Subsequent parts describe collection and analysis of residence time distribution (dye curve) data from several DMCAs. Results from DMCA tests are compared with lab and prototype tests of water and wastewater treatment basins and are presented in Part III. Improved DMCA design guidance based on these data is developed in Part IV, and methods for incorporating this improved guidance into design are presented in Part V.

11. Several of the DMCA tests were simulated using a two-dimensional numerical hydrodynamic model. Results of the modeling effort are presented as Appendix A. Appendix B contains guidance for collecting DMCA residence time distribution data, and Appendix C contains the DMCA test data.

PART II: RESIDENCE TIME DISTRIBUTION AND DMCA HYDRAULICS

12. The residence time distribution of a DMCA is controlled by flow patterns and velocity distributions. This part contains qualitative descriptions of the effects of hydraulic behavior on residence time distributions and the resultant effects on DMCA suspended solids removal. Relevant literature is surveyed, including studies containing measurements of residence time distributions for DMCAs and similar bodies of water. Applications of numerical models to the problem of simulating the hydraulics of DMCAs and predicting their residence time distributions are also briefly reviewed.

Departures from Ideal Behavior

13. As noted previously in Part I, "ideal" hydraulic behavior in a DMCA would be plug flow. Velocity distributions for plug flow are shown in Figure 5. Flow through real DMCAs strongly departs from this ideal because of unsteady flow rates, wind effects, inlet and outlet effects, and shear stresses at the sides and bottom of the DMCA. All of these effects tend to vary continuously in both time and space. The concentration and size gradation of suspended solids in the influent dredged material probably exert an influence on hydraulic behavior as well, but it is not known if these effects are as significant as those produced by the factors already mentioned. Actual DMCA conditions are probably more accurately represented by some mix of advective flow and completely mixed conditions, also shown in Figure 5.

Dead zones

14. Typical flow patterns for DMCAs are shown in Figure 6, which may be contrasted with the ideal shown in Figure 5. It should be noted that the boundaries between the various zones shown in Figure 6 are vague and indistinct, and considerable exchange can occur between different "zones." Dead zones have very little net forward flow, although they may be either stagnant or well-mixed internally. The difference between an internally mixed dead zone and a well-mixed zone is that the rate of exchange of water between the dead zone and the main advective flow zone is much slower.

15. Parcels of water that enter dead zones have very long residence times there, and a high percentage of suspended solids are removed from them. However, the presence of dead zones adversely affects the overall treatment

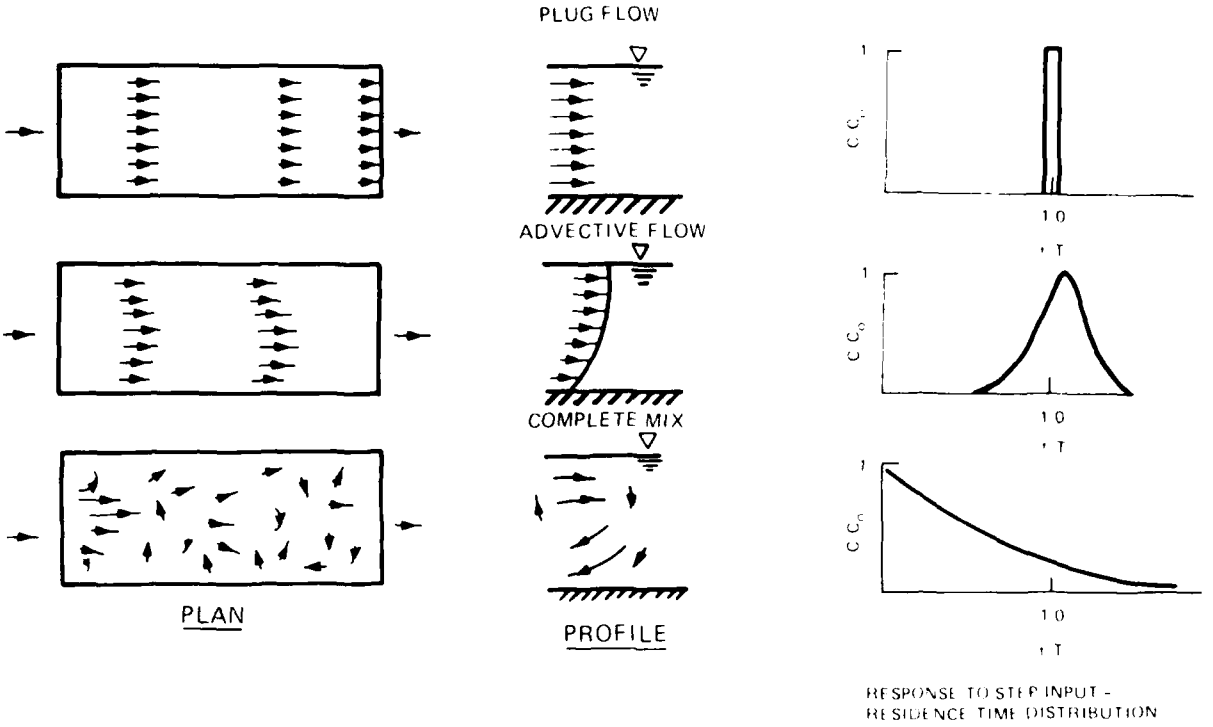

Figure 5. Velocity and residence time distributions for plug flow, completely mixed, and advective flow

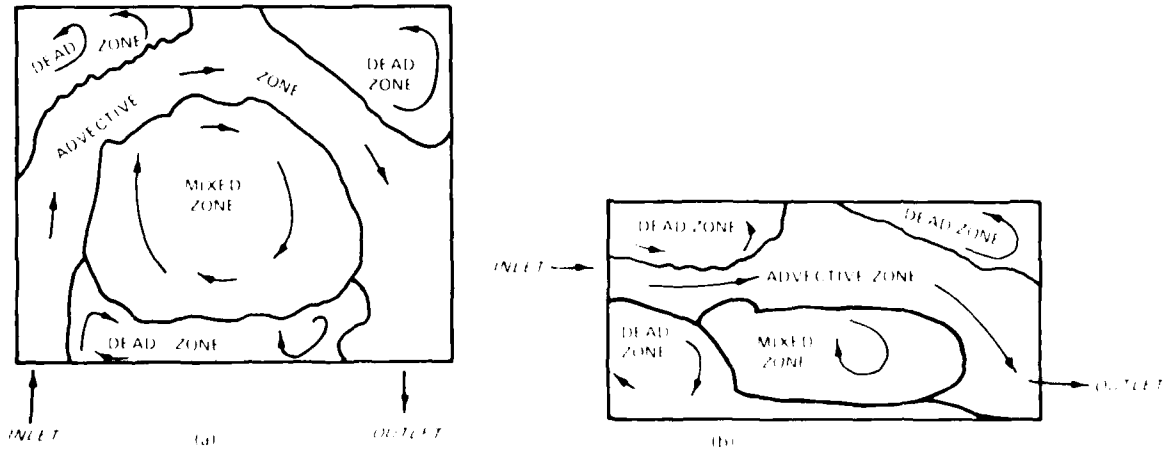

Figure 6. Plan view schematics of typical flow patterns in two DMCAs

efficiency of the DMCA because the dead zone volume is unavailable to the main flow, thus reducing the mean residence time. The expression "short-circuiting" is used to describe the effect of dead zones on residence time distribution.

16. Dead zones tend to occur in shallow or hydraulically rough areas, corners, and areas behind baffles or obstructions that are sheltered from the mixing effects of advective flow or wind. The small width of DMCA inlets and outlets relative to the width available for flow promotes formation of dead zones near inlets and outlets (Figures 2, 4, and 6). Deposition of coarse sediments at the inlet usually results in formation of a fan or delta as shown in Figure 3. Such formations have been observed at times to decrease the size of adjacent dead zones by distributing flow and at other times to promote dead zones by concentrating flow when a channel across the fan or delta evolves.

17. Dead zones can also occur in the vertical dimension, as well as the horizontal. For most dredged materials, slurries with solids concentrations greater than approximately 200 g/ℓ do not readily flow, so the point in the vertical profile where concentration exceeds 200 g/ℓ is usually defined as the bottom. Slurries with intermediate concentrations (for example, between 30 and 200 g/ℓ) flow, but at distinctly slower rates than the overlying water, which has lower solids concentrations. Therefore, the layer between the bottom and the relatively clarified surface layer could be considered a dead zone (Figure 7). The water initially contained in this layer is trapped for a relatively long time. As the layer consolidates to concentrations greater than 200 g/ℓ, the water is slowly expelled into the overlying zones.

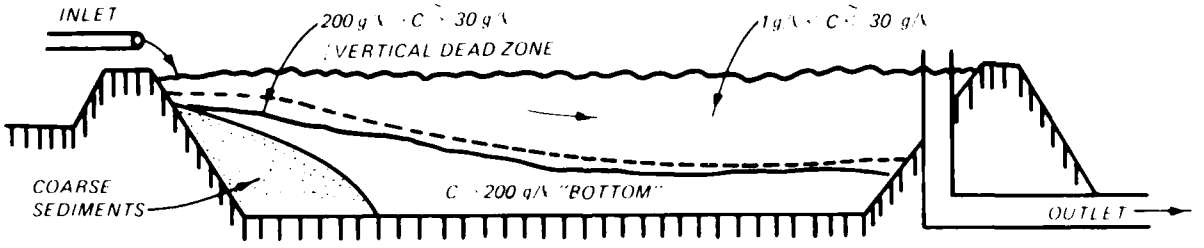

Figure 7. Dead zone in high concentration layer near bottom of DMCA

Dispersion

18. Departures from ideal flow also occur because of localized mixing in advective flow, or dispersion. Dispersion is caused by the variation in average local velocity. In general, velocities are higher at the surface and near the center of the flow than at the bottom or near the sides. In addition, dispersion is caused by turbulent mixing, although this effect is not as great as that induced by boundaries. Turbulent mixing occurs as numerous, time-varying eddies mix water in a given parcel with adjacent parcels.

As shown in the schematic of ideal flow (Figure 5), mixing occurs between "plugs."

Wind effects

19. Winds can significantly affect both short-circuiting and dispersion in DMCAs. Alterations in wind speed and direction can rapidly modify the flow patterns in a DMCA, changing zones from one type to another. Wind-induced surface velocities can be 100 times greater than mean advective flow velocities. Wind-induced surface flows are accompanied by flows in the opposite direction in lower layers and spiraling flows in corners (Liggett and Hadjitheodorou 1969). Theoretical calculations by Liu and Perez (1971) for very shallow, nonstratified small water bodies (in which the Coriolis acceleration can be neglected) showed a maximum return flow velocity of approximately 50 percent of the maximum surface velocity. The surface drift direction was found to essentially parallel the wind direction, except near the banks, and to vary from about 0.6 ft/sec for a wind speed of 10 ft/sec (6.3 mph) to about 1.8 ft/sec for a wind speed of 30 ft/sec (20 mph). The results were sensitive to the assumed value of eddy viscosity (0.5 cm^2/sec), but not to depth.

20. Wind can cause extreme short-circuiting by driving the entering flow directly from the inlet to the outlet in less than 5 percent of the theoretical residence time. However, observation of DMCAs indicates that the major effect of wind is to promote mixing and not short-circuiting. The high wind-induced surface velocities and associated underflows promote lateral and vertical mixing at the expense of dead zones and advective flow zones. Thus, wind tends to increase the fraction of the DMCA dominated by completely-mixed conditions.

Dye Tracer Curves and Residence Time Distributions

Mean residence time

21. As noted previously in Part I, the curve of DMCA effluent dye concentration versus time that results from a slug input of dye into the inflow is identical to a frequency distribution of residence times. The presence of dead zones is manifest in the dye tracer curve, the mean residence time $\bar{t}$ being less than the theoretical residence time T. The mean residence time may be computed from the dye tracer curve using Equation 1. The dimensionless

ratios, hydraulic efficiency $\bar{t}/T$, and HECF $T/\bar{t}$ are numerical measures of the influence of dead zones.

Dispersion index

22. Gross longitudinal mixing is manifested in the dye tracer curve by the spread of the base of the curve. The dispersion index d is a dimensionless number that measures the amount of mixing occurring. The dispersion index is obtained by dividing the variance of the residence time distribution by the mean residence time squared.

$$d = \frac{s^2}{\bar{t}^2} \tag{3}$$

where

s^2 = variance of the residence time distribution

$\bar{t}^2$ = mean residence time squared

The dispersion index may be computed from a digital dye tracer curve using the following formula, where previous definitions of variables apply:

$$d = \frac{1}{\bar{t}^2} \left\{ \frac{\sum_{i=1}^{n-1} \bar{t}_i^2 \, (\bar{C}_i - C_b) \, \Delta t_i}{\sum_{i=1}^{n-1} (\bar{C}_i - C_b) \, \Delta t_i} - \left[\frac{\sum_{i=1}^{n-1} \bar{t}_i \, (\bar{C}_i - C_b) \, \Delta t_i}{\sum_{i=1}^{n-1} (\bar{C}_i - C_b) \, \Delta t_i} \right]^2 \right\} \tag{4}$$

A high value for the dispersion index indicates a wide spread of flow-through times. Also, because of continuity, a high dispersion index indicates that a large fraction of the flow exits earlier than $\bar{t}$.

Efficiency, dispersion, and solids removal

23. The dispersion index and the mean residence time are entirely independent of one another. For example, Figure 8a shows four curves with identical dispersion indices but different mean residence times, and thus different hydraulic efficiencies. Conversely, Figure 8b shows three curves with identical mean residence times and hydraulic efficiencies but different dispersion indices. Although the three curves in Figure 8b have the same

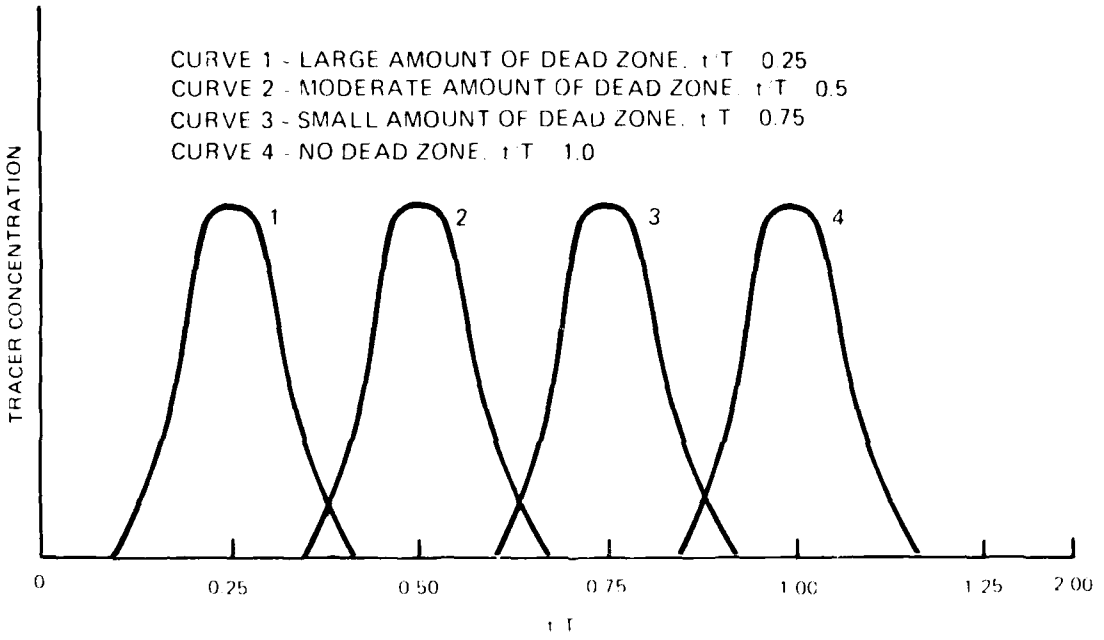

a. Dye curves with equal dispersion indices, but different mean residence times

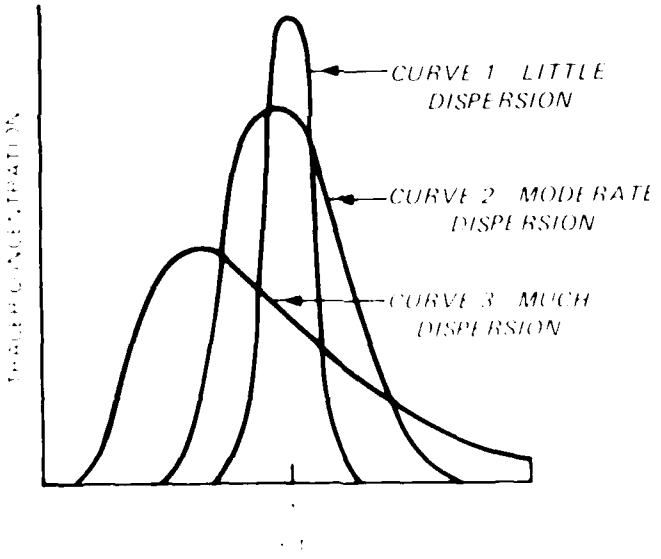

b. Dye curves with equal mean residence times, but different dispersion indices

Figure 8. Independence of dispersion and short circuiting

value for hydraulic efficiency, the DMCRs they represent would have different solids removal efficiencies. Curve three would be associated with the lowest

solids removal efficiency because of the nonlinearity of the solids removal curve (Figure 1). The greater percentage of removal of solids from parcels of water with residence times greater than $\bar{t}$ is not great enough to counterbalance the lesser percentage of removal of solids from parcels of water with residence times less than $\bar{t}$. Figure 9 contrasts the characteristics of two extreme types of residence time distributions: plug flow and complete mix.

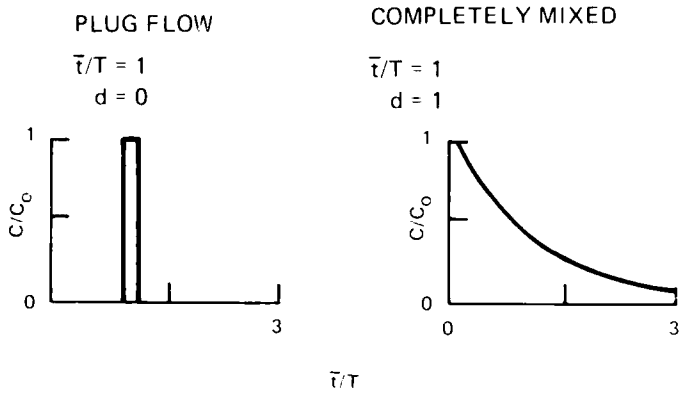

Figure 9. Residence time distributions from plug flow and completely mixed basins

Conceptual model

24. A simple conceptual model may be used to reproduce residence time distributions similar to that produced by the complex situations shown in Figure 6. Figure 10 shows a conceptual model composed of four compartments: an advective zone at the inlet, and then a completely mixed zone, an advective zone, and a dead zone to represent the main body of the DMCA. As can be seen from Figure 10, the overall DMCA residence time distribution is the sum of the outputs from the three main compartments and approximates a log-normal distribution. The exact shape of the log-normal distribution depends on the dispersion of the output from the four compartments and the relative magnitude of the compartment volumes and flow rates. Figure 10 is, of course, a simplified analogy. Some DMCAs may have small complete-mix zones in large scour holes at the point of inflow, instead of advective flow (A_1). Considerable exchange that is not part of the Figure 10 analogy occurs between well-mixed, advective, and dead zones.

25. The relative volumes of the four compartments and the division of flow among the latter three vary continuously as functions of wind, total flow, DMCA bottom topography, and plan geometry, etc., so quantitative use of

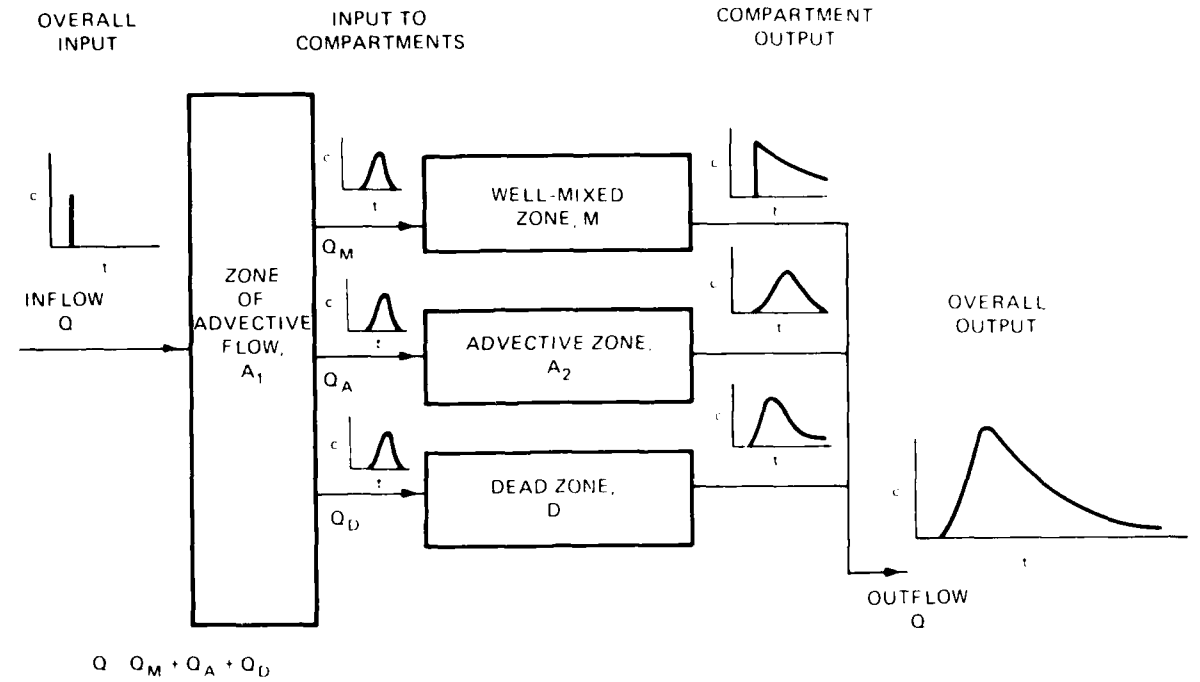

Figure 10. Analogy for DMCA hydraulic processes

the model is not possible. However, the model is useful as an aid when mentally linking the impacts of flow patterns on residence time distribution. Two hypothetical examples are presented below.

26. A hypothetical dye curve from a DMCA consisting primarily of dead zones and a small advective flow zone is shown in Figure 11a. Because the advective flow zone has a relatively low volume, the average flow-through time is much less than T, so $\bar{t}/T$ is much less than 1.0. Because the well-mixed zone is small and there is relatively little longitudinal dispersion in the advective zone, the peak of the curve is sharp. However, some dye is mixed into dead zones, from which it emerges slowly, causing the long tail of the curve. This distribution is essentially the same as that conceived by Hays (1966) and applied to natural streams by Thackston and Krenkel (1967) and Thackston and Schnelle (1970).

27. A hypothetical time-concentration curve from a DMCA with a large well-mixed zone, smaller advective flow zone, and small dead zone is shown in Figure 11b. Because much of the dye quickly enters the well-mixed zone, dye shows up at the outlet rapidly. The shape of the curve resembles that from a

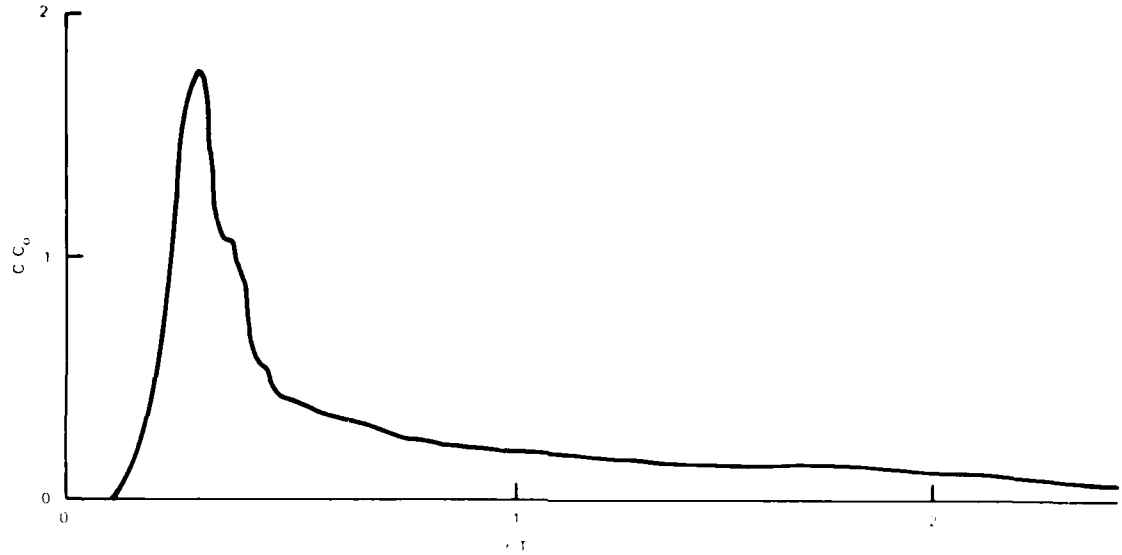

a. From a DMCA dominated by advective flow and dead zones

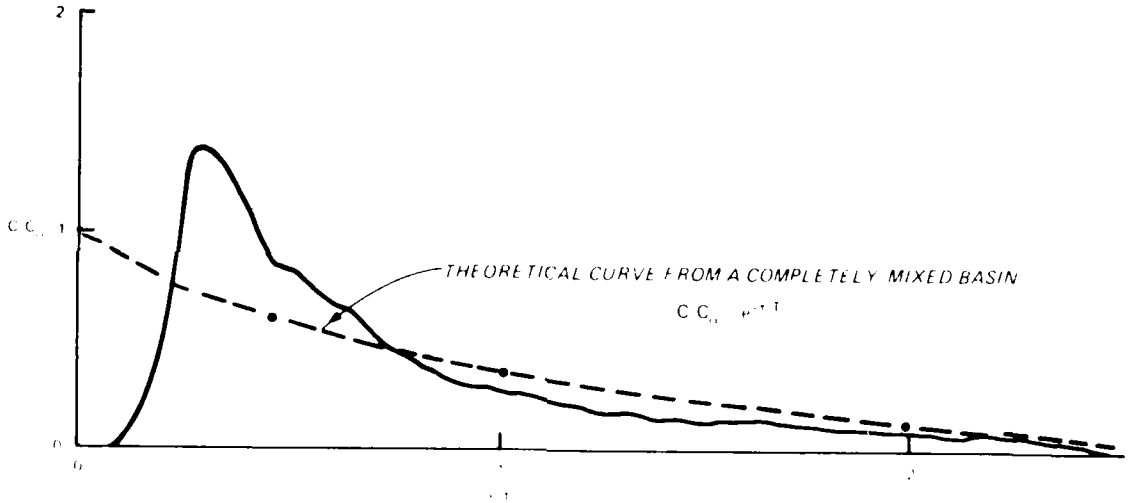

b. From a DMCA dominated by advective flow and well-mixed zones

Figure 11. Hypothetical dye curves from DMCAs

completely-mixed basin, except that there is a lag time of 0.1 to 0.2 T before dye occurs at the outlet, a higher peak dye concentration, and a decay limb slightly below the completely mixed curve.

Reported Residence Time Distributions

28. The literature contains little information about the hydraulics of large, shallow ponds, such as DMCAs, relative to the volume of information about sedimentation basins for water and wastewater treatment. This situation is partially attributable to the difficulties of performing tracer tests on large facilities with long residence times and remote locations. Relevant residence time distribution studies are summarized below.

DMCA studies

29. Montgomery (1978) reported the results of three dye tests at two DMCAs. In all three tests, short-circuiting was significant, and the hydraulic efficiency for all three tests was reported as less than 0.5.

30. Poindexter and Perrier (1980) reported the results of eight DMCA dye tests, including the three previously reported by Montgomery (1978). Results of the dye tests were sensitive to the unsteady nature of dredge discharge and wind. The sites studied had low values of length-to-width ratio (L/W) (2 to 4), and none of the numerical descriptors of the dye curves were found to be correlated with L/W ratio. However, errors were made in dye curve analysis, leading to slightly incorrect values for the statistical descriptors. Wind caused serious short-circuiting, particularly in shallow DMCAs. While wind affected the shapes of the dye curves, mean residence times were less affected.

31. Palermo (1984) reported the results of three dye tests conducted in conjunction with his research on pollutant removal in dredged material containment areas. The primary purpose of the tests was to estimate the mean residence time so that effluent sampling could be lagged from influent sampling by approximately that time. However, only two of the tests (at Mobile Harbor and Norfolk Harbor) produced complete tracer curves. Estimates of average flow rate and DMCA dimensions were not adequate for accurate determination of T, and thus $\bar{t}/T$.

32. Gallagher and Company (1978) produced a report specifically on DMCA residence time distributions. They presented results of four dye tests, one of which was obtained from Montgomery (1978). On the basis of these tests, they concluded that "... considerable short-circuiting occurs in large shallow basins, and this results in inefficient flow patterns. Actual retention times

are significantly shorter than ideal through-flow times, and wind effects can be very detrimental."

Water and wastewater
treatment basin studies

33. Marske and Boyle (1973) reported the results of dye tests on prototype chlorine contact chambers. They tested a wide variety of basin shapes and baffling arrangements. Theoretical residence times for the rectangular basins ranged from 0.46 to 7.78 hr. Flow rates ranged from 0.46 to 47 cfs.

34. Marske and Boyle (1973) ran a pair of tests with identical hydraulic conditions, but with a 20-mph wind blowing directly toward the outlet in one case and directly away from the outlet in the other case. Wind was found to cause serious short-circuiting. The ratio of initial time of dye appearance to T decreased from 0.54 with the wind blowing upstream to 0.36 with the wind blowing downstream. However, mean residences for the two tests were essentially equal.

35. The dispersion index d was recommended as the most reliable indicator of basin hydraulic performance. A value of L/W greater than 20 was necessary to reduce the dispersion index below 0.1, and a value of L/W greater than 40 was necessary to achieve the minimum value of d, which was about 0.02. Longitudinal baffling was found to be better than transverse baffling, because a larger value of L/W can be achieved with fewer baffles. In addition, fewer baffles result in fewer corners or shadow areas, which are potential dead spaces.

36. Mangelson and Watters (1972) conducted tracer tests on prototype waste-treatment lagoons at Logan, Utah, and in the laboratory on a 20- by 40- by 3.5-ft model. Various inlet and outlet conditions were used in the model tests. The average hydraulic efficiency for the lagoons was about 0.58. The lagoons had values of L/W between 1.6 and 2.3. Values of hydraulic efficiency for the unbaffled model ranged from 0.52 to 0.64 (omitting the highest and lowest values) for depths of 1.5 ft and L/W equal to 2.0. In model tests with baffles in various arrangements, a value of L/W of 5.26 produced a hydraulic efficiency of 0.72, and values of L/W from 13 to 45 produced values of hydraulic efficiency between 0.93 and 0.96, except for one experiment in which the baffles did not overlap. In this case, the value of hydraulic efficiency was 0.85.

37. In all of the prototype tests, dimensionless initial time t_i/T was less than 0.1, and dimensionless time of peak concentration t_p/T was between 0.1 and 0.2, denoting extreme dispersion. For the unbaffled model tests, t_i/T was between 0.06 and 0.18, and t_p/T was between 0.18 and 0.30. The introduction of baffles decreased the amount of dead space and significantly increased values of t_p/T and t_i/T. In general, the more baffles there were and the closer the baffles came to the opposite wall, the closer the residence time distribution approached plug flow.

Mathematical Models

38. Gallagher and Company (1978) developed a potential flow model (laminar flow) and applied it to hypothetical, rectangular DMCAs with various inlet and outlet configurations and spur dike arrangements. Although the model is not a realistic depiction of DMCA conditions, cannot be considered quantitative, cannot show flow separation or dead zones (although areas of very low predicted velocity can be interpreted as dead zones), and cannot handle wind effects, it is a qualitative indicator of hydraulic behavior. Based on model output, Gallagher and Company recommended outlet weirs as long as possible and one to four baffles extending 75 percent of the way across or along the basin. Economics of spur dikes were discussed, and tables were presented showing the increase in L/W ratio and dike construction cost associated with various spur dike arrangements.

39. Koussis, Saenz, and Thackston (1982) evaluated available hydrodynamic models with respect to their ability to reproduce the important phenomena occurring in DMCAs. Economic considerations associated with the use of models for design were also evaluated. Koussis, Saenz, and Thackston suggested development of a steady-state, two-dimensional, vertically integrated hydrodynamic model capable of handling natural topographies, realistic boundary conditions, and moderate wind effects. Such a model could be coupled with a sediment transport model for prediction of DMCA effluent solids concentration. They recognized that the two-dimensional hydrodynamic model might fail to adequately describe DMCA hydrodynamics, and in that case recommended development of a three-dimensional model.

40. In Appendix A, Bach reports the results of an effort to simulate the hydraulic behavior of DMCAs using three-dimensional and two-dimensional

computer models. Satisfactory results were obtained from initial runs of the three-dimensional model, but the modeling effort was continued with the two-dimensional codes to meet the time and money constraints of this study. The two-dimensional model was vertically averaged, and thus it could not simulate circulation in the vertical plane caused by wind shear. Nevertheless, the model was able to predict peaks and means of eight observed DMCA residence time distributions when model coefficients were chosen by trial and error.

41. Selection of model coefficients for predictive use of the model remains problematic, even though a linear regression equation for the model coefficients based on surface drift velocity, DMCA surface area, discharge, and wind direction was derived. Since only eight data points were used in fitting the equation (which has four independent variables) and since the field data used to adjust the model are of low quality, use of the regression equation for selecting model coefficients for other DMCAs is not generally recommended.

42. Tatom and Waldrop (1986) reported initial work on the adaptation of a vertically averaged, two-dimensional computer model for simulation of ash settling ponds associated with coal-fired power plants. Pond geometries are similar to large DMCAs, and flow rates are slightly lower. The model will include inputs of water to the pond from rainfall and surface runoff. Plans for calibration include collection of extensive field data. Results of this work may be useful to future DMCA designers.

Summary of Literature

43. Little information is available regarding residence time distributions of large, shallow impoundments. Field data are scarce because of the extremely long residence times and attendant time requirements for dye tests. In general, these impoundments tend to have efficiencies in the 0.4 to 0.6 range and high dispersion indices. Wind-induced currents can be two orders of magnitude greater than average advective currents.

44. Gallagher and Company (1978) present qualitative guidance for hydraulic design of DMCAs. They discuss the benefits and costs of spur dikes. Test data from chlorine contact chambers and physical models show that

dispersion and short-circuiting may be greatly reduced by increasing L/W (which may be done with spur dikes or baffles*).

45. Generation of residence time distributions by simulating DMCA hydraulics using computer models appears to be just within the state of the art. However, the costs of collecting adequate field data for calibration and running the models are obstacles to their use. Vertically averaged, two-dimensional models are not able to simulate wind-induced circulation in the vertical plane. Field studies indicate that wind-induced circulation affects the overall shape of the residence time distribution (reflected in parameters like the time to peak and the dispersion index) but not the mean residence time or hydraulic efficiency.

---

* The term "spur dikes" as used herein refers to baffles in a DMCA. DMCAs are sometimes baffled by constructing interior earthen embankments. Water and wastewater treatment basins are usually baffled with reinforced concrete walls. Wooden baffles may be used in model tests. The use of floating baffles in DMCAs is discussed in Part V.

PART III: DESCRIPTION OF FIELD TESTS

Data Sources

46. Records of 13 DMCA dye tracer tests were available. All of the dye tracer tests were conducted as part of the US Army Engineer Waterways Experiment Station (WES) research projects at active CE dredging sites. In most cases, the tests were intended to provide data to support research on subjects other than residence time distribution or hydraulic efficiency. Therefore, the quantity and quality of data from the various dye tests vary widely. In an attempt to standardize the results for analysis, all available original data were reexamined and reanalyzed in a consistent manner.

47. One of the 13 tests had to be eliminated because the dye tracer curve was incomplete and because some essential physical data were missing. The other 12 tests are listed in Table 1. Normalized dye curves, site maps, and wind data are displayed on similar scales for all 12 tests in Figures 12 through 23. Dye concentrations were normalized by dividing by C_o,

$$C_o = \frac{1}{T} \int_o^{3T} C \, dt \tag{5}$$

Physical Variables

48. The physical variables of length, width, area, and volume were all recalculated, starting with the map of the site. These maps were digitized, and the areas were calculated. Smooth flow paths from inlet to outlet were sketched, and their lengths were measured and used as L in subsequent analyses. Widths were measured as the distance from boundary to boundary perpendicular to the flow path. Several typical widths were averaged to a single value.

49. The depths of the basins were measured by various methods. Montgomery (1978) took samples at various depths, analyzed each for suspended solids, plotted the data, and defined depth as the distance from the water surface to the point where the solids concentration was about 200 g/ℓ. Poindexter and Perrier (1980) used a hydrometer consisting of a small plastic bottle filled with a sediment-water mixture, adjusted so that it was neutrally

Table 1

Location of Tests and Data Sources*

Test	Site	Date	Reference
1	Yazoo River #5, Miss.	2/23/77	Gallagher and Co. (1978) Montgomery (1978)
2	Fort Eustis, Va.	5/12/79	Poindexter and Perrier (1980)
3	Burnsville, Miss.	3/81	Schroeder (1983)
4	Yazoo River #5, Miss.	3/17/77	Montgomery (1978)
5	Yazoo River #5, Miss.	8/9/78	Poindexter and Perrier (1980)
6	Mobile (N. Blakely), Ala.	6/29/78	Poindexter and Perrier (1980)
7	Yazoo River #6, Miss.	2 or 3/77	Gallagher and Co. (1978) Poindexter and Perrier (1980)
8	Yazoo River #3, Miss.	12/12/78	Poindexter and Perrier (1980)
9	Mobile (N. Blakely), Ala.	7/7/82	Palermo (1984)
11	Norfolk (Craney Is.), Va.	2/7/83	Palermo (1984)
12	Black Rock Harbor (United Illuminating), Conn.	10/26/83	Unpublished notes, site description by Palermo and Pranger (1984)
13	Fowl River, Ala.	4/12/77	Montgomery (1978)

* Test 10 was not used because the dye curve was incomplete and site geometry data were poor.

buoyant when immersed in a slurry with a total solids concentration of 200 g/ℓ. This was lowered into the basin by a cord from a boat until it stopped, and the depth was recorded as the distance from the center of the bottle to the water surface. Schroeder (1983) estimated depths based on the difference between measured water surface elevation and elevations of the bottom taken from as-built plans. Schroeder's test occurred early in the disposal operation before much deposition had occurred in the basin.

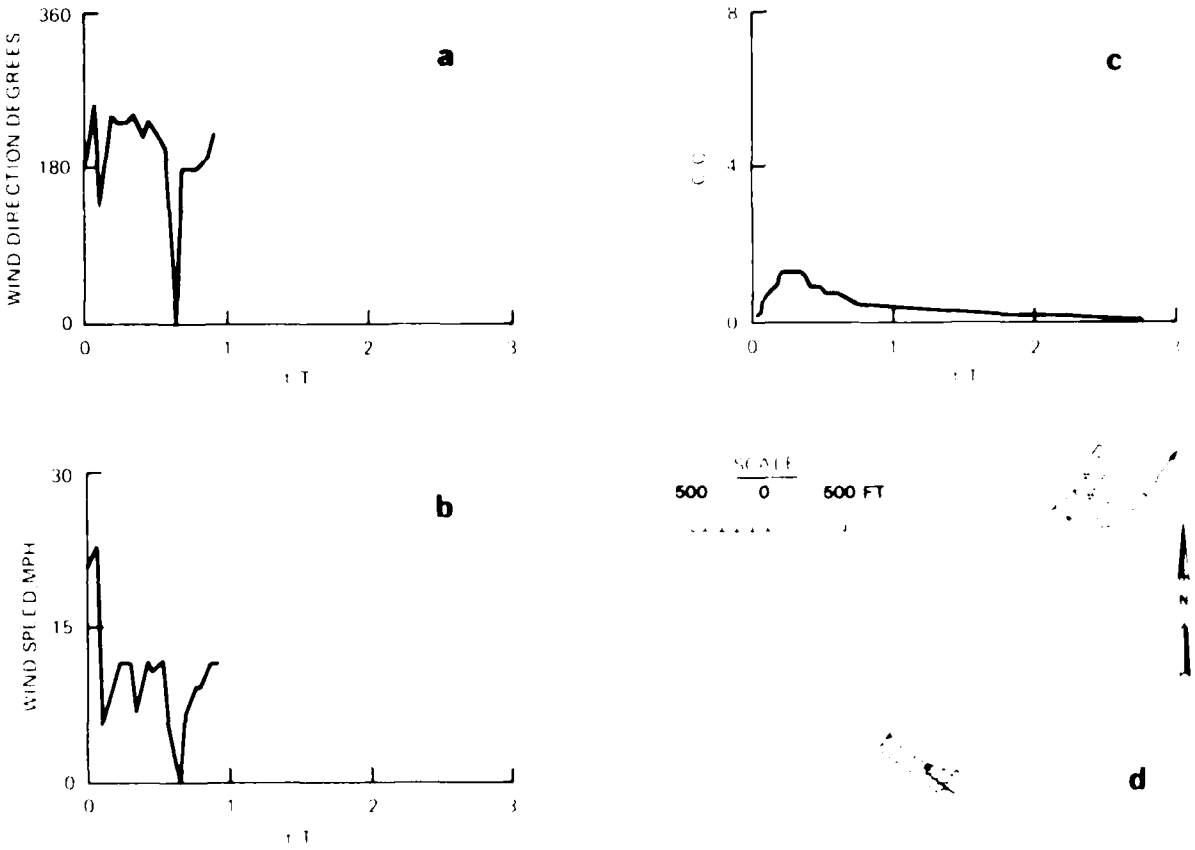

Figure 12. Test 1, Yazoo River No. 5, Mississippi. (a) Wind direction. Y-axis shows direction from which the wind blew in degrees clockwise from north, i.e., 90° for east, 180° for south, 270° for west. A wind direction of 0° indicates calm. (b) Wind speed. (c) Normalized dye curve. $C_o = \frac{1}{T}\int_o^{3T} C\,dt$. Missing values of concentration at large t/T estimated using procedure described in Part V. (d) Site plan, 1 in. = 1,000 ft. Hatching indicates dry area

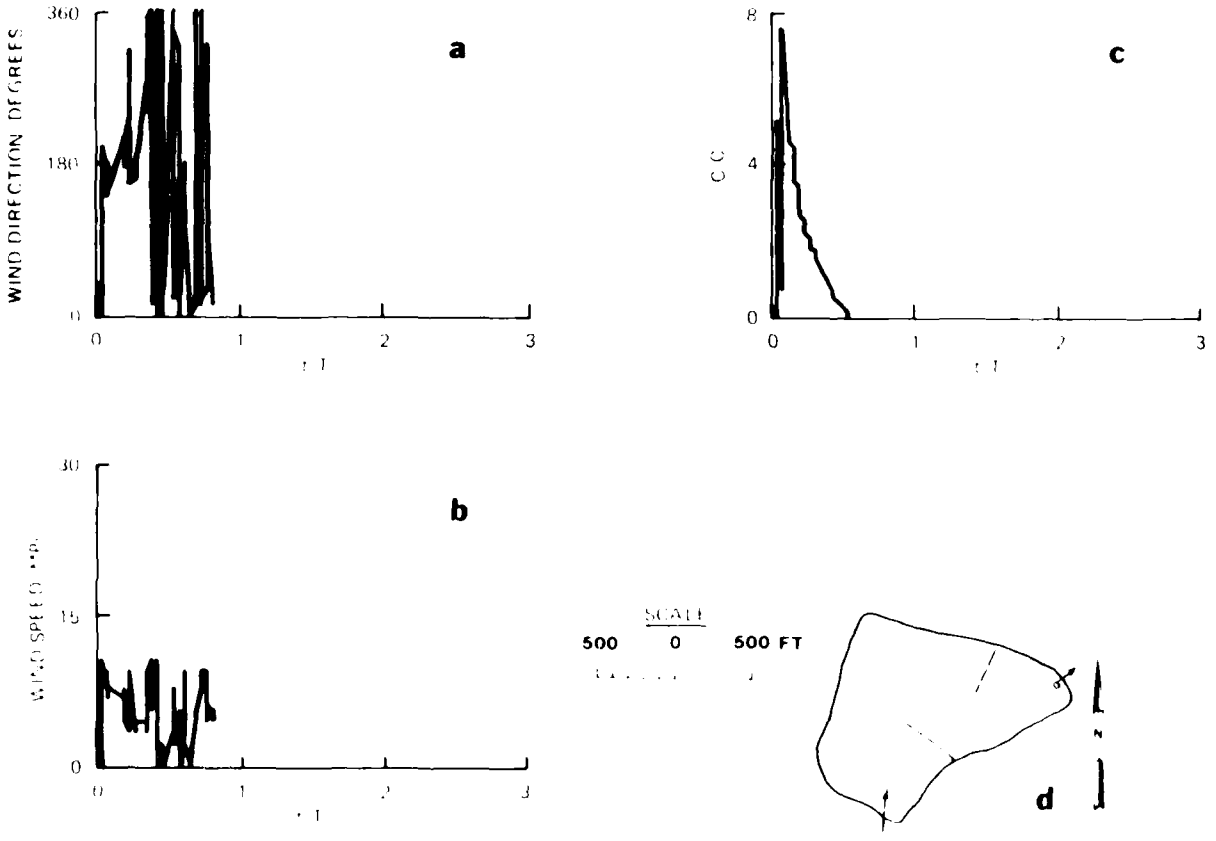

Figure 13. Test 2, Fort Eustis, Virginia. (a) Wind direction. Y-axis shows direction from which the wind blew in degrees clockwise from north, i.e., 90° for east, 180° for south, 270° for west. A wind direction of 0° indicates calm. (b) Wind speed. (c) Normalized dye curve. $C_o = \frac{1}{T}\int_0^{3T} C\,dt$. Missing values of concentration at large t/T estimated using procedure described in Part V. d) Site plan, 1 in. = 1,000 ft. Hatching indicates dry area

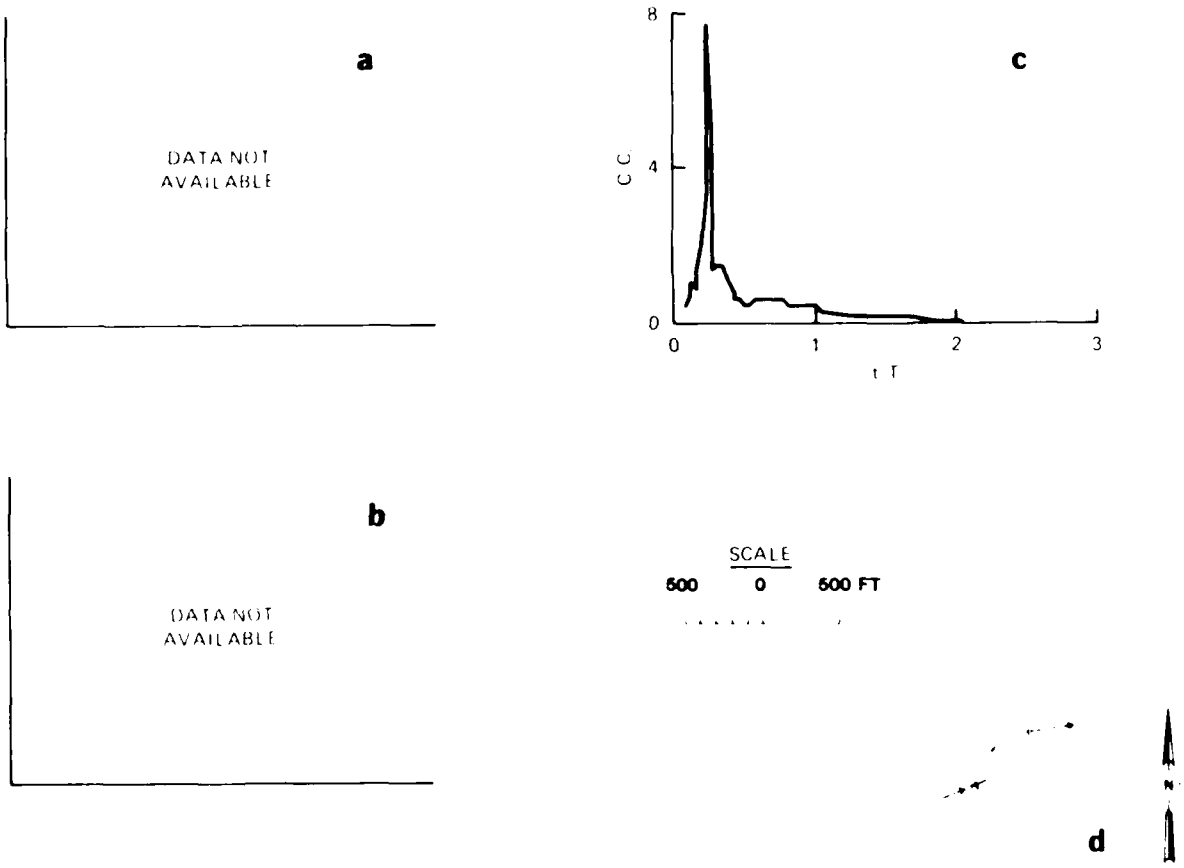

Figure 14. Test 3, Burnsville (Tenn-Tom Waterway), Mississippi. (a) Wind direction. Y-axis shows direction from which the wind blew in degrees clockwise from north, i.e., 90° for east, 180° for south, 270° for west. A wind direction of 0° indicates calm. (b) Wind speed. (c) Normalized dye curve. $C_o = \frac{1}{T}\int_o^{3T} C\,dt$. Missing values of concentration at large t/T estimated using procedure described in Part V. (d) Site plan, 1 in. = 1,000 ft. Hatching indicates dry area

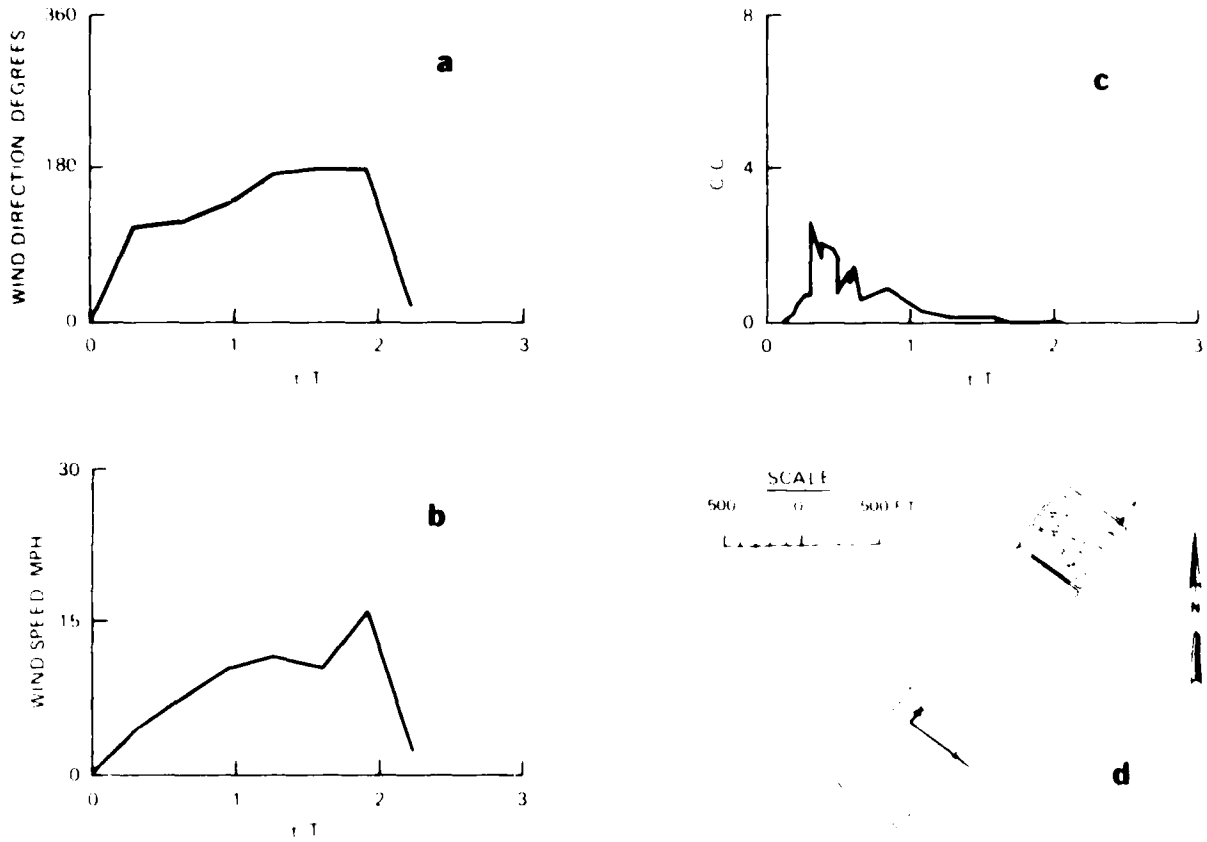

Figure 15. Test 4, Yazoo River No. 5, Mississippi. (a) Wind direction. Y-axis shows direction from which the wind blew in degrees clockwise from north, i.e., 90° for east, 180° for south, 270° for west. A wind direction of 0° indicates calm. (b) Wind speed. (c) Normalized dye curve. $C_o = \frac{1}{T}\int_0^{3T} C\,dt$. Missing values of concentration at large t/T estimated using procedure described in Part V. (d) Site plan, 1 in. = 1,000 ft. Hatching indicates dry area

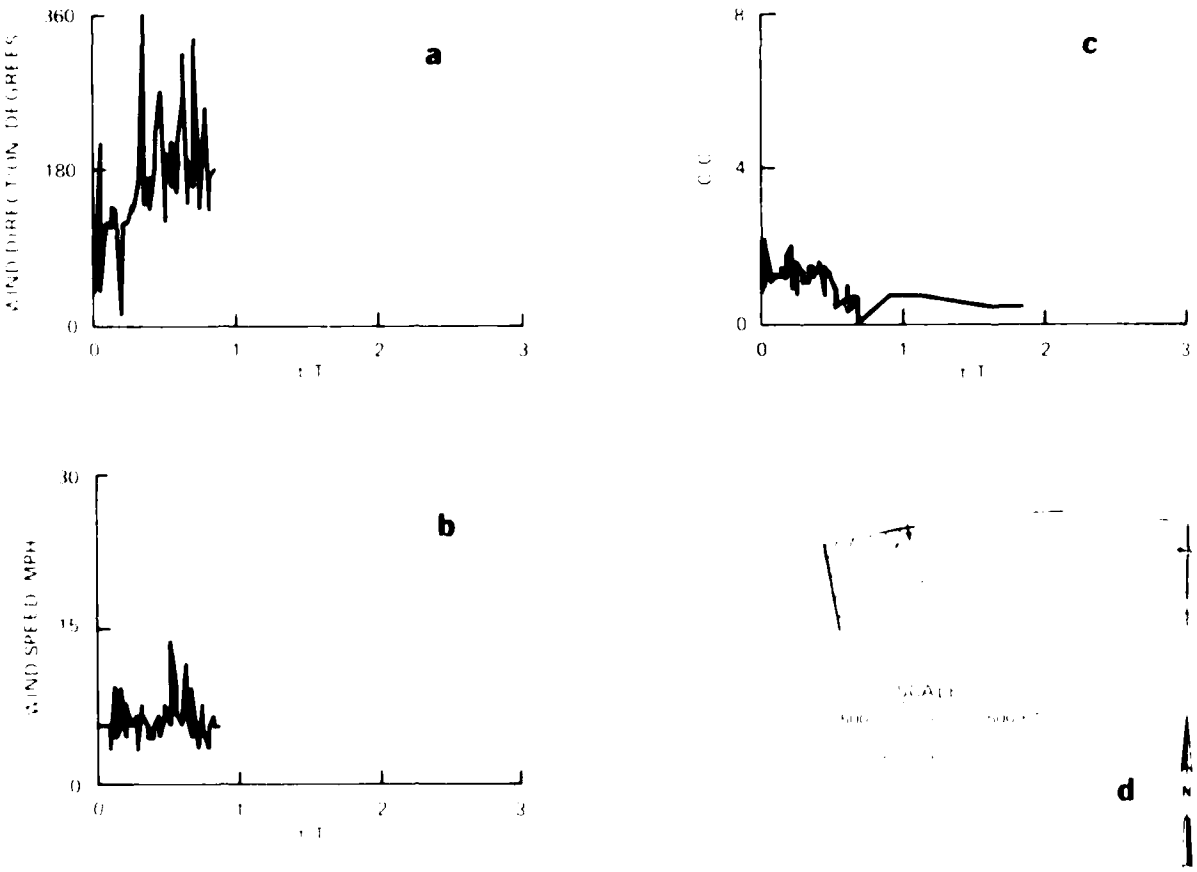

Figure 16. Test 5, Yazoo River No. 5, Mississippi. (a) Wind direction. Y-axis shows direction from which the wind blew in degrees clockwise from north, i.e., 90° for east, 180° for south, 270° for west. A wind direction of 0° indicates calm. (b) Wind speed. (c) Normalized dye curve. $C_o = \frac{1}{T}\int_0^{3T} C\,dt$. Missing values of concentration at large t/T estimated using procedure described in Part V. (d) Site plan, 1 in. = 1,000 ft. Hatching indicates dry area

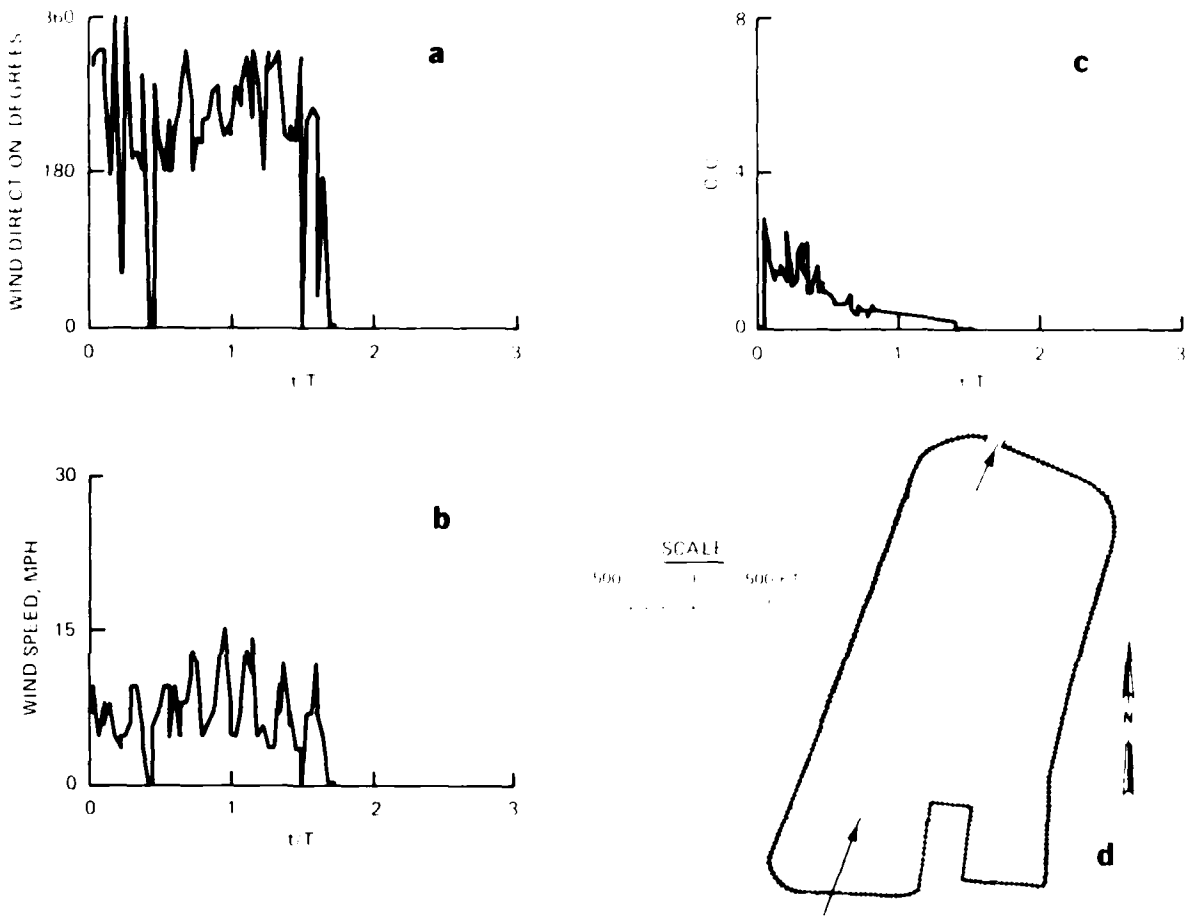

Figure 17. Test 6, Mobile (N. Blakely), Alabama. (a) Wind direction. Y-axis shows direction from which the wind blew in degrees clockwise from north, i.e., 90° for east, 180° for south, 270° for west. A wind direction of 0° indicates calm. (b) Wind speed. (c) Normalized dye curve. $C_0 = \frac{1}{T}\int_0^{3T} C\,dt$. Missing values of concentration at large t/T estimated using procedure described in Part V. (d) Site plan, 1 in. = 1,000 ft. Hatching indicates dry area

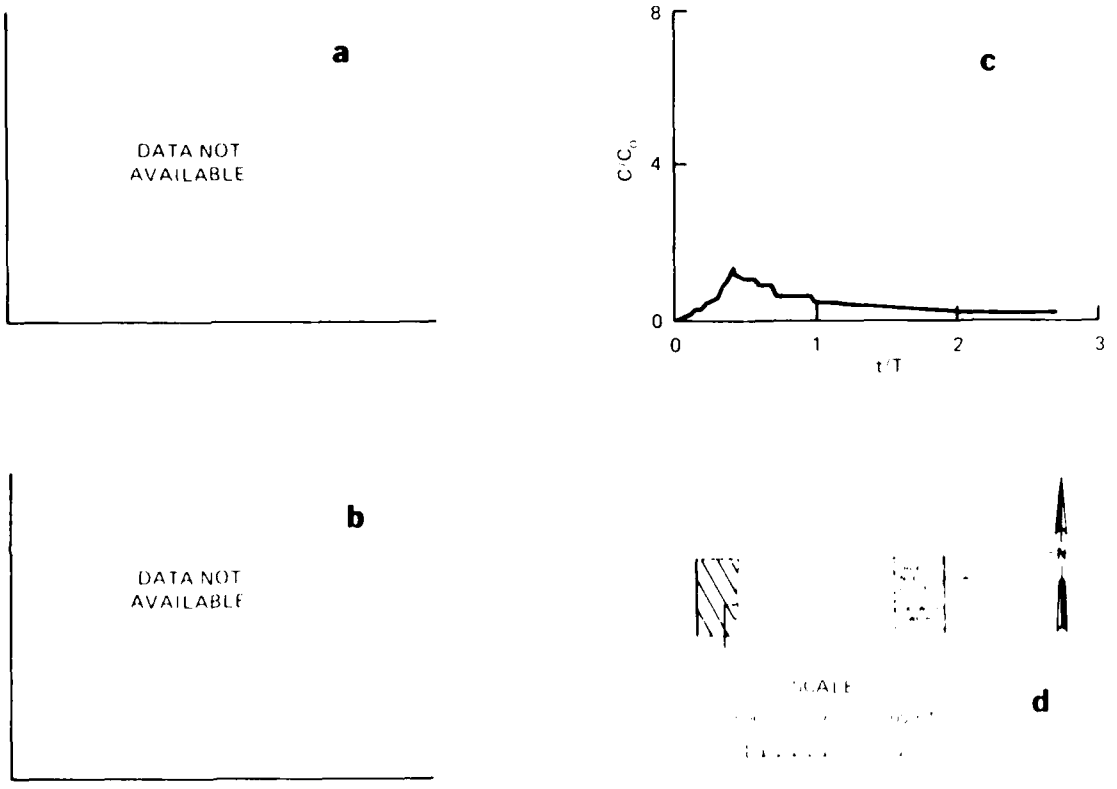

Figure 18. Test 7, Yazoo River No. 6, Mississippi. (a) Wind direction. Y-axis shows direction from which the wind blew in degrees clockwise from north, i.e., 90° for east, 180° for south, 270° for west. A wind direction of 0° indicates calm. (b) Wind speed. (c) Normalized dye curve. $C_o = \frac{1}{T}\int_o^{3T} C\,dt$. Missing values of concentration at large t/T estimated using procedure described in Part V. (d) Site plan, 1 in. = 1,000 ft. Hatching indicates dry area

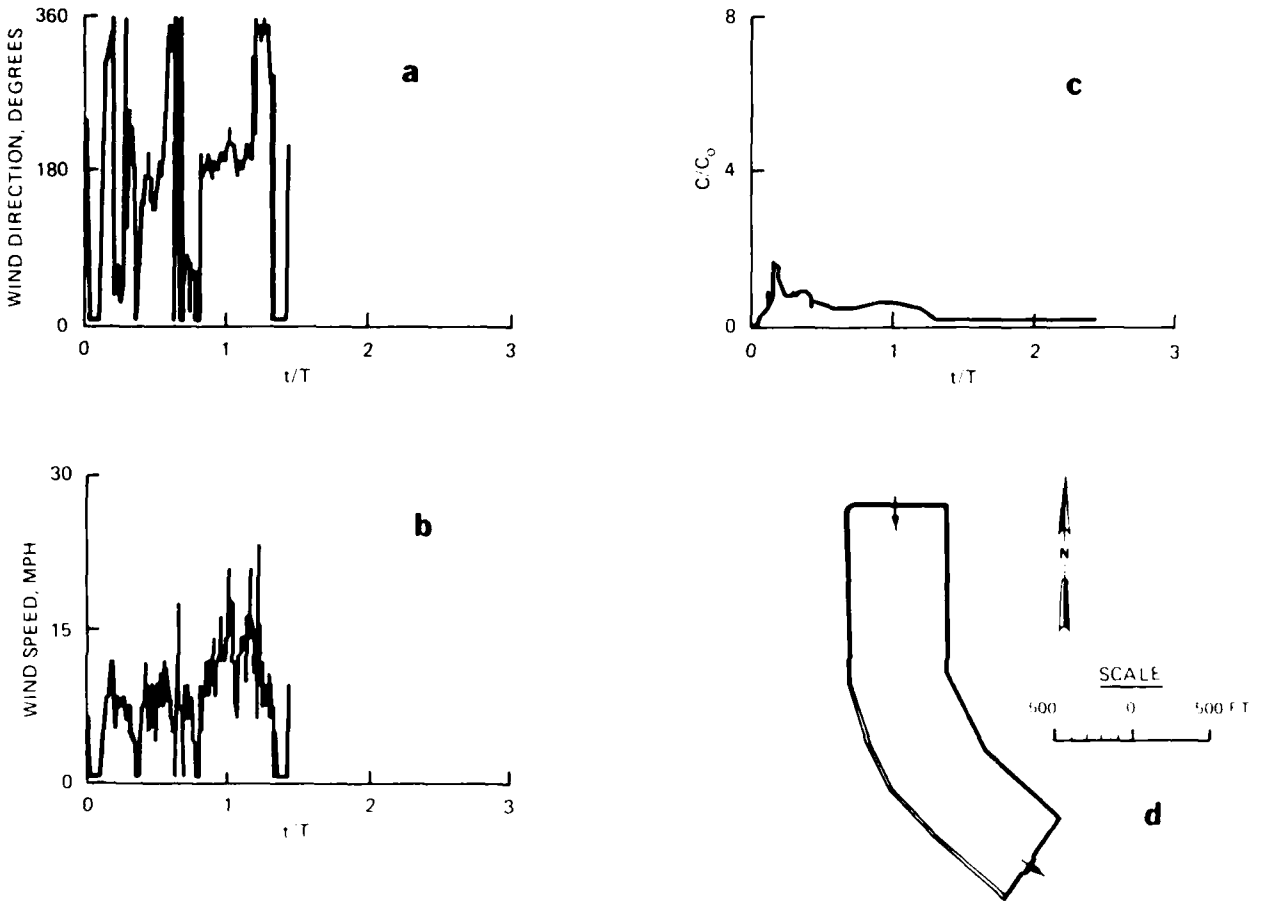

Figure 19. Test 8, Yazoo River No. 3, Mississippi. (a) Wind direction. Y-axis shows direction from which the wind blew in degrees clockwise from north, i.e., 90° for east, 180° for south, 270° for west. A wind direction of 0° indicates calm. (b) Wind speed. (c) Normalized dye curve. $C_o = \frac{1}{T}\int_o^{3T} C\,dt$. Missing values of concentration at large t/T estimated using procedure described in Part V. (d) Site plan, 1 in. = 1,000 ft. Hatching indicates dry area

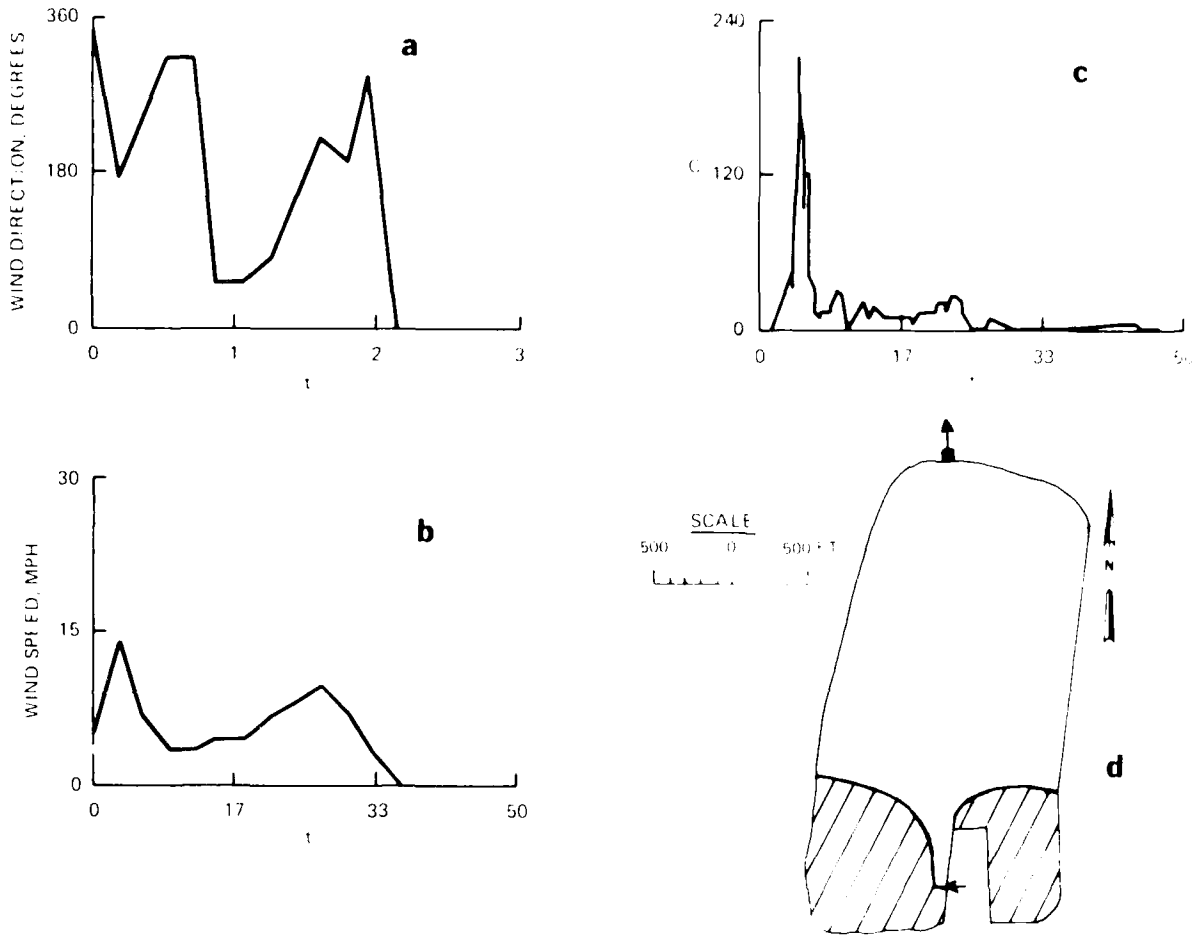

Figure 20. Test 9, Mobile (North Blakely), Alabama. (a) Wind direction. Y-axis shows direction from which the wind blew in degrees clockwise from north, i.e., 90° for east, 180° for south, 270° for west. A wind direction of 0° indicates calm. (b) Wind speed. (c) Normalized dye curve. $C_o = \frac{1}{T}\int_o^{3T} C\,dt$. Missing values of concentration at large t/T estimated using procedure described in Part V. (d) Site plan, 1 in. = 1,000 ft. Hatching indicates dry area

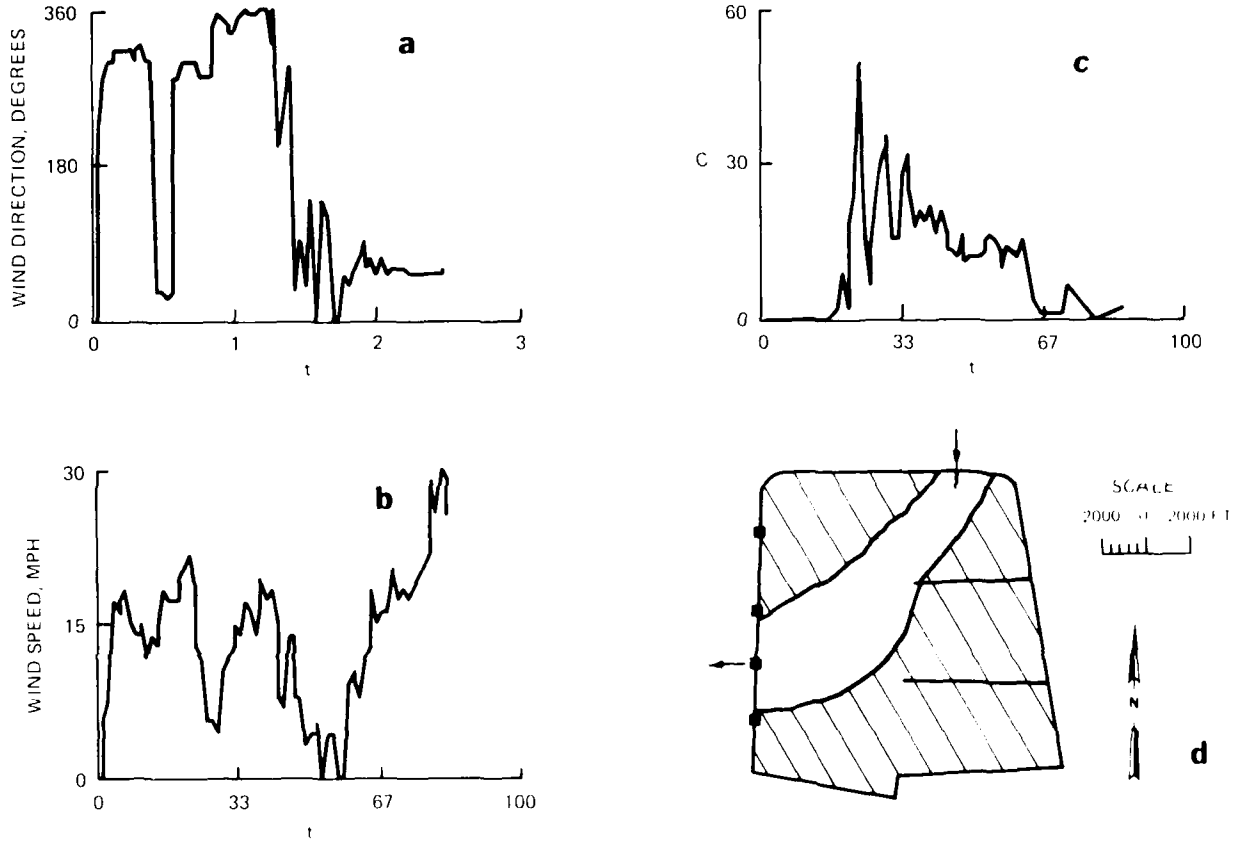

Figure 21. Test II, Norfolk (Craney Island), Virginia. (a) Wind direction. Y-axis shows direction from which the wind blew in degrees clockwise from north, i.e., 90° for east, 180° for south, 270° for west. A wind direction of 0° indicates calm. (b) Wind speed. (c) Normalized dye curve. $C_o = \frac{1}{T} \int_o^{3T} C \, dt$. Missing values of concentration at large t/T estimated using procedure described in Part V. (d) Site plan, 1 in. = 6,666 ft. Hatching indicates dry area

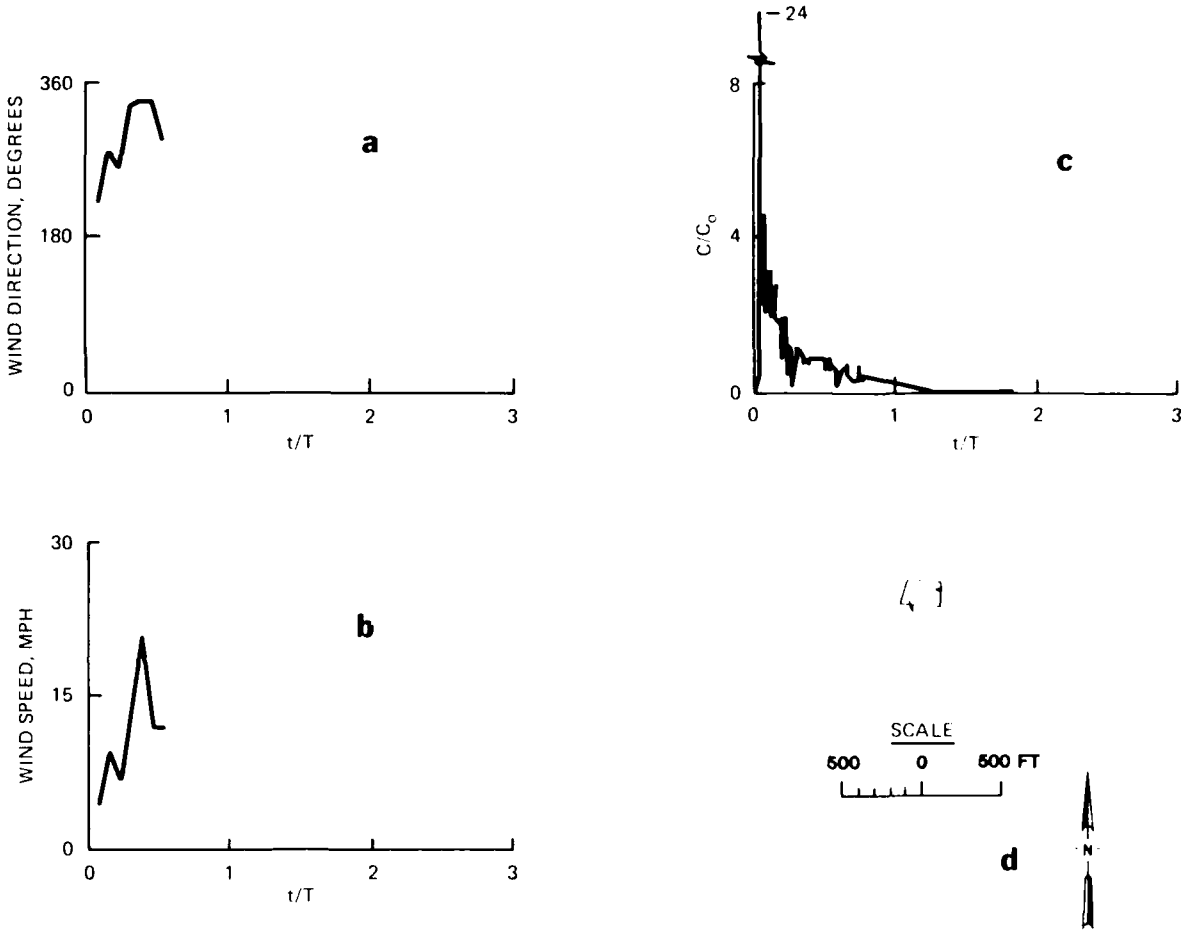

Figure 22. Test 12, Black Rock Harbor (United Illuminating), Connecticut. (a) Wind direction. Y-axis shows direction from which the wind blew in degrees clockwise from north, i.e., 90° for east, 180° for south, 270° for west. A wind direction of 0° indicates calm. (b) Wind speed. (c) Normalized dry curve.

$C_o = \frac{1}{T} \int_o^{3T} C\, dt$. Missing values of concentration at large t/T estimated using procedure described in Part V. (d) Site plan, 1 in. = 1,000 ft. Hatching indicates dry area

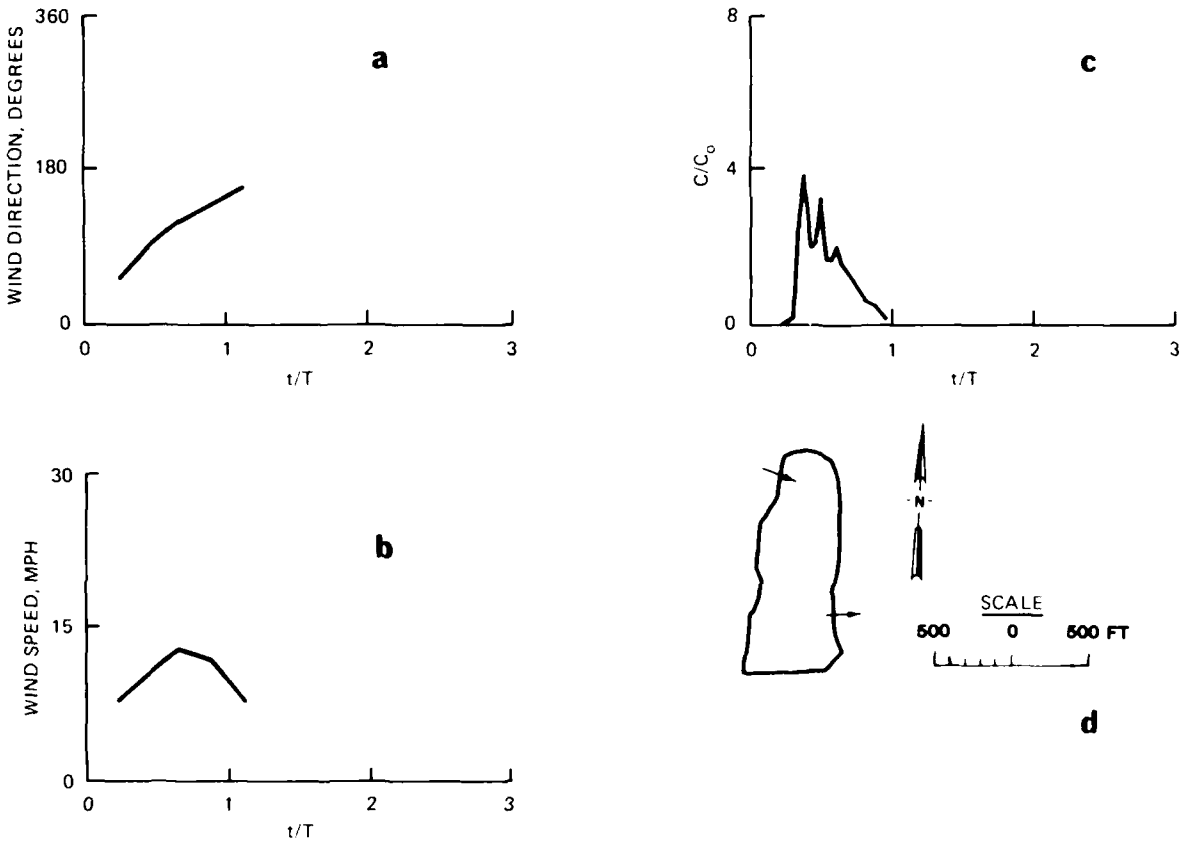

Figure 23. Test 13, Fowl River, Alabama. (a) Wind direction. Y-axis shows Y-axis shows direction from which the wind blew in degrees clockwise from north, i.e., 90° for east, 180° for south, 270° for west. A wind direction of 0° indicates calm. (b) Wind speed. (c) Normalized dye curve. $C_o = \frac{1}{T}\int_o^{3T} C\,dt$. Missing values of concentration at large t/T estimated using procedure described in Part V. (d) Site plan, 1 in. = 1,000 ft. Hatching indicates dry area

50. Volumes were calculated by multiplying area times average depth. The recalculated physical variables and dimensionless ratios for each test are shown in Table 2. Most of the sites were approximately rectangular, with L/W ratios varying from 0.7 to 4.1. Most L/W ratios were between 2.0 and 3.0. All sites except the one at Fort Pustis were unbaffled.

Table 2

Physical Variables at Each Test Site

Test No.	Length ft	Width ft	Depth ft	Area acres	Volume acre-ft	L/W	W/D	L/D
1	1,680	410	7.4	15.4	110.0	4.1	55	230
2	1,550	570	2.7	23.4	63.0	2.7	210	570
3	450	140	2.7	1.7	4.5	3.2	52	170
4	1,090	410	2.0	10.3	21.0	2.7	210	540
5	2,000	610	8.0	28.4	230.0	3.3	76	250
6	3,010	1,350	6.4	91.5	586.0	2.2	210	470
7	1,120	460	6.0	11.7	70.0	2.4	77	190
8	2,540	750	7.0	34.3	240.0	3.4	107	360
9	1,850	1,320	-	56.3	-	1.4	-	-
11	-	-	-	-	-	-	-	-
12	220	140	3.2	0.7	2.3	1.6	44	68
13	820	410	2.2	10.7	2.4	2.0	190	370

51. The inlet device in all cases except Test 3 was a single pipe of the same size as the dredge discharge pipe. Test 3 was conducted in the secondary cell of a two-celled disposal area. The inlet was the corrugated metal culvert that released water from the box-type weir draining the primary area. It was the only submerged inlet.

52. In most cases, the overflow weir was relatively short compared with the basin width, and in all cases except one (Fowl River), it was at the opposite end of the long dimension of the basin from the inlet pipe. In eight tests, the outlet device was a straight weir 100 to 450 ft in length. In three cases, a box-type drop inlet was used.

Flow Rates

53. Inflow rates were inconsistently estimated. In no case was the actual pipeline flow rate measured. Schroeder (1983) estimated the outflow rate for Test 3 by measuring the head on the overflow weir. Montgomery (1978) determined inflow by multiplying the cross-sectional area of the inflow pipe by an estimated velocity, ranging from 12 to 20 ft/sec, and checked these figures by estimating outflow by measuring the head on the overflow weir (Tests 1 and 4). In all three cases, the flow was essentially constant and uninterrupted during tests.

54. Poindexter and Perrier (1980) did not report the basis for their flow estimates. The estimated mean pipeline velocities, calculated from reported flow rates and pipe sizes, varied from 10.5 to 18.5 ft/sec for test durations of 80 to 339 hr. For a dredge to operate uninterrupted for this long is inconceivable. Montgomery (1978) analyzed operation records for two dredges and found that average operation times were 15 to 17 hr/day. Therefore, Poindexter and Perrier's flow rates were recomputed based on pipeline sizes, an average velocity of 15 ft/sec, and 16 hr/day of operation.

55. The flow rate at the North Blakely site (Test 9) was found by using records of dredge operation to determine the percentage of the dye test duration that the dredge was pumping and by assuming a pipeline velocity of 12 ft/sec. This lower value of velocity is reasonable in light of the facts that the pipeline was about 13,000 ft long and there was no booster pump. The flow rate at the Black Rock Harbor test was estimated by measuring the head on the overflow weir. Gallagher and Company (1978) did not report the flow rate at their test at the Yazoo River No. 6 site, but Poindexter and Perrier (1980) reported it as 20.4 ft^3/sec. This was assumed to be correct.

56. The inlet pipes varied in diameter from 4 in. (Black Rock) to 27 in. (North Blakely), but five were 18 in., and two were 16 in. All dredges were floating cutterhead dredges, except at Black Rock Harbor. There, a clamshell dredge filled two barges, and material was pumped from the barge by a submersible pump through a 4-in. flexible hose. The pipe diameters, flow rates, and types of dredged material are tabulated in Table 3.

Table 3

Flow Data for Tests

Test No.	Pipe Diam in.	Flow rate ft^3/sec	Theoretical Residence Time, V/Q,* hr	Duration** hr	Type of Dredged Material
1	18	27.0	52.0	44.4	Fresh water
2	10	6.0	140.0	80.0	Unknown
3	14	16.0	3.5	3.7	Fresh water†
4	18	27.0	9.4	14.0	Fresh water
5	18	18.0	155.0	107.0	Fresh water
6	24	31.0	225.0	339.5	Salt water
7	18	20.0	41.0	44.0	Fresh water
8	18	18.0	164.0	240.0	Fresh water
9	27	30.0	--	37.0	Salt water
11	-	16.0	--	83.0	Salt water
12	4	0.8	37.0	28.2	Salt water
13	16	21.0	13.5	9.0	Salt water

* V/Q = pond volume divided by average flow rate.
** Time elapsed between dye injection and collection of last sample.
† Effluent from a larger DMCA was inflow for this test. This effluent was mixed with polymer flocculant as it flowed into the tested DMCA.

Wind Conditions

57. Wind conditions varied widely at the sites, and wind speed and direction were never determined continuously. Wind data for most of the tests were obtained from nearby weather stations. Varying distances between wind instruments and test sites and differences in measurement height, surrounding terrain, and shielding introduce error when using these wind data.

Spatial variation in wind

58. The likely magnitude of error introduced by using wind data collected some distance from the test site was investigated for the DMCA tests conducted along the Yazoo River (Tests 1, 4, 5, and 8). Wind measurements at 3-hr intervals were obtained from weather stations at Greenwood and Jackson, Miss., roughly 40 miles north and 100 miles southeast of the test sites,

respectively. Wind speeds exhibited a modest positive correlation (r^2 = 0.252), but wind directions did not (r^2 = 0.028). Scatter plots showed definite associations of both speed and direction at the two stations, but correlations were influenced by extreme outliers. The Greenwood measurements were used to calculate the average windspeeds used in the analysis below. Also, wind data in Figures 12, 15, 16, and 19 are from Greenwood. Slade (1968) noted that wind measurements at adjacent stations in flat terrain show high levels of association, but spatial variation is much greater in rugged terrain.

59. Analysis of wind speed and direction data was hampered by a lack of data regarding test starting times. No dates were found for Test 7, and dates but not times were found for Tests 1, 4, 5, 6, and 7. A summary of wind data is in Table 4. Most of the wind statistics in Table 4 are based on observations at 3-hr intervals. When exact test starting times were unavailable, reasonable times were assumed. Resultant wind directions (the direction from which the wind blows) were determined by summing the wind vectors measured at 3-hr intervals. Observations at 3-hr intervals were not available for any locations in close proximity to Test 3.

60. Surface drift velocities were computed at 3-hr intervals using the method described by Gallagher and Company (1978). Gallagher and Company (1978) gave equations for surface drift velocity as a function of wind speed and eddy viscosity. A power function was fitted to Kaurashev's data (1960, in Gallagher and Company 1978) to express eddy viscosity as a function of depth. When constants are combined, the formula for drift velocity becomes:

$$V_S = 0.00925\ V_w^2\ d^{-0.34} \tag{6}$$

where

V_S = surface drift velocity, ft/sec
V_w = windspeed, mph
d = mean depth, ft

Mean surface drift velocities are shown in Table 4. Arithmetic means of drift velocities were used for analysis of wind effects instead of vector sums, because wind tends to act on DMCAs more as a mixing agent than as a transporting agent. An exception would be a strong wind blowing toward the weir of a small, shallow area, causing an early release of dye at high concentrations

Table 4

Wind Data for Dye Tracer Tests

Test No.	Average Speed mph	Standard Deviation mph	Resultant Direction* Degrees Counter-clockwise from Site Axis	Standard Deviation of Wind Direction Degrees	Source of Data	Average Surface Drift Velocity, ft/sec
1	12	5	120	40	NWS,† Greenwood, Miss.	0.6
2	5	3	45	130	NWS, Fort Eustis, Va.	0.3
3	12	-	330	-	Schroeder, p.c.††	1.0
4	10	5	165	70	NWS, Greenwood, Miss.	0.9
5	6	3	120	70	NWS, Greenwood, Miss.	0.2
6	7**	4	95	90	NWS, Mobile, Ala	0.3
7	"Calm"	-	-	-	Gallagher and Co. (1978)	0.0
8	5	4	355	130	NWS, Greenwood, Miss.	0.2
9	6**	3	165	110	NWS, Mobile, Ala.	-
11	14	7	125	130	Craney Island, Va.	-
12	11	4	175	100	NWS, Bridgeport, Conn.	0.7
13	9	3	90	50	NWS, Mobile, Ala.	0.7

* Vector sum of wind measurements. Directions from which the wind blows, measured counterclockwise from site axis. Inflow point is roughly at 180° and outflow is at 0°.

** Storms and frequent gusting winds.

† NWS = National Weather Service.

†† p.c. = personal communication.

(Test 3 and 12). As Figures 12 through 23 show, many of the tests experienced diurnal cycling of wind direction typical of coastal areas. Resultant wind velocity for these tests is quite small, but wind mixing is important.

61. Wind conditions varied widely, with average velocities ranging from 0 to 14 mph. Most resultant wind directions tended to be between 90 and 180 deg relative to the site axes. Temporal variations of wind speeds and directions are depicted graphically in Figures 12 through 23.

Dye Tests

62. In each test, a 20-percent solution (by weight) Rhodamine WT fluorescent dye in water was used as a tracer. In all cases, the dye was added to the inflow essentially instantaneously at the point where the discharge from the dredge pipeline entered the basin. The amounts used ranged between 1 and 15 gal, but was usually about 10 gal.

63. The dye concentration at the overflow weir was sometimes measured by pumping water continuously through either a Turner Model III or series 10-005 fluorometer, and sometimes by taking grab samples at irregular intervals and measuring the dye concentration in a fluorometer at the site or in the lab later. In one case (Test 12, Black Rock Harbor), both lab and field measurements were made. Results were reported in units of either relative dye concentration (fluorometer reading or deflection) or absolute dye concentration (ppb). The raw data are presented in digital form in Appendix C.

64. The duration of the tests ranged from 4 to 329 hr, but most were between 30 and 100 hr. Test durations were usually between one and two times the estimated theoretical volumetric detention time. In general, test durations were not sufficiently long enough to observe decay of fluorescence to background or near-background levels.

Effects of sample handling and dye type

65. The effects of different sample handling procedures and the use of different dyes were tested by running replicate experiments at the Black Rock Harbor site (Test 12). Two fluorescent dyes, Rhodamine WT and Lissamine FF, were simultaneously added at the inlet. Samples collected at the outlet weir were split into three portions: the first was immediately tested for Rhodamine fluorescence, and the other two were returned to the laboratory. These second and third portions of each sample were tested in the laboratory several

weeks after collection for Rhodamine and Lissamine fluorescence, respectively. The same Turner Series 10-005 fluorometer was used in the laboratory as in the field. Fluorescence levels were read in the laboratory before and after vigorous shaking (2 to 3 sec) to determine the effect of resuspension of fine particles on fluorescence.

PART IV: DATA ANALYSIS AND RESULTS

Overview

66. This part contains a description of the procedures that were used to process and reduce the residence time distribution field data collected as described in Part III. Results of the experiment conducted at the Black Rock site to determine the effects of dye type and sample handling are reported first. The remainder of the data analysis had as its objective derivation of a method for predicting hydraulic efficiency based on design variables such as site geometry, discharge, and expected or "worst-case" wind conditions. Briefly, the steps followed were:

a. Most of the dye curves were incomplete because measurement of dye concentration was not continued long enough for return to background levels to be observed. The missing decay limbs or "tails" of the dye curves were estimated by fitting the measured dye concentration values to a log-normal distribution curve using least-squares best-fit regression. The best-fit functions were then used to predict the decay limbs.

b. Next, the extrapolated curves were used to calculate numerical descriptors such as mean residence times, hydraulic efficiencies, and dispersion indices.

c. A matrix of correlation coefficients was computed for the numerical curve descriptors.

d. The mean residence time, hydraulic efficiency, and dispersion index were used as dependent variables in regression analyses with site geometry, flow rate, and wind conditions as independent variables. Coefficients were computed for regression functions based on both dimensional variables and dimensionless groups of variables.

e. The values of mean residence time, hydraulic efficiency, and dispersion index computed using the regression equations were compared with observed values. Hydraulic efficiencies and dispersion indices for hypothetical but reasonable site conditions were computed using the regression equations and were evaluated.

f. A simplified predictive equation for hydraulic efficiency as a function of only L/W was fit to a data set that included the DWCS data as well as published data for chlorine contact chambers, wastewater lagoons, and a physical model.

Effects of Sample Handling and Dye Type

67. Results of the experiments of effects of dye type and sample handling are shown in Table 5 and Figure 24. The Lissamine curves produced mean residence times and dispersion indices that were roughly 50 percent larger than for Rhodamine. The decay limbs of the Lissamine curves had more gradual slopes, suggesting that the Lissamine did not degrade under the influence of conditions in the DMCA as quickly as Rhodamine. Shaking the samples had insignificant, though observable, effects on $\bar{t}$ and the dispersion index. Differences between the field and lab curves were also slight and appear to be mainly because of a higher peak concentration measured in the lab.

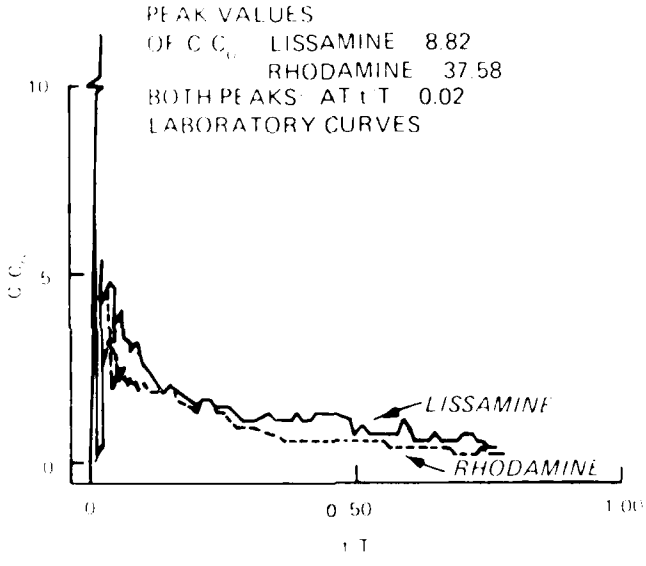

Figure 24. Residence time distributions measured simultaneously using two different tracer dyes

Extrapolation of Incomplete Curves

68. The 12 dye tracer curves were classified as either complete or incomplete (Table 6). Complete curves were those that had decay limbs that terminated in a mild fluctuation about the background concentration. Background concentrations were determined based on the initial readings immediately after dye addition, but prior to initiation of the rising limb. Ideally, background levels would have been based on a period of monitoring

Table 5

Effect of Dye Type and Sample Handling, Test 12

	$\bar{t}$ hr	Background ppb	Maximum Concentration ppb	t_{50}, hr	Dispersion Index
Rhodamine WT					
Field*	8.0	0.05	53.45	5.5	0.82
Lab-unshaken	7.0	0.10	199.90	4.5	0.99
shaken	6.9	0.10	179.90	4.4	1.01
Lissamine					
Lab-unshaken	10.6	20.0	96.00	9.2	0.53
shaken	11.0	19.0	83.00	10.3	0.52

* This curve was used in the analysis described in Table 6 because all other tests were run with Rhodamine.

Table 6

Dye Curve Analysis

Test No.	Complete or Incomplete	Background Conc.	Regression Coefficients b_1	b_2	b_3	Coefficients of Determination r^2
1	I	1.0	-0.55	2.8	-0.06	0.90
2	I	12.0	-0.88	5.1	-3.0	0.83
3	I	0.1	-0.83	6.5	-11.3	0.59
4	I	1.0	-1.6	4.6	0.50	0.85
5	I	15.0	-0.19	1.0	2.8	0.54
6	C	1.5	-0.49	3.4	-2.5	0.84
7	I	1.0	-0.57	3.4	-2.5	0.85
8	I	7.5	-0.16	1.2	1.1	0.63
9	C	1.0	0.27	-2.8	7.8	0.59
11	I	0.04	-4.5	32.0	-53.5	0.59
12	C	0.05	-0.26	0.30	1.8	0.58
13	I	4.0	-5.1	19.0	-13.3	0.74

prior to dye addition, but such measurements, if any were made, were not reported. Furthermore, dye concentrations were variously reported either as relative concentrations (fluorometer scale readings) or in absolute concentrations (ppb of dye), thus complicating selection of reasonable values for background.

69. Most curves were incomplete. However, since they exhibited overall shapes similar to the log-normal distribution, log-normal curves were fitted to the measured points using a regression approach. The log-normal distribution function is given by

$$C = \frac{1}{\sqrt{2\pi}\,\sigma t} \exp\left\{\frac{-1}{2\sigma^2}\,[\ln(t) - \mu]^2\right\} \qquad (7)$$

where C is dye concentration and t is time. If μ and σ are taken as constants, this expression reduces to

$$\ln(C) = b_1\,[\ln(t)]^2 + b_2\,\ln(t) + b_3 \qquad (8)$$

which is a quadratic equation for $\ln(C)$ in terms of $\ln(t)$. Values for the coefficients b_1, b_2, and b_3 were obtained using a multiple linear regression program with $\ln(t)$ and $[\ln(t)]^2$ as the independent variables and $\ln(C)$ as the dependent variable. Resultant values of the coefficients b_1, b_2, and b_3 and associated coefficients of determination r^2 are shown in Table 6. Coefficients were determined for complete as well as incomplete curves for purposes of comparison. Fitted curves and measured points are shown in Figure 25. The fitted curves tended to give rather poor fits to the measured peak dye concentrations, but extremely good fits to the decay limbs; thus, the primary objective was met. The regression coefficients were used to estimate missing values for decay limbs of incomplete curves. Curves were extended either to background concentration or three times the theoretical residence time, whichever occurred first. The dye curves shown in Figures 12 through 23 include estimated values for incomplete curves. Values of C_o used to normalize dye concentrations for Figures 12 through 23 were computed using the estimated missing values.

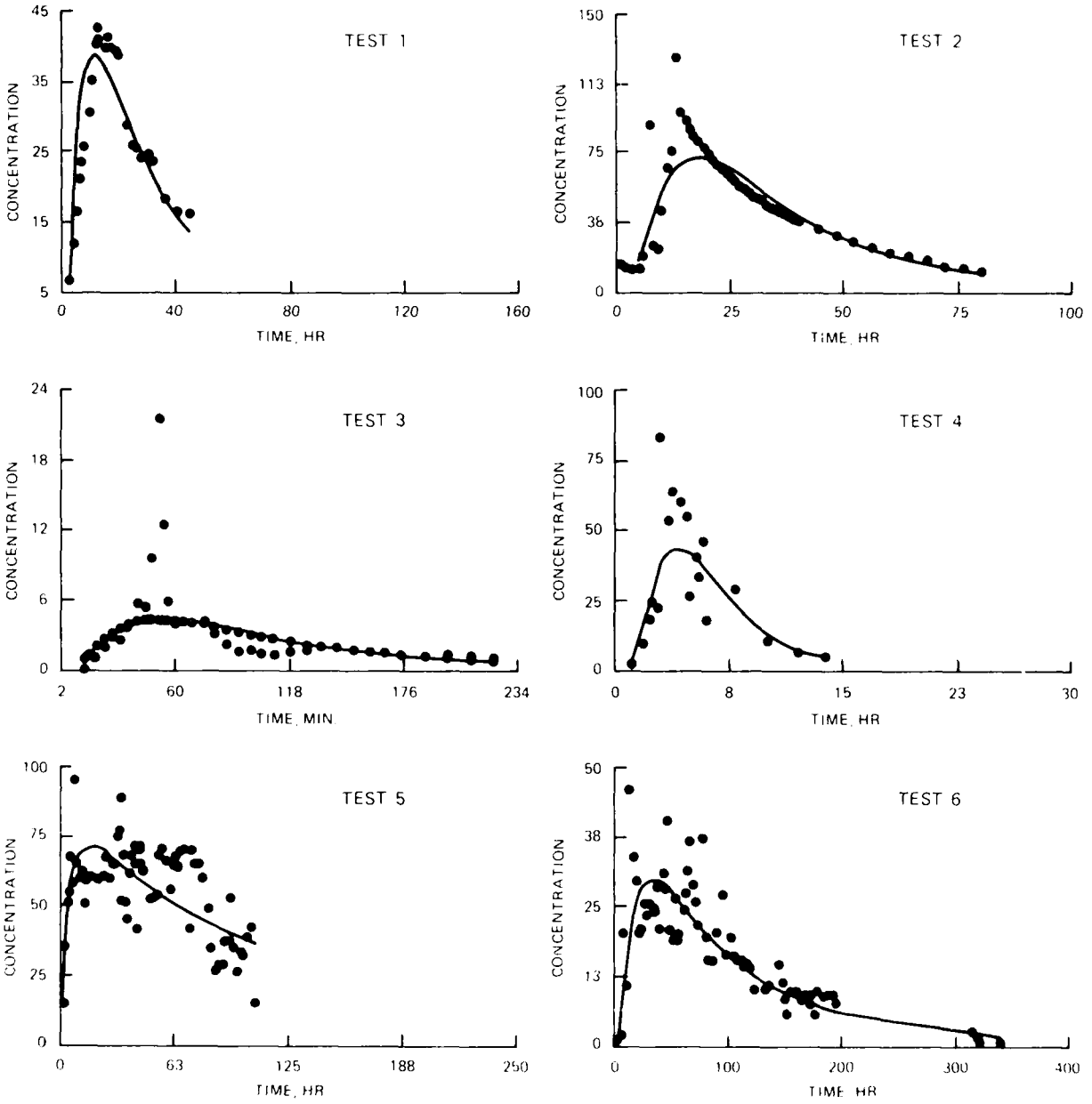

Figure 25. Observed and log-normal best-fit dye tracer curves. Solid dots are field measurements. Smooth curves are plots of Equation 8 with coefficients from Table 6 (Tests 1 through 6) (Continued)

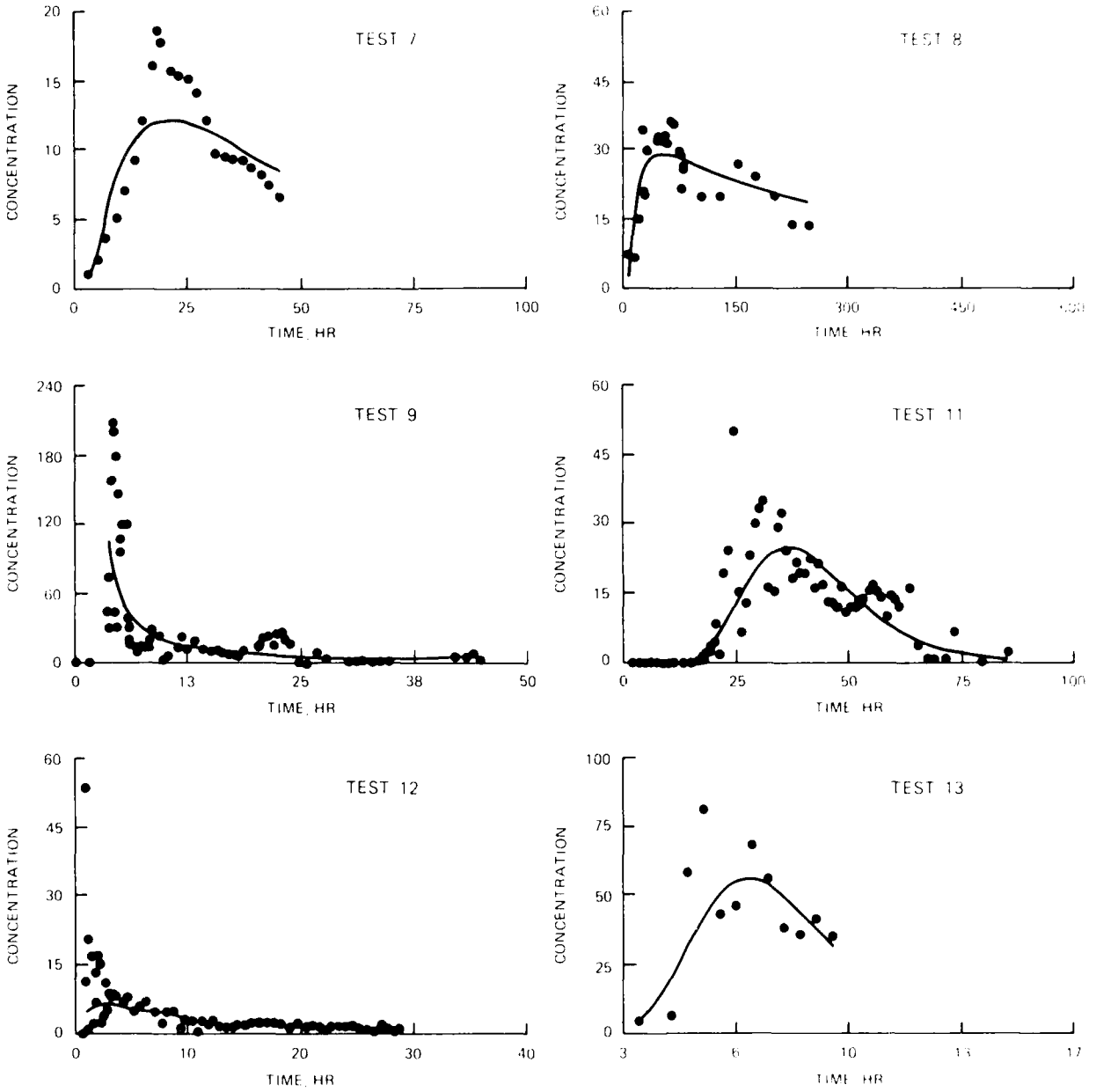

Figure 25. (Tests 7 through 13) (Concluded)

Numerical Description of Dye Curves

Computation of descriptors

70. The dye tracer curves provide representative residence time distributions from the tested DMCAs. In order to quantitatively describe these distributions, the measured times and concentrations and the estimated values for missing portions of incomplete curves were entered as input to DYECON, a dye concentration analysis routine of the Automated Dredging and Disposal Alternatives Management System (ADDAMS) computer program (Hayes et al. 1985). DYECON computed the following numerical descriptors for each curve:

Mean time	= mean residence time (Equation 2)
Hydraulic efficiency	= mean residence time divided by the theoretical residence time × 100%
Minimum time	= the time at which the first dye reading above background is recorded
Modal time	= the time at which the maximum observed dye reading is recorded
t_{10}, t_{50}, t_{90}	= the time at which the 10, 50, and 90 percentiles of the area beneath the dye curve occur, respectively
Morrill index	= t_{90}/t_{10}
Dispersion index	= dispersion variance as computed by Equation 4

DYECON also provides a variety of plot options. Full documentation for the DYECON program is found in Hayes et al. (1985).

71. Results of the DYECON runs are in Table 7. Computed mean residence times ranged from 2 to 100 hr, hydraulic efficiencies from 19 to 105 percent, and dispersion indices from 0.03 to 0.60. Hydraulic efficiency was not computed for Tests 9 and 11 because pond volume (and thus T) was unknown. The two impossibly high values for hydraulic efficiency (Tests 7 and 8, Table 7) were both associated with curves with extremely jagged profiles and no definite peak. Although practically impossible, these two values were retained and used in subsequent analysis for the sake of consistency. Marske and Boyle (1973) also reported a value of hydraulic efficiency in excess of 100 percent.

72. The extremely low value of efficiency for Test 2 is also suspect. Estimates of site volume and average flow rate are tenuous for this test, and

Table 7

Numerical Curve Descriptors

Test No.	Mean Time hr	Hydraulic Efficiency %	Minimum Time hr	Modal Time hr	t_{90} hr	Median Time hr	t_{10} hr	Morrill Index	Dispersion Index
1	37.7	72.8	2.0	12.2	81.0	28.4	9.72	8.3	0.60
2	26.9	19.4	1.0	13.0	49.4	23.1	11.51	4.3	0.30
3	1.7	49.2	0.23	0.9	3.6	1.2	0.7	5.53	0.51
4	5.9	62.7	1.1	3.0	10.03	4.93	2.91	3.5	0.27
5	76.2	49.2	2.0	8.0	168.1	61.4	14.0	12.01	0.60
6	100.0	44.4	4.0	12.0	218.1	80.0	19.4	11.3	0.55
7	42.5	103.0	4.0	17.0	85.4	34.0	15.0	5.91	0.42
8	172.0	105.0	14.0	28.0	383.0	143.0	32.0	12.0	0.55
9	9.8	--	3.8	4.4	22.2	5.7	4.0	5.6	0.55
11	40.9	--	2.0	23.0	60.9	38.0	23.1	2.64	0.14
12	8.0	22.0	0.33	0.33	19.6	5.5	0.7	29.2	0.82
13	7.0	51.4	4.0	5.0	9.7	6.7	4.7	2.1	0.08
means	44.0	57.9	3.2	10.5	92.5	35.8	11.4	8.5	0.45

the normalized dye curve has a shape that is somewhat atypical relative to the others (Figures 12 to 23).

Comparison of descriptors

73. Relationships among dimensionless forms of the various curve descriptors (i.e., $\bar{t}/T$, t_i/T , t_m/T , etc.) were investigated by computing a matrix of linear correlation coefficients (Table 8). All of the curve descriptors except t_{min}/T , the Morrill index, and the dispersion index were strongly and positively correlated with $\bar{t}/T$. The Morrill index was strongly and positively correlated with the dispersion index. Additional analysis was therefore focused on $\bar{t}$, $\bar{t}/T$, and the dispersion index. Marske and Boyle (1973) recommended use of the dispersion index because it has the highest potential for statistical reliability.

Table 8

Correlation Coefficients r for Numerical Curve Descriptors

	$\frac{\bar{t}}{T}$	$\frac{t_{min}}{T}$	$\frac{t_{modal}}{T}$	$\frac{t_{50}}{T}$	$\frac{t_{90}}{T}$	$\frac{t_{10}}{T}$	Morrill Index	Dispersion Index
$\bar{t}/T$	1.00							
t_{min}/T	0.21	1.00						
t_{modal}/T	0.58	0.72	1.00					
t_{50}/T	0.99	0.32	0.61	1.00				
t_{90}/T	0.97	-0.00	0.39	0.93	1.00			
t_{10}/T	0.63	0.77	0.98	0.68	0.43	1.00		
Morrill index	-0.28	-0.54	-0.69	-0.32	-0.12	-0.68	1.00	
Dispersion index	-0.06	-0.81	-0.66	-0.18	0.15	-0.70	0.84	1.00

Dimensional Variables

74. In order to generate a predictive relationship for use in DMCA design, an effort was made to study the relationship of mean residence time to site conditions. The mean residence time of water in a DMCA is a function of geometry, surface drift velocity (produced by wind shear), the wind direction, and the mean advective flow velocity $\bar{Q}/WD$. Algebraically,

$$\bar{t} = f(L,W,D,V_{adv}, V_s, \cos \theta) \quad (9)$$

where

$\bar{t}$ = mean residence time, hr

L,W,D = average site dimensions, ft

V_{adv} = mean advective flow velocity, $\bar{Q}/WD$, ft/sec

$\bar{Q}$ = average flow rate through the DMCA during the dye test of period of interest

V_s = surface drift velocity (Equation 6), ft/sec

$\cos \theta$ = cosine of the angle between the site axis and the resultant wind direction

For wind blowing directly from the inlet to the outlet $\theta = 0$, and for wind blowing directly from outlet to inlet $\theta = 180$. θ is measured in a

counterclockwise direction from the site axis (a line from inflow to outlet) to the direction from which the wind blows.

75. A correlation matrix was computed for log-transformed values of the variables $\bar{t}$, d, L, W, D, V_{adv}, V_s, and cos θ from the 10 dye tracer tests for which theoretical residence times were available (Table 9). The value of zero for V_s for Test 8 was transformed by assigning a value of 0.01 to it before transformation. Cos θ was transformed by using the function:

$$\text{Transform } \cos\theta = \text{sgn}(\cos\theta) * \left\{\log\ [\text{abs}(\cos\theta) + .01]\right\} \qquad (10)$$

because θ of 90° and 270° should have the same effect on residence time distribution.

Table 9

Correlation Coefficients r for Log-Transformed Dimensional Variables

	Log($\bar{t}$)	Log(L)	Log(W)	Log(D)	Log(V_s)	Log(cos θ)	Log(V_{adv})
Log($\bar{t}$)	1.00						
Log(L)	-0.002	1.00					
Log(W)	-0.10	0.94	1.00				
Log(D)	0.60	0.59	0.50	1.00			
Log(V_s)	-0.08	-0.15	-0.20	-0.37	1.00		
Log(cos θ)	0.10	0.04	-0.10	-0.05	-0.19	1.00	
Log(V_{adv})	-0.54	-0.20	-0.32	-0.55	0.16	0.09	1.00

76. The set of independent variables was then edited to eliminate redundant or collinear combinations (r greater than or equal to 0.5). The resultant set of transformed, uncorrelated, independent variables (W, V_{adv}, V_s, cos θ) was input to a stepwise regression procedure (Hunt and Delagran 1984), and regression coefficients were calculated for mean residence time as a function of the independent variables. The resultant equation is:

$$\bar{t} = 0.00019\ W^{1.4} V_{adv}^{-0.64} \qquad r^2 = 0.87 \qquad (11)$$

When the Test 2 data were left out, the equation became:

$$\bar{t} = 0.00014\ W^{1.4} V_{adv}^{-0.69} \qquad r^2 = 0.90 \tag{12}$$

Figure 26 shows the observed values of $\bar{t}$ plotted against values predicted by Equation 12. The difference between observed and predicted values is greater for larger areas with higher observed values of $\bar{t}$. Large residual errors for Tests 6 and 8 may be due to inaccurate extrapolation of dye curve decay limbs.

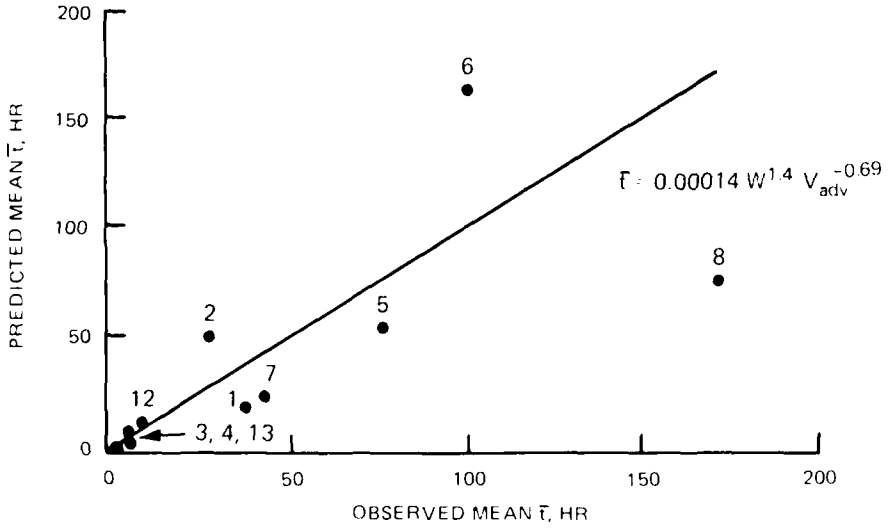

Figure 26. Observed values of $\bar{t}$ for DMCAs versus values predicted by Equation 12

Nondimensional Variables

77. If experimental data are placed in dimensionless form by combining the variables in groups, the numerical results will be independent of the system of units of measurement used. Results of such analysis may be more generally applicable to situations not included in the original data set. Accordingly, the set of independent variables listed in the paragraph above may be reduced to a group of dimensionless terms:

$$d \text{ or } \bar{t}/T = f(L/W,\ L/D,\ V_s/V_{adv},\ \cos\ \cdot) \tag{13}$$

A correlation matrix for log transforms of these variables (Table 10) revealed little collinearity. Nonpositive values were log-transformed as before. Stepwise regression was again used to calculate regression coefficients with the results:

$$\bar{t}/T = 0.29\left(V_s/V_{adv}\right)^{-0.11}\left(L/W\right)^{0.94} \qquad r^2 = 0.53 \tag{14}$$

and dispersion index:

$$d = 7.1\left(L/D\right)^{-0.51} \qquad r^2 = 0.26 \tag{15}$$

When the Test 2 data were omitted, stepwise regression yielded:

$$\bar{t}/T = 0.087\left(L/W\right)^{0.81}\left(L/D\right)^{0.25}\left(V_s/V_{adv}\right)^{-0.093} \qquad r^2 = 0.84 \tag{16}$$

and

$$d = 7.8\left(L/D\right)^{-0.53} \qquad r^2 = 0.24 \tag{17}$$

Table 10

Correlation Coefficients r for Log-Transformed Dimensionless Variables

	Log					
Field	Dispersion Index	$\bar{t}/T$	L/W	L/D	V_s/V_{adv}	cos θ
Log(dispersion index)	1.00					
Log($\bar{t}/T$)	-0.02	1.00				
Log(L/W)	0.29	0.48	1.00			
Log(L/D)	-0.51	0.12	0.29	1.00		
Log(V_s/V_{adv})	0.13	-0.55	-0.02	-0.04	1.00	
Log(cos θ)	0.10	0.05	0.35	0.09	-0.22	1.00

78. Predicted and observed values of $\bar{t}/T$ and the dispersion index are plotted in Figures 27 and 28. Table 11 shows observed and predicted values for Equations 12, 16, and 17. Figure 27 shows that Equation 16 predicted $\bar{t}/T$ reasonably well for all tests except 2 and 8. Once again, the extrapolation

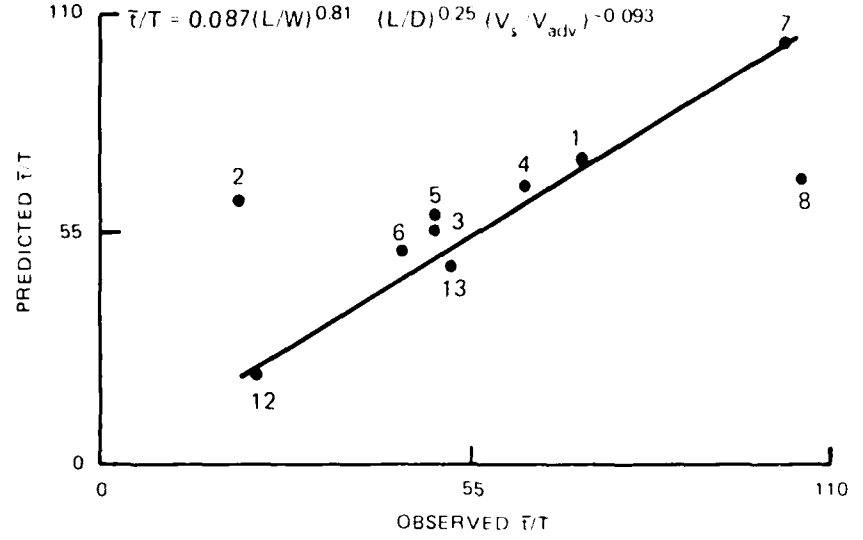

Figure 27. Observed values of $\tilde{t}$ for DMCAs versus values predicted by Equation 16

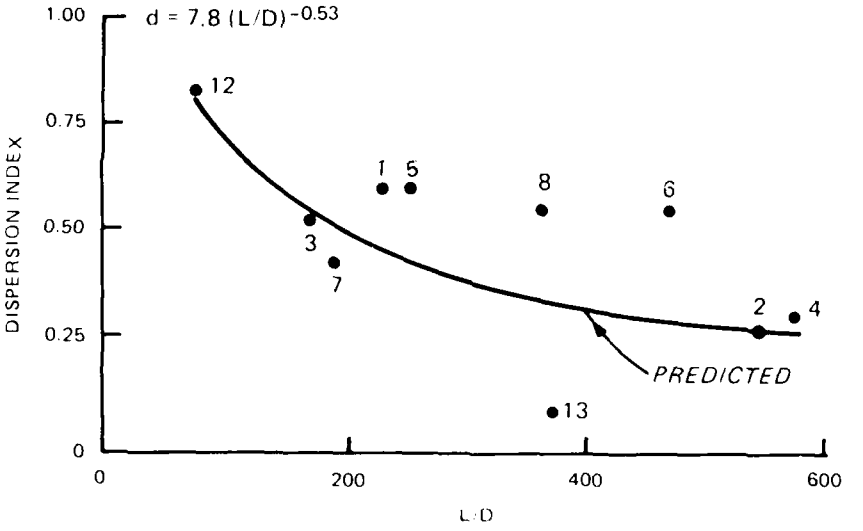

Figure 28. Observed and predicted dispersion index for DMCAs as a function of length-depth ratio L/D (predicted curve from Equation 17)

procedure may be the source of error. Equation 17 exhibited poor fit to the observed dispersion indices, with best fits for the smaller DMCAs.

Table 11

Observed and Predicted Values

Test	Obs $\bar{t}$ hr	Pred $\bar{t}$* hr	Obs $\bar{t}/T$ %	Pred $\bar{t}/T$** %	Obs d	Pred† d
1	38.0	17.0	73	74	0.60	0.44
2	27.0	49.0	19	66	0.30	0.27
3	1.7	1.3	49	62	0.51	0.52
4	5.9	6.8	63	70	0.27	0.28
5	76.0	54.0	49	64	0.60	0.42
6	100.0	163.0	44	53	0.55	0.30
7	43.0	22.0	103	103	0.42	0.49
8	172.0	75.0	105	73	0.55	0.34
9	9.8	--	--	--	0.55	--
11	41.0	--	--	--	0.14	--
12	8.0	11.0	22	21	0.82	0.83
13	7.0	8.5	51	49	0.08	0.34

* Equation 12.
** Equation 16.
† Equation 17.

Discussion of Results

Reproducibility of dye tests

79. The observed data exhibit considerable scatter about values predicted by Equations 12, 16, and 17 (Figures 26 through 28 and Table 11). Mangelson and Watters (1972) observed experimental absolute errors of about 10 percent in hydraulic efficiency while working with an indoor model basin 40 ft long by 20 ft wide by 3.5 ft deep. There was no wind, and sources of error were more tightly controlled than for any of the DMCA field tests. Conversely, Marske and Boyle (1973) reported that the results of dye tests in chlorine contact chambers were not sensitive to experimental procedure, and "When the dye test was repeated on the same basin under identical flow conditions, the results were essentially identical." Eight of the predicted values of $\bar{t}/T$ are within 0.13 of the observed value, with two predictions (Tests 3

and 8) exhibiting much larger errors (0.46 and 0.34, respectively). Sources of error for the DMCA tests include incomplete data for decay limbs, the aforementioned variation in methods for determining mean depth, inaccurate estimate of mean flow rates, unsteady flows, and errors introduced by using wind data collected some distance away from the test site.

Predictions for extreme conditions

80. Although Equations 12 and 16 provide reasonably good fit to most of the observed values, they do not provide realistic values when values of independent variables outside the observed range are used. Although Equation 12 does indicate that mean residence time becomes infinite as Q approaches zero, it also implies that mean residence time is completely independent of basin length, which is intuitively false. Equation 16 gives impossibly large hydraulic efficiencies when even fairly modest values of L/W or small values of D/W are input. Hydraulic efficiency becomes infinite when wind speed and thus V_s are zero.

81. Since Equation 16 is based on dimensionless variables, predictions from it can be compared with data from other studies. Unfortunately, published results were found for only two other similar investigations: a study of chlorine contact chambers by Marske and Boyle (1973) and a study of model and prototype waste stabilization ponds by Mangelson and Watters (1972). Marske and Boyle include wind and depth observations for only two of their tests. Most of Mangelson and Watters's data were from an indoor model pond with no wind. Although they did note the presence of wind effects for their prototype tests, they did not record wind speeds.

82. Marske and Boyle (1973) reported values of hydraulic efficiency of 83 and 84 percent for tests run in a basin 336 ft long by 16 ft wide by 3 ft deep. Details of the two tests were virtually identical except for wind direction. Wind was 20 mph directly downstream in the first test and 20 mph directly upstream for the second. Equation 16 predicts a hydraulic efficiency of 280 percent. The ratios L/W and D/W were both an order of magnitude greater for these tests than for the tests on DMCAs, and the ratio V_s/V_{adv} was smaller than for all DMCA tests except the one with zero wind speed (Test 7). It therefore appears that Equation 13 is not generally applicable outside the range of conditions encountered in the DMCA tests, even though it is based on dimensionless variables.

83. Equation 12 is heavily influenced by width and is insensitive to changes in wind speed. Use of Equation 12 to estimate the effects of adding spur dikes is particularly misleading because length-width ratio is not included in any form. Similarly, Equation 16 gives unreasonable values for hydraulic efficiency when length-width ratios exceed maximum observed values (3 to 4).

84. In summary, the regression Equations 12 and 16 give unreasonable values where used outside the observed ranges of the independent variables. However, they do highlight the influence of L/W on DMCA mean residence time and hydraulic efficiency. (In Equation 12, note that $V_{adv} = Q/WD$.) They also highlight the lack of influence exerted by other variables such as wind speed and direction on hydraulic efficiency. Less definitive results were obtained for the dispersion index.

Relative Effects of Site Condition Variables

Effect of length-width ratio

85. Regression equations based on only DMCA data fail to adequately describe effects of changing L/W on hydraulic efficiency because the observed range of L/W was so small. The model study by Mangelson and Watters (1972) and the chlorine contact chamber study by Marske and Boyle (1973) made measurements of $\bar{t}/T$ over a much wider range of L/W. Both sets of investigators found a direct relationship between L/W and hydraulic efficiency. Marske and Boyle (1973) recommended use of $L/W = 40$ for design of chlorine contact chambers. Using regression equations based on their data, they predicted a hydraulic efficiency of 81 ± 24 percent and a dispersion index of 0.02 for such a basin.*

86. Figure 29 shows all of the available data for the effect of L/W on hydraulic efficiency. Data from DMCAs, chlorine contact chambers, wastewater lagoons, and the physical model described previously are included. Regression coefficients were calculated using these data for the following equation:

---

* The dispersion index was estimated from a plot of d vs. L/W. Hydraulic efficiency was predicted using a regression equation with d as the independent variable and $\bar{t}/T$ as the dependent variable.

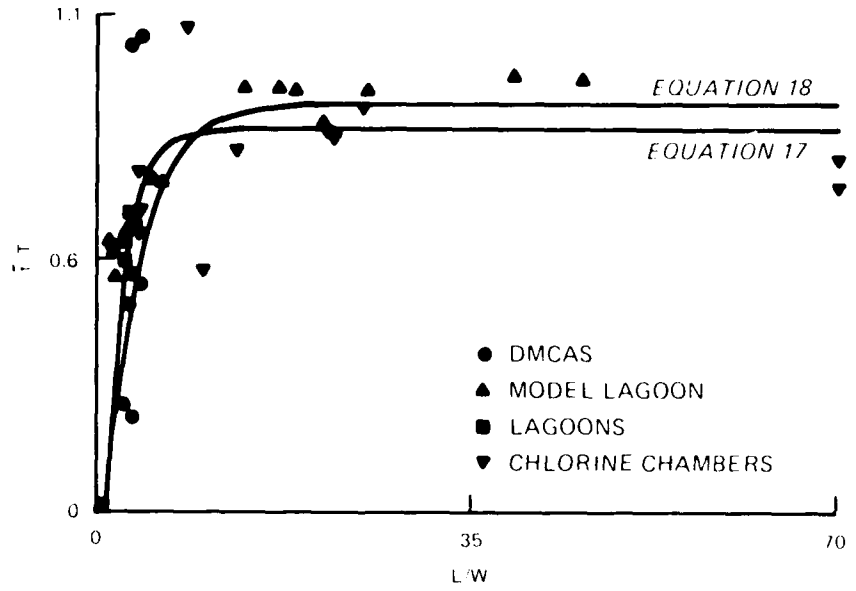

Figure 29. Hydraulic efficiency as a function of length-width ratio

$$\bar{t}/T = 0.84\left[1 - \exp\left(-0.59\ L/W\right)\right] \quad (n = 38,\ r^2 = 0.80) \qquad (18)$$

Mangelson and Watters (1972) reported results for 24 physical model experiments with $L/W = 2.0$. Hydraulic efficiencies for these experiments were averaged to a single point ($t/T = 0.605$, standard deviation = 0.06) prior to use in the regression analysis. The regression Equation 18 is plotted in Figure 29. Also shown in Figure 29 is a plot of the equation:

$$\bar{t}/T = 0.9\left[1 - \exp\left(-0.3\ L/W\right)\right] \quad (n = 7,\ r^2 = 0.61) \qquad (19)$$

Equation 19 is based only on DMCA data with hydraulic efficiencies between 25 and 100 percent and is more appropriate than Equation 18 for DMCA design. Equation 18 is heavily influenced by the laboratory model and chlorine contact chamber tests, which had much more ideal inlet-outlet conditions, usually no wind, and more uniform geometries than the typical DMCA.

Effect of depth-width ratio

87. Mangelson and Watters (1972) found only a weak inverse relationship between D/W and hydraulic efficiency, while Marske and Boyle (1973) did not comment on the effects of depth. If all other variables (L, W, Q, and wind speed) are held constant, Equations 12 and 16 imply that hydraulic efficiency

is proportional to the -0.3 and -0.25 power of depth, respectively. This confirms the findings of Mangelson and Watters (1972). In other words, increases in depth for a given width tend to increase the fraction of volume in dead zones.

88. On the other hand, depths that are too shallow can degrade DMCA performance. Montgomery (1978) suggests 2 ft as a minimum DMCA ponding depth and attributes some observed DMCA short-circuiting to inadequate ponding depths. Walski and Schroeder (1978) present a design procedure for DMCA outlet weirs that links effluent quality, weir length, and ponding depth. Therefore, DMCA depths should generally be 2 to 8 ft.

Effect of wind speed and direction

89. In Gallagher and Company (1978), the results of two DMCA dye tests in the same DMCA indicated that a 10- to 15-mph wind toward the weir reduced t_p/T by 0.13 relative to a no-wind condition. However, the dye "curve" for the wind test was only two points. Marske and Boyle (1973) concluded that wind effects on performance of a basin with $L/W = 21$ were relatively unimportant based on the results described above. Although the 20-mph wind toward the weir resulted in a reduction of dimensionless initial time t_i/T of 0.18 relative to a test with 20-mph wind away from the weir, the other dye curve descriptors were unchanged. Conversely, Mangelson and Watters (1972) noted that simultaneous dye tests in two adjacent waste stabilization ponds, with one oriented transverse and the other parallel to the wind produced significantly different results. The pond parallel to the wind (wind blowing from inlet to outlet) experienced "serious short-circuiting." Quantitative results were not reported. Data for the DMCAs were insensitive to wind direction, although the high, early spikes in curves for Tests 3 and 12 are doubtless the result of wind blowing across relatively small areas toward the weir. Equation 16 indicates that hydraulic efficiency is proportional to wind speed to the -0.2 power. Based on the above evidence, it seems that wind effects on hydraulic efficiency are slight, but wind effects on the overall residence time distribution are presently uncertain, but probably significant.

Effect of inlet and outlet configuration

90. Mangelson and Watters (1972) found model pond performance most efficient when vertical or horizontal diffusers placed at perimeter locations were used to distribute inflow. Most changes in $\bar{t}/T$ resulting from changes in inlet and/or outlet configurations were 0.1 or less, although the

configuration most similar to a typical rectangular DMCA had the lowest value of $\bar{t}/T$ (0.456), and one configuration using a long diffuser for inflow had $\bar{t}/T = 0.672$. Marske and Boyle (1973) demonstrated that a sharp-crested weir is superior to a Cipolleti weir and recommended minimization of weir overflow rates for greater hydraulic efficiency. The DMCA data base did not contain sufficient data to adequately compare the effects of various types of inlets and outlets. Walski and Schroeder (1978) present guidance for the design of DMCA weirs based on typical solids concentration profiles and weir withdrawal zones.

PART V: DESIGN GUIDANCE

Introduction

91. Residence time distribution is an important consideration in the design of most DMCAs. All but the largest and most permanent DMCAs experience periods when residence time distribution is critical to effluent quality, usually near the end of filling, when DMCA pond volume and surface area are least. If a DMCA is sized large enough to provide adequate effluent quality even when hydraulic efficiency is low and dispersion is high, consideration of residence time distribution in design is not necessary. However, such a DMCA design is economically inefficient with regard to effluent quality constraints on size. As shown in Part I, improving hydraulic efficiency from 40 to 60 percent reduces the required ponded volume by 33 percent.

92. Plug flow represents the ideal residence DMCA time distribution. Although this ideal is not achievable in practice, low dispersion indices and high hydraulic efficiency should be the designer's goal. Design decisions generally determine residence time distribution; operational actions to improve effluent quality such as reducing flow rates or increasing ponding depth are often infeasible because of other constraints.

Determining Residence Time Distributions for Existing DMCAs

93. The residence time distribution of an existing DMCA may be determined by performing a dye tracer test during disposal operations with flow rates, wind conditions, ponding depths, and surface areas similar to the conditions of interest. Recommended procedures for dye tracer tests are provided in Appendix B of this report. If the results of such tests indicate inadequate hydraulic efficiency, residence times may be increased by reducing inflow rates or by using the techniques for improving hydraulic efficiency.

94. In the absence of site-specific field data, the hydraulic efficiency of a given site may be estimated using Equation 19 from Part IV.

$$\bar{t}/T = 0.9 \left[1 - \exp\left(-0.3\ L/W\right)\right] \qquad (19)$$

This relationship is plotted in Figure 30 along with the DMCA data. Values of $\bar{t}/T$ from this equation should be rounded to the nearest 0.1. L for use in this equation is the distance from the DMCA inlet to the outlet measured along the center line of the flow, and W is the average width of the flow path.

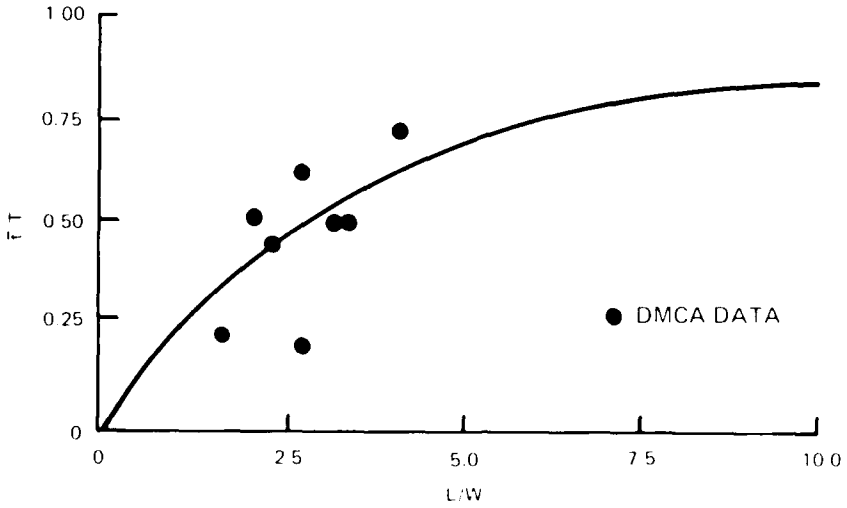

Figure 30. DMCA design curve. Hydraulic efficiency as a function of L/W . Solid curve is Equation 19

95. The hydraulic efficiency correction factor HECF will be the reciprocal of $\bar{t}/T$. If the correction factor is used in additional analysis for the prediction of effluent quality, the engineer should be careful to multiply the HECF by the DMCA pond volume (or surface area for zone settling analysis) likely to exist at the time of interest instead of its initial condition. For example, use of the surface area enclosed by the perimeter dikes could introduce error since DMCA surface area is usually significantly reduced during filling by the formation of deltas or fans of coarse material at the points of inflow.

Predicting Hydraulic Efficiency of Proposed DMCAs

96. Hydraulic efficiency is incorporated into sizing of proposed DMCAs by multiplying the required surface area for effective settling (as determined from lab tests) by the reciprocal of hydraulic efficiency, HECF, if zone settling analysis is employed, or by multiplying the required residence time by the HECF if flocculent settling analysis is used. Dredged material will normally exhibit zone settling, and that type

where saltwater sediments are to be dredged. A detailed description is given by Palermo, Montgomery, and Poindexter (1978). The flocculent settling analysis is normally used for design of DMCAs to receive freshwater sediments with significant clay fraction and for situations where sediments exhibit zone settling but DMCA effluent contaminant concentrations are of concern. A detailed description of the procedure and an example are given by Palermo (1985).

97. Thus in the zone settling analysis, the design surface area A_d is equal to:

$$A_d = HECF * A_\ell = \left(\frac{1}{\bar{t}/T}\right) * A_\ell \tag{20}$$

where A_ℓ is the required surface area determined from laboratory tests. For flocculent settling, the design residence time T_d is equal to the required residence time determined from laboratory tests T_ℓ multiplied by the HECF:

$$T_d = HECF * T_\ell = \left(\frac{1}{\bar{t}/T}\right) * T_\ell \tag{21}$$

98. A simple approach for evaluating the layout of a proposed DMCA would be simply determining L/W from site plans and using Equation 19 to predict $\bar{t}/T$. As noted above, L should be the distance from inlet to outlet along the center line of the flow, and W should be the average width of the flow path. The computed value of $\bar{t}/T$ could then be used in either Equation 20 or 21 (whichever is appropriate) to determine if the DMCA size is adequate to ensure good effluent quality. Design would proceed by trial and error: (a) choose a layout, (b) compute efficiency, (c) check site area or volume, and (d) repeat if necessary. The DMCA area (or volume and flow rate) used in Equation 20 or 21 should be values representative of critical conditions.

99. However, since hydraulic efficiency and surface area of square or rectangular DMCAs are both functions of L and W, a more appropriate design procedure would be to combine Equations 18 and 19 or 20 to economically optimize DMCA dimensions and the number of spur dikes. A simplified procedure for

such a cost analysis is given in the following section. A similar analysis might be used to evaluate the economics of adding spur dikes or baffles to an existing DMCA.

Improving Residence Time Distributions

100. Site conditions that promote nonuniform flow tend to degrade residence time distribution away from the plug-flow ideal. To promote uniform flow, the bottom of the DMCA should be free of vegetation larger than grasses. Major topographic variations such as ridges and swales should be graded smooth. Inlets and outlets should be designed and located so as to avoid concentration of flow and adjacent dead zones.

Spur dikes

101. Baffles or internal spur dikes are by far the most effective and reliable devices that can be used to significantly reduce short-circuiting and dispersion. One well-placed spur dike can nearly double the length and halve the width, thereby increasing the length-to-width ratio by a factor of 3 to 4. Figure 31 shows several good spur dike arrangements. In general, spur dike length should be 0.75 times the length of the side parallel to the dike. Spur dikes should subdivide the DMCA pond into sections with near-equal surface areas. Equation 19 indicates that L/W ratios above 10 provide very little improvement in the hydraulic efficiency, and therefore use of spur dikes to achieve L/W ratios greater than 10 is probably unnecessary. Extremely high L/W ratios might produce advective velocities high enough to scour and resuspend deposited sediments.

102. Spur dikes force the flow to reverse direction, which can have several advantages. The first turn breaks the momentum caused by the inflow jet and/or wind, and each subsequent turn redistributes the flow, eliminating any tendency for the flow to concentrate in a narrow band. The influence of wind on short-circuiting is reduced, since the wind cannot establish a surface current that travels directly from the inlet to the outlet. The wind is forced to blow across or against the flow over a portion of the flow path, which reduces large wind-induced circulation patterns.

103. Commercially available floating baffles may offer several advantages to permanent spur dikes (Figure 32). They can be installed quickly, even after disposal has begun. They can be moved after deltas form to

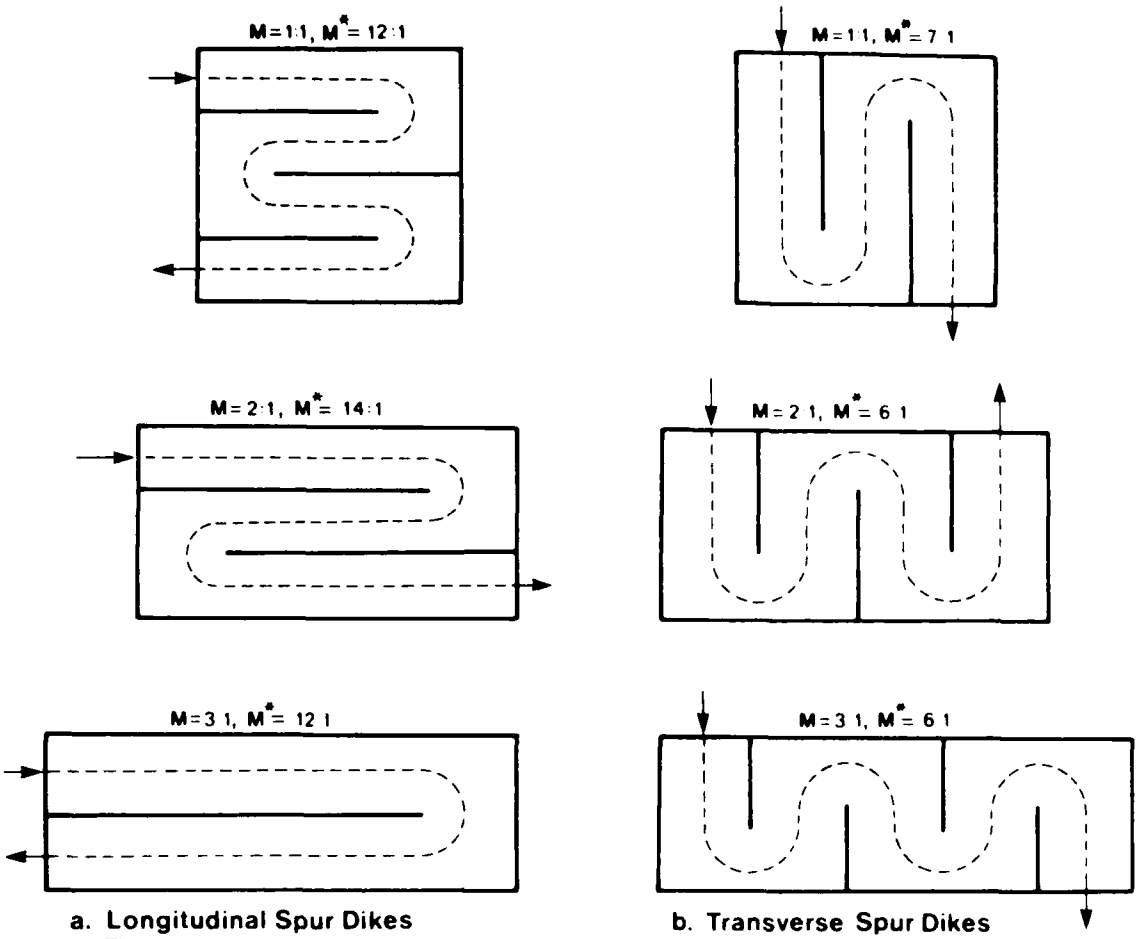

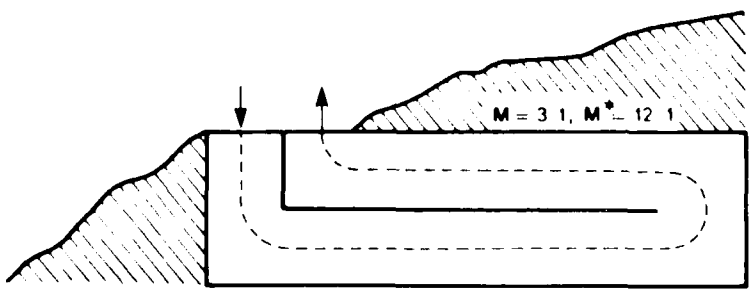

Figure 31. Examples of longitudinal and transverse spur dike configurations. M is L/W without spur dikes and M* approximate L/W ratio with spur dikes (from Gallagher and Company (1978))

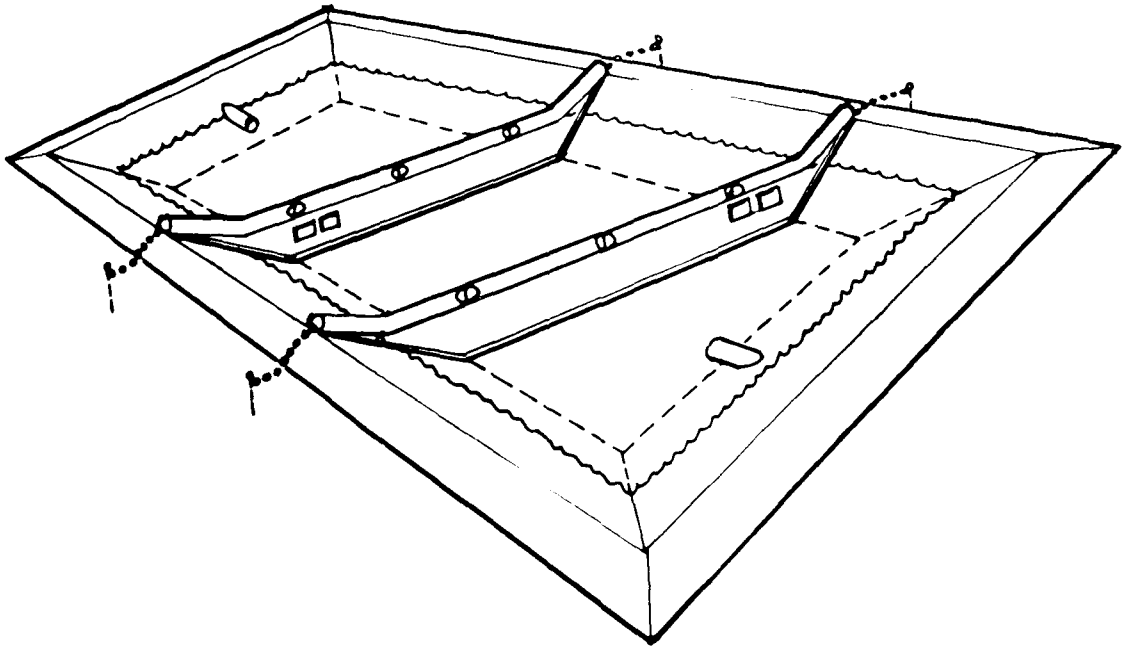

Figure 32. Floating baffles. Illustrations courtesy of Environetics, Inc., Bridgeview, Illinois

increase the L/W ratio near the end of the disposal life of the DMCA. Unlike spur dikes, baffles use very little of the DMCA volume, thus allowing more volume for storage and settling.

Inlet devices

104. The most important design aspect of inlet devices is the necessity of destroying the forward momentum jet and distributing the flow throughout the width of the basin. Ways to achieve this design goal include the following:

a. Attach a flow splitter to the end of the dredge pipe to split the flow and direct it toward the sides of the DMCA.

b. Attach a spoon to the end of the dredge pipe to spread the flow as a fan in all directions from the inlet.

c. Use a wye or a manifold to distribute the inflow across the entire inlet end; preferably, each point of inflow should have a device to break the forward momentum.

d. Install a splash baffle in front of the inlet pipe.

Inlet devices like manifolds that divide the flow should be designed to avoid clogging. During many disposal operations, it is necessary to move the dredge pipe to different inflow points. In such cases, special inlet devices must be portable.

Outlet devices

105. The outlet device for a DMCA is typically a weir. Weirs concentrate flow in the area directly in front of them, creating dead zones on either side (Figure 33). The size of the dead zones can be reduced by increasing the length of the weir or by installing several weirs along the outlet end. However, care must be taken to ensure that all of the weir crests are at the same elevation to avoid concentrating the flow at locations where the weir crests are lower. Walski and Schroeder (1978) provide guidance and design nomograms for DMCA weir design.

Placement of inlets, outlets, and spur dikes

106. The objective of the placement of inlets, outlets, and spur dikes is to reduce wind effects, maximize the L/W ratio, and ensure that water flows through the entire DMCA pond, keeping dead zones to a minimum. The placement of the inlet and outlet is frequently controlled by site and project constraints such as the location with respect to the dredge and receiving

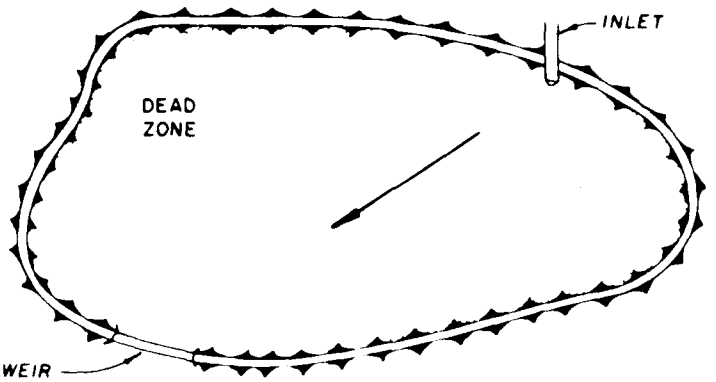

a. Weir placement and dead zones

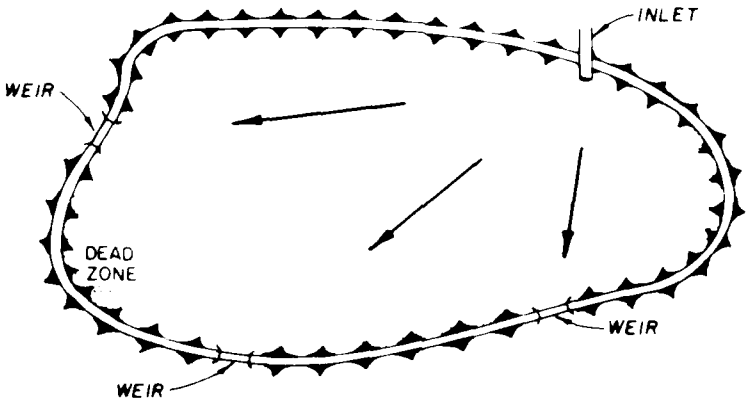

b. Dead zone size reduced by using two weirs

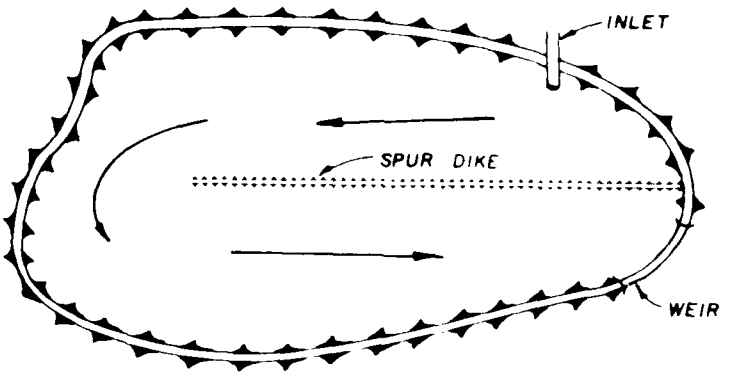

c. A spur dike and a longer weir

Figure 33. DMCA designs with weirs as outlet devices from Walski and Schroeder (1978)

water body. Nevertheless, efforts should be made to maximize the distance between the inlet and outlet and to place the inlet and outlet on opposite sides of the DMCA, unless they are separated by a spur dike.

Cost Analysis

107. The surface area and length-width ratio for a square or rectangular DMCA are both functions of length and width. If baffles or spur dikes are installed, the number and dimensions of the spur dikes enter the functions, but area and L/W are still functionally related. By means of equations to describe these relationships, the least-cost configuration of site length, width, and number of spur dikes may be determined for a given value of site area A_ℓ (or T_ℓ for flocculent analysis).

Constraint function

108. The following relationships may be used to transform Equations 20 and 21 into functional relationships between L, W, and the number of spur dikes or baffles N. Assuming a rectangular DMCA with points of inflow and outflow at the midpoints of the shorter sides (Figure 34), pond surface area = pond length × pond width - area occupied by spur dikes, or

$$A_d = LW - L'NW_s L \tag{22}$$

where

L = pond length, inlet to outlet, ft

W = average pond width, ft

N = number of spur dikes (all spur dikes assumed to be longitudinal)

W_s = width of spur dikes at water surface elevation

The theoretical residence time is

$$T_d = \text{volume}/Q \tag{23}$$

where

Q = average flow rate, cfs

Pond volume is pond length × pond width × pond depth - volume occupied by spur dikes, or

$$\text{Pond volume} = LWD - L'NV_u L \tag{24}$$

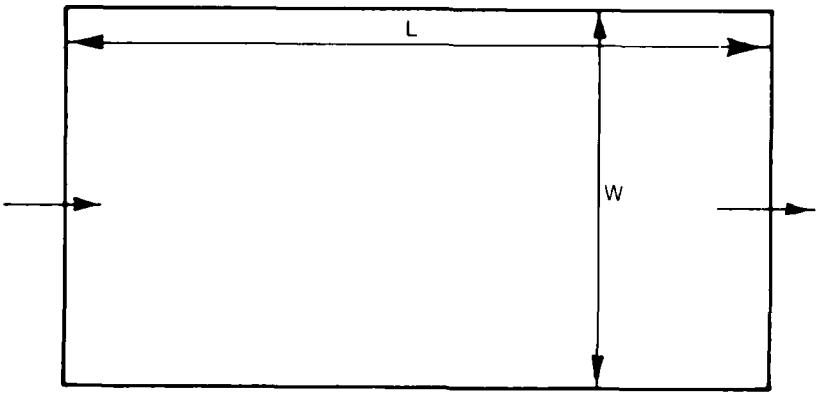

a. Rectangular DMCA with no spur dikes (N = 0)

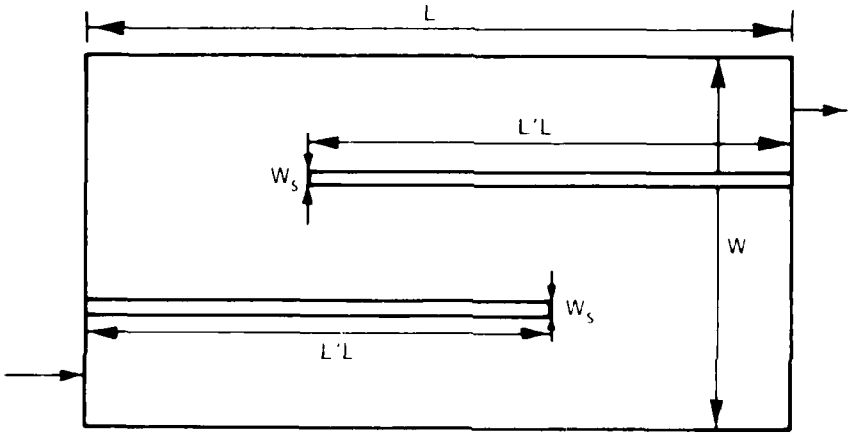

b. Rectangular DMCA with two longitudinal spur dikes (N = 2). Width of spur dikes at water surface is W_s. Length of spur dikes is L' L

Figure 34. Definition sketch for DMCA layout cost analysis

where

L' = ratio of spur dike length to parallel perimeter dike length

V_u = unit volume of spur dike below waterline, ft^3/ft

109. The flow path length-width ratio of a DMCA with longitudinal spur dikes (as shown in Figure 34b) may be approximated by $(L/W)(1' (N+1)$ if L' is between 0.8 and 1.0. If this expression is substituted into Equation 19 for L/W and the reciprocal of both sides is taken, the following is obtained:

$$HECF = 0.9\left|1 - \exp\left[-0.3L'(L/W)(N + 1)^2\right]\right|^{-1} \quad (25)$$

By substituting Equation 25 into Equation 20, the following is derived:

$$L(W - L'NW_s) = \frac{A_\ell}{0.9\left|1 - \exp\left[-0.3L'(L/W)(N + 1)^2\right]\right|} \quad (26)$$

Substituting Equation 25 into Equation 21 gives:

$$\frac{L(WD - L'NV_u)}{Q} = \frac{T_\ell}{0.9\left|1 - \exp\left[-0.3L'(L/W)(N + 1)^2\right]\right|} \quad (27)$$

110. If all variables in Equations 26 and 27 are fixed except N, L, and W, the two equations become identical:

$$L(W - aN) = \frac{b}{1 - \exp\left[c(L/W)(N + 1)^2\right]} \quad (28)$$

where a, b, and c are constants. If $W>>aN$, then

$$LW \approx \frac{b}{1 - \exp\left[c(L/W)(N + 1)^2\right]} \quad (29)$$

Equations 28 and 29 may be referred to as constraint functions, since DMCA design must satisfy these equations in order to provide acceptable effluent quality.

Cost function

111. The cost of a DMCA consists of the cost of dikes, land, and other items like outlet structures, channels, access roads, and miscellaneous items. The area of land required (excluding land necessary for access and rights-of-way) will be (Figure 35):

$$\text{Site area} = (L + 2w)(W + 2w) \quad (30)$$

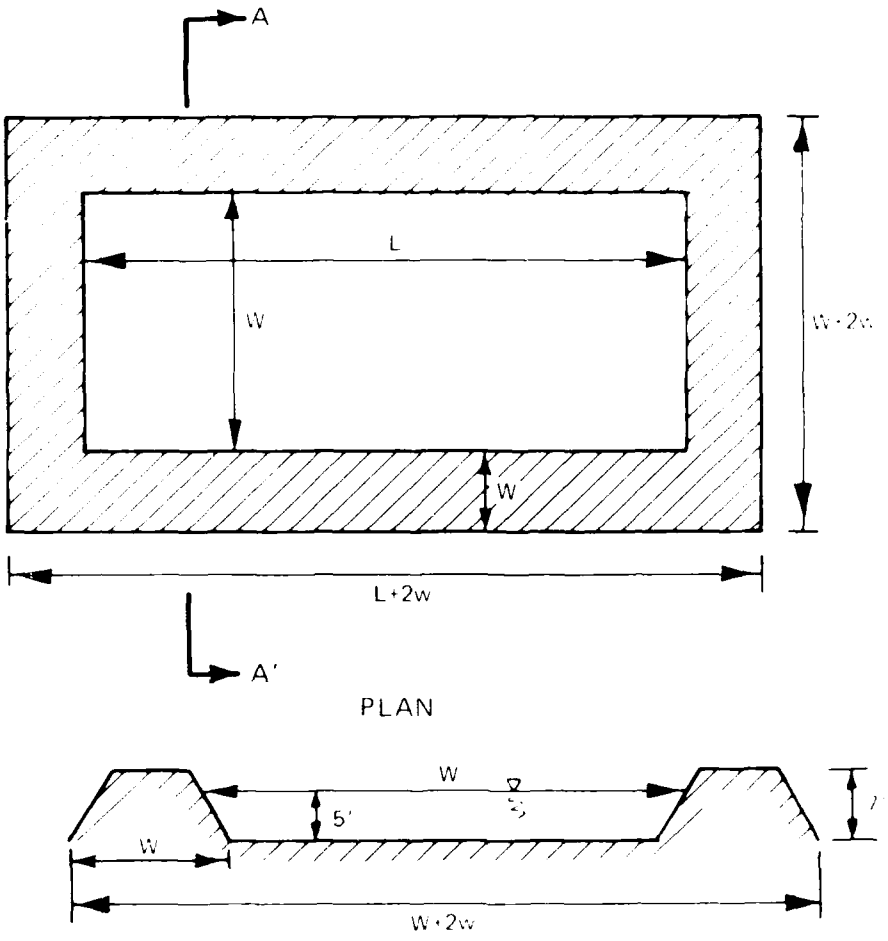

Figure 35. Definition sketch for cost analysis

where w is the base width of the perimeter dike.

The length of the perimeter dike will be (Figure 35):

$$\text{Perimeter dike length} = 2(L + 2w + W) \tag{31}$$

The total length of the spur dikes will be (Figure 34):

$$\text{Spur dike length} = NL \tag{32}$$

If f is the ratio of the unit cost of the spur dike to the unit cost of the perimeter dike, then the cost of the DMCA dikes and land will be:

$$\$ = \left[2(L + 2w + W) + fNL'L\right]C_d + \left[(L + 2w)(W + 2w)\right]C_\ell \qquad (33)$$

where C_d is the cost of the perimeter dike in \$/ft and C_ℓ is the cost of land in $\$/ft^2$.

112. A designer may optimize the portion of DMCA costs represented by Equation 33 subject to the constraint imposed by Equation 28. In other words, the least costly combination of L, W, N, and L' that will provide acceptable effluent quality may be selected. Some simplified examples follow. The basic assumptions in these examples are the same as those used by Gallagher and Company (1978) in their Appendix D.

Basic assumptions

113. The following assumptions are used in all examples:

a. All spur dikes are longitudinal, and L', the ratio of spur dike length to pond length, is 0.75.

b. Perimeter dikes have side slopes of 1:3, crown widths of 10 ft, and heights of 7 ft. Their unit volume is 217 ft^3/ft.

c. Spur dikes have side slopes of 1:2, crown widths of 10 ft, and heights of 7 ft. Spur dike width at the water surface elevation is 10 ft, and unit volume below the waterline V_u is 100 ft^3/ft.

d. Ponding depth D is fixed at 5 ft, so all dikes have 2 ft of freeboard.

e. The average flow rate Q is 27 cfs.

f. The required residence time T_ℓ from laboratory tests (flocculent analysis) is 44.75 hr, while the required surface area A_ℓ from lab tests (zone settling analysis) is 20 acres.

g. The unit cost of perimeter dikes C_d is \$16/ft. Unit cost for spur dikes is half as much, so $f = 0.5$.

h. The unit cost of land is \$500/acre or $\$0.011/ft^2$.

i. The DMCA is rectangular in shape with uniform depth so that $A = LW$ and volume $= LWD$.

Example 1--neither length nor width fixed

114. In the case that neither DMCA width nor length are constrained by site conditions, costs are a function of L/W and N. Given N and L/W values, Equation 29 may be used to compute LW. LW may then be combined with the given value of L/W to find L and W, and then Equation 33 can be used to find the total cost of land and dikes. Table 17 and Figure 40 show

the effects of L/W and N on the total cost of land and dikes under the set of assumptions listed in paragraph 113. Both Table 12 and Figure 36 show that spur dikes reduce costs when the above assumptions hold. However, the incremental rate of return on spur dikes diminishes rapidly, so one to three longitudinal spur dikes will be the best arrangement for most situations.

Table 12

Minimum Cost Configuration for DMCA with Neither Length nor Width Fixed

Spur Dikes No.	Overall L/W	Cost, $K	L, ft	W, ft	LW, acres
0	5	125.6	2,675	535	32.9
1	2	101.0	1,520	760	26.6
2	1	98.2	1,055	1,055	25.6
3	1	98.4	1,000	1,000	22.8

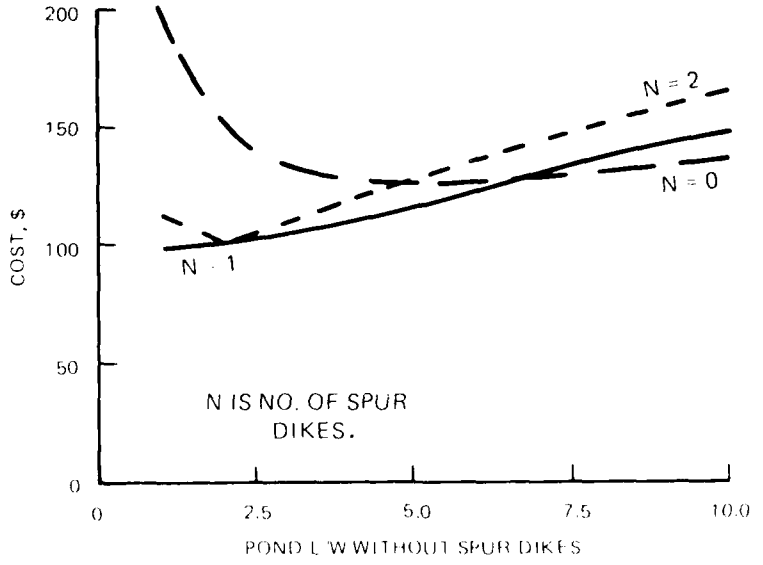

Figure 36. Relationship of cost of DMCA land and dikes to the number of spur dikes and the overall pond L/W ratio

Example 2--width fixed

115. In most cases, the designer cannot freely vary the length and width of the DMCA because available tracts of land are limited in size and shape. In a case where the pond width of the proposed DMCA is set at 300 ft but the length may take on any value greater than or equal to 300 ft, Equation 29 may be solved by trial and error for L using several different values of N, the number of spur dikes. Table 13 shows the effect of N on DMCA cost. A comparison of Tables 12 and 13 shows that restricting DMCA shape can be costly.

Table 13

Variation of Cost with Number of Spur Dikes for DMCA with Width Fixed at 300 Ft

Spur Dikes No.	L/W	Overall Cost, $K	L, ft	W, ft	LW, acres
0	11.7	140.9	3,500	300	24.1
1	11.0	153.4	3,300	300	22.8
2	11.3	178.0	3,400	300	23.4
3	11.7	203.9	3,500	300	24.1

116. In summary, the relationship between L/W and hydraulic efficiency allows economic optimization of DMCA layout--pond shape, size, and the number of spur dikes. Floating baffles are often economically attractive relative to earthen spur dikes both because of their cost and because they occupy so little of the DMCA pond volume. Certainly more sophisticated approaches to optimization with fewer simplifying assumptions (such as fixing pond depth) are warranted for some projects.

PART VI: CONCLUSIONS AND RECOMMENDATIONS

Conclusions

117. Flow residence time distribution is a critical factor in DMCA design. Underestimation of hydraulic efficiency can result in increase cost, whereas overestimation can result in poor effluent quality. Current design procedure relies on the hydraulic efficiency instead of the overall residence time distribution. Water quality is determined by the product of the solids removal characteristics and the residence time distribution.

118. DMCAs tend to have log-normal residence time distributions. Most DMCAs have hydraulic efficiencies between 20 and 70 percent with dispersion indices between 0.3 and 0.6. Wind tends to affect the minimum and modal residence times, and thus the overall shape of the residence time distribution, but not the hydraulic efficiency. Wind tends to increase the fraction of the DMCA dominated by completely mixed conditions.

119. Residence time distribution data for DMCAs and similar large, shallow basins are scarce and are of generally poor quality. The remote locations of most of these sites and the extremely long sampling times required for adequate data collection are partially responsible. Residence time distribution data from similar, but smaller water and wastewater treatment basins indicate a strong direct relationship between basin length-width ratio (L/W) and hydraulic efficiency and an inverse relationship between L/W and the dispersion index. DMCA hydraulic efficiency data seem to follow the same general relationship with L/W as data from the other sources.

120. The functional relationship between hydraulic efficiency and L/W allows economic optimization of layouts of DMCAs. Use of one to three longitudinal spur dikes is economically justified for most situations. Constraining DMCA size in one dimension (for example, width) results in higher costs than for an unconstrained configuration.

121. Mathematical computer models can be used to simulate flow patterns and the transport of solids and dyes in DMCAs. Three related obstacles to their use as design tools remain, however: (a) computer costs for model runs are quite high, (b) the use of existing knowledge to select appropriate model

coefficients for a given DMCA is difficult, and (c) detailed, high-quality field data are needed for refinement of modeling techniques.

Recommendations

122. Part V of this report should be used when sizing DMCAs until superseded by superior information.

123. The relationships between hydraulic efficiency and L/W developed in this document rely on dye tracer data from basins other than DMCAs for values of L/W greater than 4.1. Residence time distributions from DMCAs with higher L/W should be measured in order to verify the equations presented in this report. Collection of highly detailed quality field data for DMCAs of a variety of shapes would allow verification of the relationship between hydraulic efficiency and L/W , allow formulation of design guidance based on the entire residence time distribution instead of hydraulic efficiency, and also allow further development of computer modeling capability.

124. If additional field data allow formulation of a relationship between solids removal and L/W with greater precision than the relationship between hydraulic efficiency and L/W presented above, consideration should be given to developing a more sophisticated approach to DMCA design optimization. An optimization study might include consideration of DMCA shape, spur dikes, design of spur and exterior dikes, weir design and placement, and inlet structures.

125. Field tests to determine DMCA residence time distribution should include frequent measurements of wind speed, wind direction, and flow rate as well as effluent fluorescence. Measurement of effluent fluorescence should commence prior to dye addition at the inlet to allow determination of background fluorescence and should continue until fluorescence levels return to background levels. Field tests should also comply with guidance contained in Appendix B.

126. Additional investigations are needed to determine the relative merits of different types of tracer dyes when used in DMCA tests.

127. Future work should also focus on prediction of DMCA effluent quality by combining solids removal curves (Figure 1) with residence time distributions. Use of the mean residence time for design can be misleading

because solids removal curves are nonlinear. A method similar to that of Thackston (1972) would be more appropriate.

REFERENCES

Abood, K. A., Lawler, J. P., and Disco, M. D. 1969. "Utility of Radioisotophy Methodology in Estuary Pollution Control Study; 1: Evaluation of the Use of Radioisotopes and Fluorescent Dyes for Determining Longitudinal Dispersion," Report NYO-3961-1, US Atomic Energy Commission, New York.

Ariathurai, Ranjan. 1982. "Two and Three Dimensional Models for Sediment Transport," Report No. RMA 9180, Resource Management Associates, Lafayette, Calif.

Deaner, G. G. 1973. "Effect of Chlorine on Fluorescent Dyes," Journal of the Water Pollution Control Federation, Vol 45, No. 3, pp 507-514.

Feuerstein, D. L., and Selleck, R. E. 1963. "Fluorescent Tracers for Dispersion Measurements," Journal of the Sanitary Engineering Division, American Society of Civil Engineers, Vol 89, No. SA4, pp 1-21.

Francingues, N. R., Jr., et al. 1985. "Management Strategy for Disposal of Dredged Material: Contaminant Testing and Controls," Miscellaneous Paper D-85-1, US Army Engineer Waterways Experiment Station, Vicksburg, Miss.

Gallagher, Brian J., and Company. 1978. "investigation of Containment Area Design to Maximize Hydraulic Efficiency," Technical Report D-78-12, US Army Engineer Waterway Experiment Station, Vicksburg, Miss.

Hayes, Donald F., et al. 1985. "Automated Dredging and Disposal Alternative Management System," Draft Instruction Report D-85- , US Army Engineer Waterways Experiment Station, Vicksburg, Miss.

Hays, J. R. 1966. "Mass Transport Mechanisms in Open Channel Flow," Ph.D. Dissertation, Vanderbilt University, Nashville, Tenn.

Hunt, John P., and Delagran, Louise. 1984. Statpro User's Manual, Wadsworth Professional Software, Inc., Boston.

Johnson, M. 1984. "Fluorometric Techniques for Tracing Reservoir Inflows," Instruction Report E-84-1, US Army Engineer Waterway Experiment Station, Vicksburg, Miss.

Kavaushev, A. V. 1960. Dynamics of Natural Water Courses, State Publishing House on Hydrometeorology, Leningrad.

King, Ian P. 1982. "A Finite Element Model for Three Dimensional Flow," Report No. RMA 9150, Resource Management Associates, Lafayette, Calif.

Koussis, Antonis D., Saenz, Melio A., and Thackston, Edward L. 1982. "Evaluation of Hydraulic Models for Dredged Material Containment Areas," Department of Civil and Environmental Engineering, Vanderbilt University, Nashville, Tenn.

Liggett, James A., and Hadjitheodorou, Christos. 1969. "Circulation in Shallow Homogeneous Lakes," Journal of the Hydraulics Division, American Society of Civil Engineers, Vol 95, No. HY2, pp 609-725.

Liu, Henry, and Perez, Himerio J. 1971. "Wind-Induced Circulation in Shallow Water," Journal of the Hydraulics Division, American Society of Civil Engineers, Vol 97, No. HY7, pp 923-935.

Mangelson, Kenneth A., and Watters, Gary Z. 1972. "Treatment Efficiency of Waste Stabilization Ponds," Journal of the Sanitary Engineering Division, American Society of Civil Engineers, Vol 98, No. SA2, pp 407-425.

Marske, D. M., and Boyle, J. D. 1973. "Chlorine Contact Chamber Design--A Field Evaluation," Water and Sewage Works, Vol 120, No. 1, pp 70-77.

Miller, I., and Freund, J. E. 1977. Probability and Statistics for Engineers, Prentice-hall, Inc., Englewood Cliffs, N. J.

Montgomery, Raymond L. 1978. "Methodology for Design of Fine-Grained Dredged Material Containment Areas for Solids Retention," Technical Report D-78-56, US Army Engineer Waterways Experiment Station, Vicksburg, Miss.

Nie, Norman H., et al. 1975. Statistical Package for the Social Sciences, 2d ed., McGraw-Hill, New York.

Palermo, M. R. 1984. "Prediction of the Quality of Effluent from Confined Dredged Material Disposal Areas," Ph.D. Dissertation, Vanderbilt University, Nashville, Tenn.

_____. 1985. "Interim Guidance for Predicting Quality of Effluent Discharged from Confined Dredged Material Disposal Areas," Environmental Effects of Dredging Technical Notes, EEDP-04-1, -2, -3, -4, US Army Engineer Waterways Experiment Station, Vicksburg, Miss.

Palermo, M. R., Montgomery, R. L., and Poindexter, M. E. 1978. "Guidelines for Designing, Operating, and Managing Dredged Material Containment Areas," Technical Report D-78-10, US Army Engineer Waterways Experiment Station, Vicksburg, Miss.

Palermo, M. R., and Pranger, S. P. 1984. "Field Verification Program: Upland/Wetland Disposal Site Design, Construction, and Operation," Attachment to ETL 1110-X-XXX, Office, Chief of Engineers, Washington, DC.

Poindexter, Marion E., and Perrier, Eugene R. 1980. "Hydraulic Efficiency of Dredged Material Impoundments: A Field Evaluation," Proceedings of ASCE Symposium on Surface Water Impoundments, Minneapolis, Minn.

Pritchard, D. W., and Carpenter, J. H. 1960. "measurement of Turbulent Diffusion in Estuarine and Inshore Water," Bulletin of the International Association of Science and Hydrology, Vol 20, pp 37-50.

Schroeder, Paul R. 1983. "Chemical Clarification Methods for Confined Dredged Material Disposal," Technical Report D-83-2, US Army Engineer Waterways Experiment Station, Vicksburg, Miss.

Slade, David H., ed. 1968. Meteorology and Atomic Energy 1968, US Atomic Energy Commission, Silver Spring, Md.

Smart, D. L., and Laidlaw, I. M. S. 1977. "An Evaluation of Some Fluorescent Dyes for Water Tracing," Water Resource Research, Vol 13, pp 15-33.

Tatom, F. B., and Waldrop, W. R. 1986. "Hydrodynamics of Settling Ponds," Third International Symposium on River Sedimentation, Jackson, Miss.

Thackston, E. L. 1972. "Sedimentation," Water Quality Engineering, E. L. Thackston and W. W. Eckenfelder, Jr., ed, Jenkins Publishing Co., Austin, Texas.

Thackston, E. L., and Krenkel, P. A. 1967. "Longitudinal Mixing in Natural Streams," Journal of the Sanitary Engineering Division, American Society of Civil Engineers, Vol 93, No. SA5, pp 67-90.

Thackston, E. L., and Schnelle, K. B. 1970. "Predicting Effects of Dead Zones on Stream Mixing," Journal of the Sanitary Engineering Division, American Society of Civil Engineers, Vol 96, No. SA2, pp 319-331.

Thomas, William A., and McAnally, William H., Jr. 1985. "User's Manual for the Generalized Computer Program System, Open Channel Flow and Sedimentation, TABS-2," Instruction Report HL-85-1, US Army Engineer Waterways Experiment Station, Vicksburg, Miss.

Walski, T. M., and Schroeder, P. R. 1978. "Weir Design to Maintain Effluent Quality from Dredged Material Containment Areas," Technical Report D-78-18, US Army Engineer Waterways Experiment Station, Vicksburg, Miss.

Watt, J. P. C. 1965. Development of the Dye-Dilution Method for Measuring Water Yields from Mountain Watersheds, M.S. Dissertation, Colorado State University, Fort Collins, Colo.

Watters, Gary Z., Mangelson, Kenneth A., and George, Robert L. 1973. "The Hydraulics of Waste Stabilization Ponds," Utah Research Laboratory/College of Engineering, Utah State University, Logan, Utah.

Wilson, J. F. 1968. "Fluorometric Procedures for Dye Tracing," Techniques of Water Resources Investigations of the US Geological Survey, Vol 3, US Geological Survey, Washington, DC.

Yotsukura, N., and Kilpatrick, F. A. 1973. "Tracer Simulation of Soluble Waste Concentration," Journal of the Environmental Engineering Division, American Society of Civil Engineers, Vol 99, No. 8, pp 499-515.

APPENDIX A: NUMERICAL MODELING

PART I: INTRODUCTION

Purpose

1. The purpose of this study was to evaluate the potential of the TABS numerical modeling system as a tool to predict residence time distributions of dredged material containment areas (DMCAs).

Scope

2. The study consisted of trial applications of two-dimensional (2-D) and three-dimensional (3-D) numerical models from the TABS system to DMCAs for which measurements of residence time distribution were available. This report describes the models, explains how they were used to model DMCAs, provides results of model runs for DMCAs, and offers conclusions about the usefulness of these tools in DMCA design.

Approach

3. The TABS numerical modeling system (Thomas and McAnally 1985)* was used to simulate eight DMCA test cases. Model performance was evaluated based on two criteria: reproduction of measured dye tracer curves (which are residence time distributions) and prediction of hydraulic efficiency. Regression equations were derived for the model coefficients to allow the models to be used in a predictive mode. The models were used to simulate a hypothetical DMCA generated by adding spur dikes to one test case geometry to show the response of the models to such changes in geometry.

---

* See References at the end of the main text.

PART II: NUMERICAL MODELS

4. Finite element hydrodynamic models, RMA-10 (King 1982) and RMA-2V (Thomas and McAnally 1985), and transport models, SED-8 (Ariathurai 1982) and RMA-4 (Thomas and McAnally 1985) from the TABS system, were used in this study. Computations are performed in two horizontal directions within RMA-2V and RMA-4. Two-dimensional horizontal models are applicable to DMCAs when there is little variation in velocity in the vertical plane. Adjustment of some of the two-dimensional model coefficients can compensate for such three-dimensional phenomena as vertical mixing and return flow. RMA-10 and SED-8 perform fully three-dimensional computations.

The Hydrodynamic Models, RMA-10 and RMA-2V

5. RMA-10 and RMA-2V are finite element solutions of the Reynolds form of the Navier-Stokes equations for turbulent flow. In RMA-2V, the equations are depth-integrated. Bottom friction is calculated with Manning's equation, and eddy viscosity coefficients are used to define the turbulent exchanges. A velocity form of the basic equation is used. Side boundaries are treated as either slip (flow parallel to the boundary) or no-slip (zero flow) as specified by the user. Boundary conditions may be water levels, velocities, or discharges and may occur inside the mesh as well as along the edges.

The Transport Models, SED-8 and RMA-4

6. The transport models, SED-8 and RMA-4, solve the convection-diffusion equation, which has general source-sink terms. In RMA-4, the equations are depth-integrated, and up to six dissolved or suspended constituents can be routed. In SED-8, transport of dissolved or suspended material, including cohesive sediment, may be modeled. RMA-4 uses hydrodynamics generated by RMA-2V and the same computational mesh. SED-8 uses hydrodynamics generated by RMA-10.

Mesh Generation

7. For the finite element method, the DMCAs were subdivided into smaller areas called elements. Within the TABS system, elements can be either quadrilateral or triangular in shape and can have curved sides. Each element is defined by a number of points called nodes that are connected by lines (element sides). Within TABS, quadrilaterals are defined by eight nodes, and triangles are defined by six nodes. Bed elevations are defined at each node, and a linear interpolation is performed along each element side. Output is readily available at each node, but, due to the continuous solution within the element, solution values may be obtained anywhere within the element domain.

8. For each disposal area tested, the limits of the area were digitized into regions for input to the TABS mesh generator program, AUTOMESH (Thomas and McAnally 1985). Where allowed by area geometry, elements of uniform dimension 50 by 50 ft were used for all of the sites modeled in order to eliminate element size as one possible source of a difference in eddy viscosity and diffusion coefficients. Bed elevations were specified to produce a slope of 1 ft/1,000 ft from the inflow point to the outflow weir. The deltaic sediment deposits around the inflow pipes were not modeled because of lack of data describing the formations. Figure A1 shows a sample computational mesh.

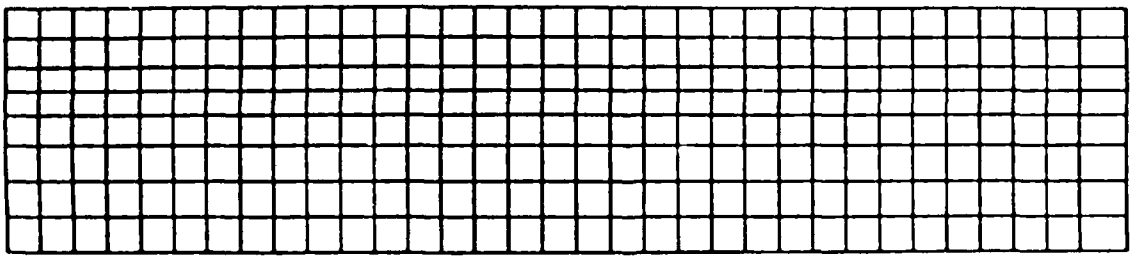

Figure A1. Numerical model mesh, Test 1

Boundary Conditions

9. For each test, smooth sides of each disposal area were specified as slip flow. Sharp corners were specified as no-slip flow. Inflows were specified as uniform velocity along a single element side, approximately 50 ft wide. The 50-ft width was used in an effort to simulate the immediate spread of the flow over the delta of coarse sediments deposited under the

inflow pipe. An exit water surface elevation equal to the DMCA water surface elevation was specified to simulate the outflow weir. For the RMA-10 test, slip flow was specified at the subsurface nodes of the outflow weir. The hydrodynamics programs were used to simulate steady-state velocity and depths fields, which were then input to the transport model.

10. Dye tracer tests were simulated by setting an initial concentration value of one at the inflow and zero for the rest of the DMCA. After one or two time-steps (depending on the test), the inflow concentration was reduced to zero. The inflow concentration was left at one for enough time so that measurable concentrations could be seen near the outflow weir. Hour or half-hour time-steps were used depending on the size of the DMCA.

PART III: FIELD DATA

Measured Characteristics

11. Table A1 shows geometric and hydraulic properties of each field test. Test numbers are the same as those used in the main body of the report. Data from Tests 9, 11, 12, and 13 were not available in time for incorporation in this numerical model study. Methods for determining site length, surface area, average depth, discharge, average wind-speed, surface drift velocity, and wind angle are given in the main body of this report.

Descriptive Calculations

12. Mean residence time, hydraulic efficiency, modal time, and dispersion index were computed for both the field test dye curves and the dye curves output by RMA-4 using the DYECON computer program (Hayes 1985). Formulas and definitions for these statistical descriptors are given in the main body of this report.

Table A1

Some Properties of the Test Disposal Areas

Test No.	Length ft	Avg. Depth ft	Surface Area ft²	Inflow Width ft	Outflow Width ft	No. of Elements	No. of Nodes	Discharge cfs	Average Wind Speed mph	Surface Drift Velocity ft/sec	Wind Angle from Weir, deg
1	1,680	7.4	670,400	50	100	264	875	26.6	10	0.6431	122.0
2	1,550	2.7	1,016,000	50	50	438	1,433	5.5	5	0.2518	45.0
3	449	2.7	73,182	25	40	35	132	15.6	12	0.9500	-30.0
4	1,090	2.0	449,100	50	100	176	589	26.6	10	0.9243	164.4
5	1,996	8.0	1,234,120	50	55	650	2,081	17.7	6	0.2206	119.5
6	3,010	6.4	3,980,000	50	105	1,464	4,583	31.4	7	0.2214	94.0
7	1,115	6.0	506,800	150	100	204	671	20.4	0	0.0000	0.0
8	2,540	7.0	1,493,000	50	80	569	1,834	17.7	5	0.1835	-5.5

AD-A187 235 DREDGING OPERATIONS TECHNICAL SUPPORT PROGRAM DESIGN AND MANAGEMENT OF DR..(U) ARMY ENGINEER WATERWAYS EXPERIMENT STATION VICKSBURG MS ENVIR.. 2/2

UNCLASSIFIED F D SHIELDS ET AL. JUN 87 WES/TR/D-87-2 F/G 13/2 NL

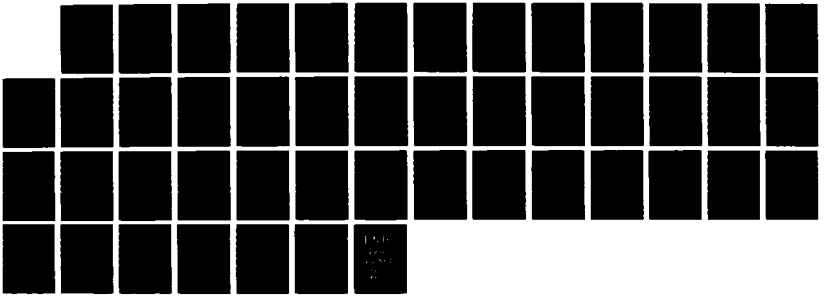

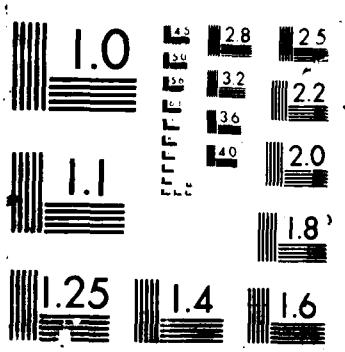
1.0
1.1
1.25
1.4
1.6
1.8
2.0
2.2
2.5
2.8
3.2
3.6
4.0

Table A1

Some Properties of the Test Disposal Areas

Test No.	Length ft	Avg. Depth ft	Surface Area ft^2	Inflow Width ft	Outflow Width ft	No. of Elements	No. of Nodes	Discharge cfs	Average Wind Speed mph	Surface Drift Veloc ft/sec	Wind Angle from Weir, deg
1	1,680	7.4	670,400	50	100	264	875	26.6	10	0.6431	122.0
2	1,550	2.7	1,016,000	50	50	438	1,433	5.5	5	0.2518	45.0
3	449	2.7	73,182	25	40	35	132	15.6	12	0.9500	-30.0
4	1,090	2.0	449,100	50	100	176	589	26.6	10	0.9243	164.4
5	1,996	8.0	1,234,120	50	55	650	2,081	17.7	6	0.2206	119.5
6	3,010	6.4	3,980,000	50	105	1,464	4,583	31.4	7	0.2716	94.0
7	1,115	6.0	506,800	150	100	204	671	20.4	0	0.0000	0.0
8	2,540	7.0	1,493,000	50	80	569	1,834	17.7	5	0.1835	-5.5

PART IV: MODEL RESULTS

Three-Dimensional Model

13. The TABS-3 modeling system was applied to Test 1. Results showed insufficient vertical circulation to warrant the extra time and cost of running a three-dimensional model. Therefore, the modeling effort was continued using TABS-2.

Two-Dimensional Model

Model adjustment criteria

14. Coefficients within the TABS modeling system were adjusted to obtain accurate simulation of measured residence time distributions. The following paragraphs describe the adjustment criteria that were used for eddy viscosity* in the hydrodynamic model and diffusion coefficients* in the transport model.

15. The hydrodynamic portion of the modeling system was adjusted in order to produce realistic eddy patterns while keeping the model numerically stable. Eddy viscosity coefficients were adjusted in the hydrodynamic model. Values of 0.5 $lb/sec/ft^2$ produced the most desirable velocity field. Lower values caused the hydrodynamic model to become numerically unstable, whereas higher values damped out the eddy patterns. A sample plot of the velocity field is shown in Figure A2. The presence of eddies slowed the simulated transport of dye.

16. The transport portion of the modeling system was adjusted by varying the diffusion coefficients. Diffusion coefficients were selected for each of the eight field tests by trial and error. First, the diffusion coefficient was varied to obtain the best fit of the peak of the simulated curve to the observed peak. The resulting eight values are hereinafter referred to as the best peak fit (BPF) coefficients. Then the diffusion coefficient was adjusted until the simulated dye curves had mean residence times within 10 percent of

---

* Identical values were used for lateral and longitudinal eddy viscosity. Lateral and longitudinal diffusion coefficients were also assumed to be equal.

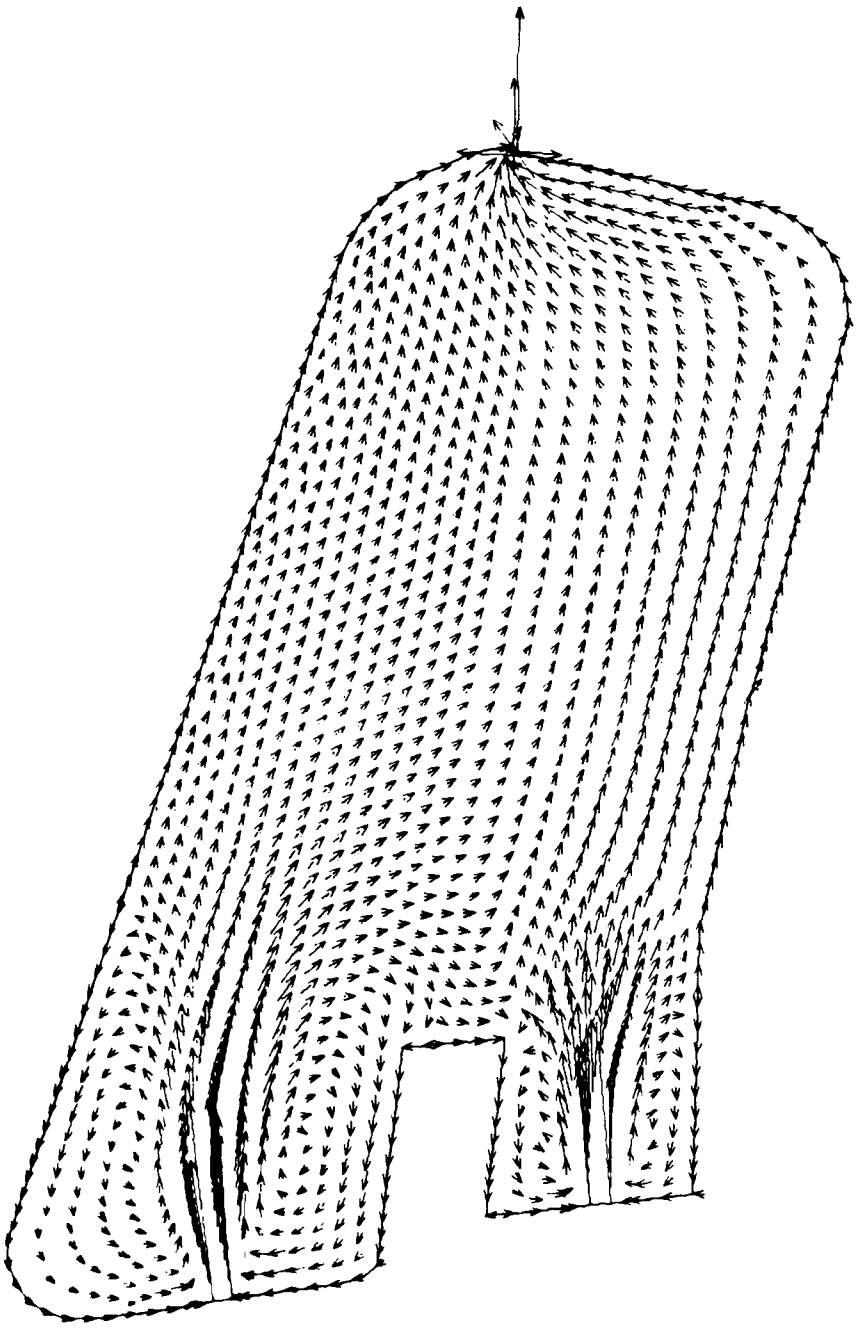

Figure A2. Velocity vector field, Test 6

[illegible] the retical residence time of the observed mean residence times. The re- [illegible] coefficients are referred to hereinafter as the best hydraulic [illegible] (BHD) coefficients.

Results

17. The diffusion coefficients that best fit the BPF and BHE adjustment criteria are presented in Table A2. Table A2 also shows that when the model was adjusted to meet the BPF criteria, mean residence times were predicted within 40 percent of the observed values in all but one case and within 14 percent of the observed value in half of the cases. Except for Test 2, in cases where the BPF-adjusted model achieved good fit for mean residence time, reasonably good fit was also obtained for the dispersion index. Evidently, the model provided much better simulation of some of the field tests than others, but the reasons why are not obvious. For Tests 1, 3, 7, and 8, the BPF and the BHE adjustment criteria did not produce the same diffusion coefficients. The observed and simulated dye tracer curves are shown in Figure A3. Normalized dye concentrations (the y-coordinate in Figure A3) were obtained by dividing the actual values by the peak concentration for each curve. Raising the diffusion coefficients moved the peak of the dye tracer curve to the left on the time axis (faster transport), whereas lowering the coefficients moved the peak of the curve to the right (slower transport).

Regression Analysis

18. As noted above, a common value for eddy viscosity was used in the hydrodynamic model for all simulations, but different values for the transport model diffusion coefficient were used in each test to meet the BPF and BHE criteria (Table A2). A multiple linear regression analysis was performed to formulate an equation for predicting the diffusion coefficient based on selected physical characteristics of the field tests. The regression analysis was performed using the Statistical Package for the Social Sciences (SPSS) system of computer programs (Nie et al. 1975).

19. Regression analyses were performed using both BPF and BHE diffusion coefficients as the dependent variable. A noncollinear set of independent variables, consisting of the surface drift velocity, surface area, discharge, and wind angle, was selected in a stepwise manner. Surface area was selected instead of depth or length because it was uncorrelated with the other variables of interest and because it was measured directly from site plans for all tests. For the BPF regression, the independent variables were added to the regression equation one at a time until the coefficient of determination (R^2) exceeded

Table A2

Best Model Diffusion Coefficients and Calculated Parameters*

Test No.	Longitudinal Diffusion Coefficient m^2/sec		Mean Residence Time, hr			Hydraulic Efficiency			Modal Time, hr			Dispersion Index		
	BPF	BHE	Field	BPF	BHE	Field	BPF	BHE	Field	BPF	BHE	Field	BPF	BHE
1	0.6	0.18	37.7	29.6	37.4	72.8	57.2	72.1	12.2	16.5	28.5	0.60	0.36	0.18
2	1.8	1.8	26.9	30.7	30.7	19.3	22.2	22.2	13.0	12.0	12.0	0.30	0.58	0.58
3	1.2	2.2	1.73	2.39	1.80	49.2	68.3	51.4	0.87	1.5	1.00	0.51	0.37	0.29
4	0.90	0.90	5.89	6.52	6.52	62.7	69.4	69.4	3.00	4.25	4.25	0.27	0.23	0.23
5	1.2	1.2	76.2	72.4	72.4	49.2	46.8	46.8	8.0	28.0	28.0	0.60	0.58	0.58
6	0.90	0.90	100.0	104.0	104.0	44.4	46.5	46.5	12.0	38.0	38.0	0.55	0.51	0.51
7	0.18	0.09	42.5	31.9	34.7	103.0	77.0	83.8	17.0	19.5	24.5	0.46	0.34	0.24
8	0.60	0.03	172.0	87.7	130.0	105.0	53.5	79.2	27.5	44.0	98.0	0.69	0.46	0.14

* BPF = best peak fit; BHE = best hydraulic efficiency (paragraph 16).

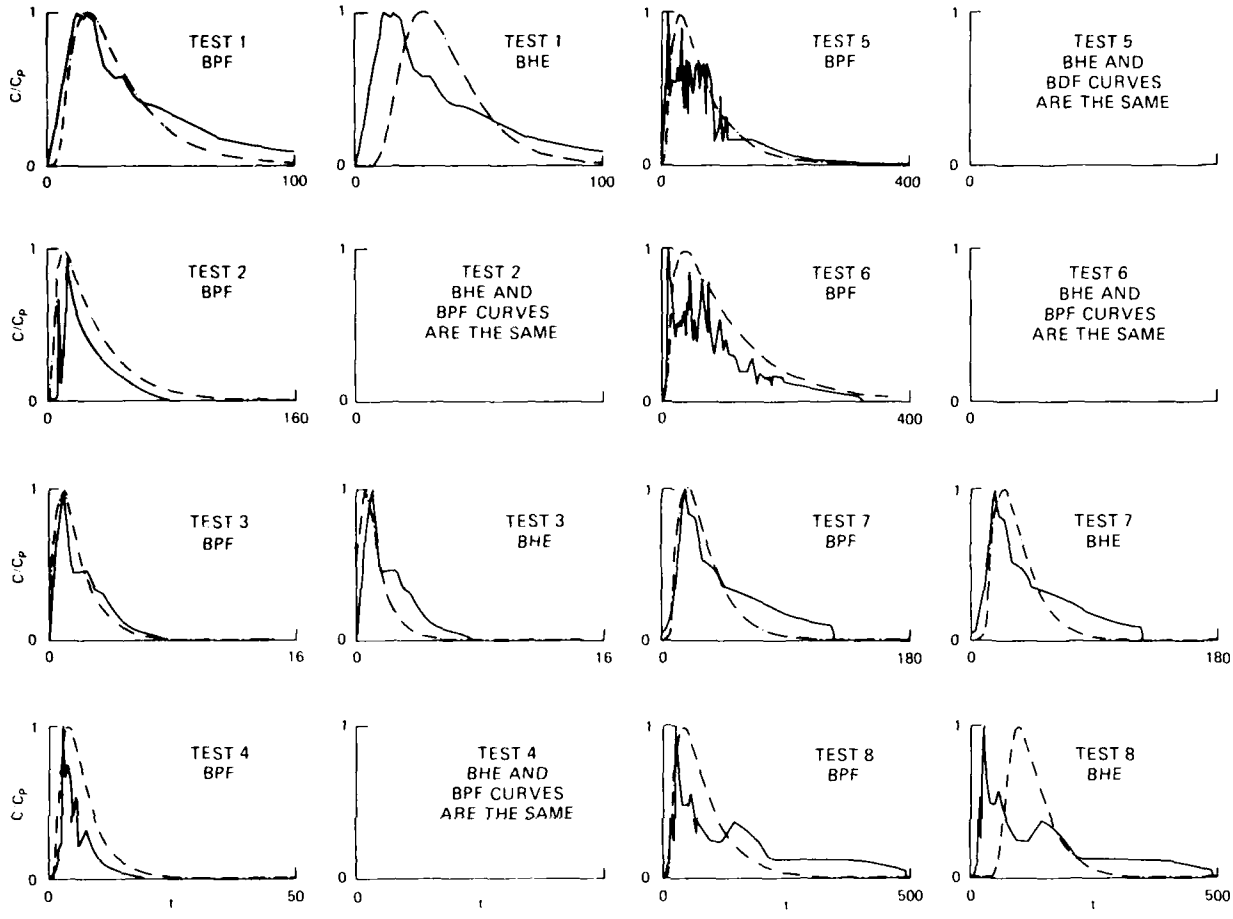

Figure A3. Observed dye tracer curves (solid lines) and simulated curves from TABS model output (dashed lines). The x-axis is time after dye injection in hours, and the y-axis is dye concentration divided by peak dye concentration. BPF curves show output from model with coefficients adjusted to achieve the best fit of the model output to the observed dye curve peak. BHE curves show model output with coefficients adjusted to obtain values of hydraulic efficiency close to observed values

0.950. The same independent variables produced the highest R^2 for BHE regression. Table A3 shows the correlation matrix for the independent variables tested.

20. Table A4 shows the multiple linear regression coefficients resulting from the calculations. Table A5 shows calculated values of the model coefficients from the regression analysis and the best-fit model coefficients from the modeling exercise. Table A6 shows some statistics from the regression analysis. R^2 is the coefficient of determination, and values above 0.90 indicate a "good" fit to the data. Lower values for the standard deviation

Table A3

Independent Variable Correlation Matrix

	BHE Diffusion Coefficient	BCF Diffusion Coefficient	Discharge	Wind Speed	Surface Drift Velocity	Wind Angle	Length	Surface Area
Discharge	-0.486	-0.572						
Wind speed	0.456	0.331	0.237					
Surface drift velocity	0.430	0.216	0.198	0.919				
Wind angle	-0.122	0.110	0.517	0.303	0.249			
Length	-0.406	-0.0735	0.334	-0.261	-0.553	0.224		
Surface area	-0.128	-0.0415	0.433	-0.151	-0.409	0.185	0.876	
Average depth	-0.628	-0.489	0.322	-0.350	-0.581	0.087	0.634	0.385

Table A4

Multiple Linear Regression Coefficients*

Variable Number n	Independent Variable, X_n	Mean	BHE, $\bar{Y}$ = .913 Regr. Coef. B_n	BPF, $\bar{Y}$ = .922 Regr. Coef. B_n
1	Surface drift velocity	4.3061×10^{-1}	1.9373	9.2825×10^{-1}
2	Surface area	1.1778×10^{6}	4.1555×10^{-7}	3.1817×10^{-7}
3	Discharge	2.0189×10^{1}	-9.4459×10^{-2}	-7.8079×10^{-2}
4	Angle	6.3675×10^{1}	4.0914×10^{-4}	3.1558×10^{-3}
	Constant	0.0000	6.2500×10^{-3}	1.1125×10^{-2}

* Coefficients for the equation $Y = B_1 X_1 + B_2 X_2 + B_3 X_3 + B_4 X_4 + B_o$

Table A5

Calculated* and Observed** Diffusion Coefficients

	RMA-4 Diffusion Coefficient, m^2/sec			
	BHE		BPF	
Test No.	Observed	Calculated	Observed	Calculated
1	0.18	0.54	0.60	0.65
2	1.8	1.9	1.8	1.8
3	2.2	1.9	1.2	1.1
4	0.90	1.0	0.90	0.98
5	1.2	0.79	1.2	1.1
6	0.90	0.73	0.90	0.90
7	0.090	-0.24	0.18	0.10
8	0.030	0.78	0.60	0.78

* From trial model runs.
** From regression.

Table A6

Selected Statistics of Regression Results

Item	BHE	BPF
R^2	0.750	0.967
Standard deviation	0.614	0.135
F	2.25	22.1

indicate less error in fitting the data. The values for F can be compared with a table of F values for the degrees of freedom within the regression. For this regression (4 variables, 8 tests), F values above 3.84 show a 95-percent confidence level, and values above 7.01 show a 99-percent confidence level (Miller and Freund 1977). However, reliable regression analysis requires 15 to 20 observations per variable. Since these analyses included a total of 5 variables, 75 to 100 observations are needed to establish a reliable regression equation instead of just 8. Figures A4 and A5 show calculated versus observed scatter plots for the best hydraulic efficiency and the best curve fit, respectively. The regression fit was better using the BPF diffusion coefficients and the resulting regression equation might be used as a starting point for selection of diffusion coefficients for future TABS-2 simulations of DMCAs.

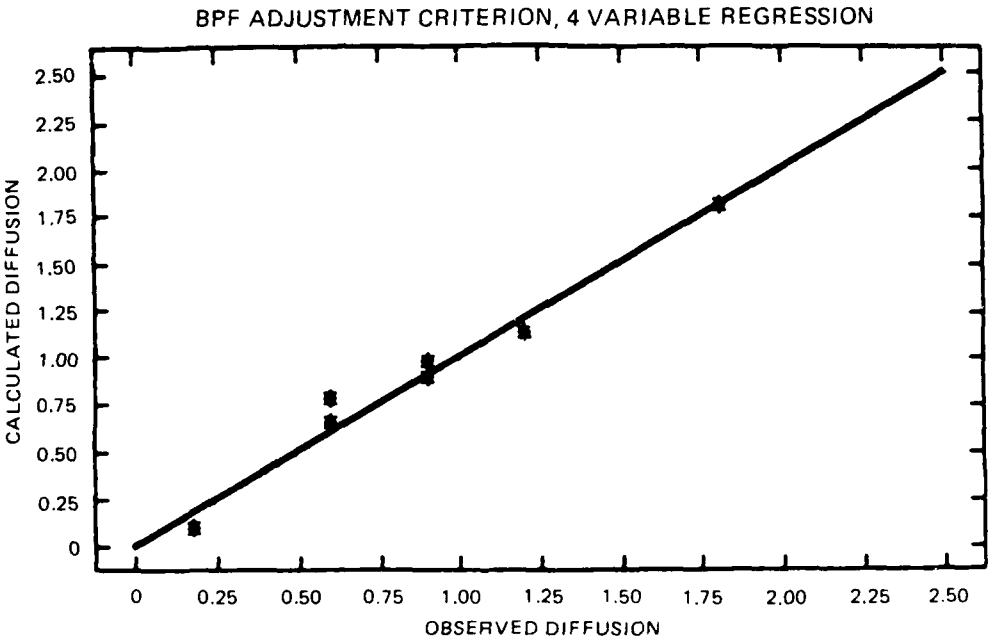

Figure A4. Calculated versus observed diffusion coefficients for regression analysis using BPF adjustment

Reasons for Differences Between Observed and Simulated Residence Time Distributions

21. Sources of variation between model simulations and field tests could have been caused by improper definition of the bed geometry and inflow or outflow conditions, not modeling vertical circulation, the presence of

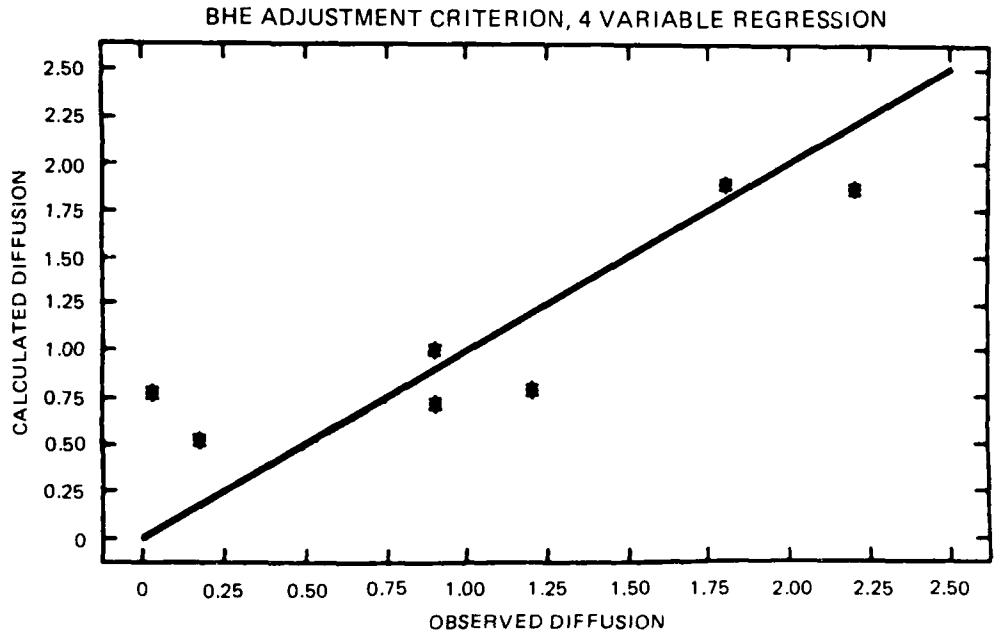

Figure A5. Calculated versus observed diffusion coefficients for regression analysis using BHE adjustment

suspended sediment within the flow, and errors in field data measurement. Despite the variations, the TABS-2 models were adjusted to closely reproduce four of eight observed dye curves. Specifically, sources of error included:

a. Inflows for the larger areas were unsteady since dredges start and stop many times during a typical dye test. The TABS-2 models used constant inflows.

b. Assuming a uniform slope for the bed is an oversimplification. Each area's bed will have irregularities. Since sediment is entering at the inflow, shoaling of this area will occur.

c. Vertical mixing caused by wind is not modeled directly within the two-dimensional models, but is compensated for by adjusting the diffusion coefficients.

d. Suspended sediment tends to make water denser and may also adsorb dye.

e. Some of the field dye curves are noisy, and some of the calculations from them may not be meaningful. Monitoring of effluent dye concentration was not continued long enough to adequately define the decay limbs of the curves in most of the tests. Accurate background dye concentration was not available for some of the tests. Field data for Tests 7 and 8 are suspect as the hydraulic efficiency was calculated to be greater than 100 percent.

Geometric Sensitivity Test

22. To further test the applicability of the TABS-2 modeling system to DMCA design, the geometry of one DMCA was modified while keeping the hydraulic properties and model coefficients constant. Spur dikes were added to Test 7 (Figure A6). The dye tracer curve moved to the right (slower transport, Figure A7) when compared with Test 7 without spur dikes (Figure A3).

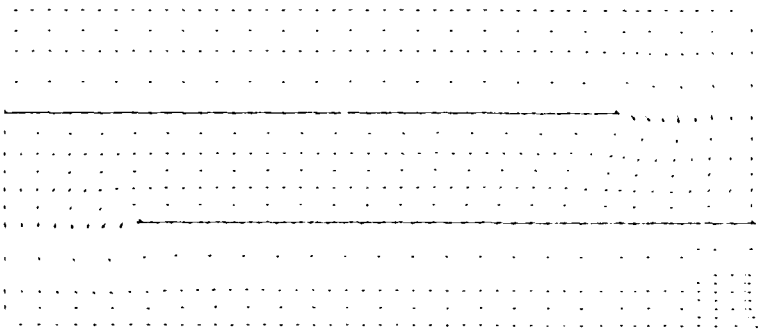

Figure A6. Velocity vector field, Test 7 with spur dikes

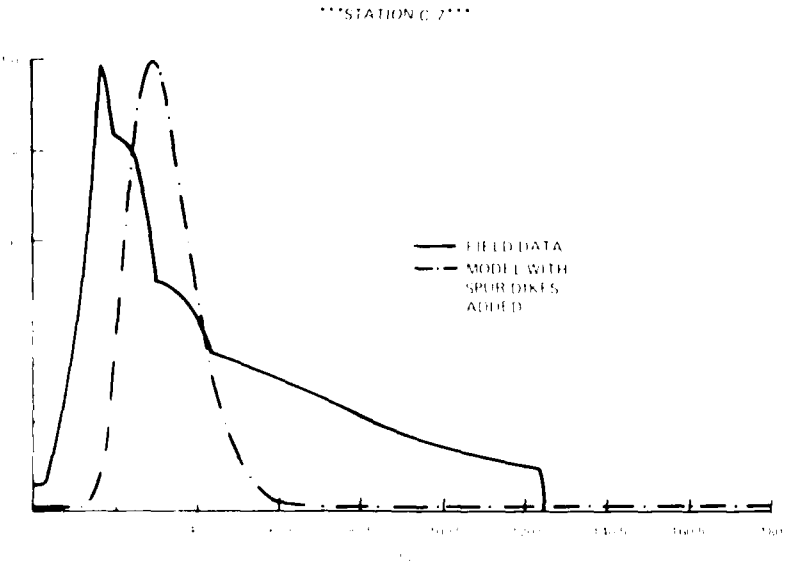

Figure A7. Dye tracer curve, Test 7 with spur dikes

PART V: CONCLUSIONS

23. The tests conducted with the numerical models showed the potential usefulness of the TABS system for design of dredged material disposal areas. The following conclusions can be drawn from these tests:

a. The tests clearly showed the impact of various eddy viscosity and diffusion coefficients on the results. The results were sensitive to changes in both parameters.

b. An eddy viscosity coefficient of 0.5 lb/sec/ft^2 produced reasonable current patterns and realistic travel times for the tracer dye in the disposal areas tested.

c. There exists a definite lower limit for the eddy viscosity coefficients where results produced are unrealistic and unstable. The possibility exists that for a given disposal area and mesh, a value of 0.5 lb/sec/ft^2 may be too low.

d. Equations that will predict the transport model's diffusion coefficients have been derived. The diffusion coefficients depend upon DMCA surface area, discharge, and wind conditions.

e. Changes in site geometry by the addition of spur dikes influence the numerical model results in a reasonable manner.

f. Better field data with more accurate measurement of the tracer background concentration and the decay limb of the dye curve are needed.

g. Given more time, it is felt that the three-dimensional TABS models can be tuned to better reproduce the effects of wind.

APPENDIX B: PROCEDURES FOR MEASURING DMCA RESIDENCE TIMES

Fluorescent Dyes

General

1. The most common method to measure the residence time distribution of a body of water is by the use of a dye tracer, typically a fluorescent dye. Fluorescent materials used for tracing are unique in that they efficiently convert absorbed light into emitted light in a characteristic pair of spectra. With the proper light source and filters, a fluorometer can measure small amounts of fluorescent material in a sample. Thus, when a fluorescent dye is mixed with a given parcel of water, that parcel may be identified and traced through a water system. The mean residence time and the amount of mixing of the water parcel in the system can be quantified by measuring the dye concentration of the water leaving the system.

Physical-chemical considerations

2. For a given fluorescent dye, the interaction of the dye with surrounding environmental conditions should be considered. Use of a dye in fresh water normally is not affected by chemical changes; however, if the dye were to be used in waters having high chloride concentrations (salt water), the dye loss could be significant. Photochemical decay of dye concentration must also be considered when planning a dye-tracer study. Factors influencing photochemical decay are light intensity, cloud cover, water turbidity, and water column depth. Other physical-chemical impacts on dyes are related pH, temperature, and salinity. Under acidic conditions, adsorption occurs more freely, resulting in a loss of dye and a reduction in fluorescence. A general rule of thumb on temperature impacts is that fluorescence of a given concentration of dye decreases 5 percent for every 2° C increase in temperature. Tests have shown that dye decay occurs at a slower rate under saline conditions (7.02-m sodium chloride solution) (Smart and Laidlaw 1977).* Additional guidance for designing dye-tracer studies and details of physical-chemical effects on dyes are found in the following: Abood, Lawler, and Disco 1969; Pritchard and Carpenter 1960; Feuerstein and Selleck 1963; Watt 1965; Smart and Laidlaw 1977; Yotsukura and Kilpatrick 1973; Deaner 1973; and Wilson 1968.

---

* See References at the end of the main text.

Dye types

3. Fluorescent dyes have been used since the early 1900s. Several have been developed and used with varying degrees of success in the tracing of surface and ground waters. Smart and Laidlaw (1977) evaluated eight dyes: Fluorescein, Rhodamine B, Rhodamine WT, Sulpho Rhodamine B, Lissamine FF, Pyramine, Amino G Acid, and Photine CU. Rhodamine B is stable in sunlight; however, it is readily adsorbed to sediments in water. Rhodamine WT was developed specifically for water tracing and is recommended for such use by Johnson 1984, Montgomery 1978, and Wilson 1968. Although Rhodamine WT is generally thought to have a very low toxicity level, ingestion should be restricted to 0.75 mg/day, and concentrations should be limited to less than 10 ppb near water intakes (Johnson 1984). Because of its color, sustained effluent concentrations above 50 ppm should be avoided.

Measurement Techniques

Theory of operation

4. Unlike sophisticated and complex analytical laboratory spectrofluorometers, filter fluorometers are relatively simple instruments. Basically, filter fluorometers are composed of six parts: light (excitation energy) source, primary or "excitation" filter, sample compartment, secondary or "emittance" filter, photomultiplier, and readout device.

a. When a fluorescent material is placed in a fluorometer, the spectral portion of the light source that coincides with the known excitation spectrum of the test material is allowed to pass through the primary filter to the sample chamber. This energy is absorbed by the fluorescent material, causing electrons to be excited to higher energy levels. In returning to its ground state, the fluorescent material emits light that is always at a longer wavelength and lower frequency than the light that was absorbed. It is this property that is the basis of fluorometry, the existence of a unique pair of excitation and emission spectra for different fluorescent materials. Finally, only a certain band of the emitted light is passed through the secondary filter to the photomultiplier, where a readout device indicates the relative intensity of the light reaching it. Thus, with different light sources and filter combinations, the fluorometer can discriminate between different fluorescent materials.

b. The selection of light sources and filters is crucial since they determine the sensitivity and selectivity of the analysis.

Fluorometer manufacturers recommend and supply lamps and filters for most applications, including Rhodamine WT applications.

c. Two types of fluorometers are in common field use today. The standard instrument used in water tracing by many groups, including the US Geological Survey (Wilson 1968), has been the Turner Model III manufactured by G. K. Turner Associates. Turner Designs has capitalized on recent advances in electronics and optics and developed a fluorometer, the Model 10 series, that is better adapted to field use than the Turner Model III.

Field use

5. Once a fluorometer is calibrated, it must be decided where and how field samples will be analyzed--in situ or in a laboratory, continuously or discretely. During in situ analysis, the operation of the fluorometer in flow-through mode (where water from a given discharge point in the containment area is pumped continuously through the sample chamber in the fluorometer) is advantageous over its operation in cuvette mode (where a discrete sample is analyzed). Specifically, in situ flow-through analysis (a) allows the homogeneity and variation of fluorescence in the discharge to be easily observed and (b) eliminates the need for handling individual samples. Also during in situ flow-through analysis, a strip chart recorder can be attached to the fluorometer, simplifying data collection by providing a continuous record of the fluorescence measured. During laboratory analysis, however, the flow-through system is seldom used since discrete samples are homogeneous and usually lack the volume needed to fill the system. Instead, the fluorometer is operated in cuvette mode where only a small portion of a sample is required for analysis. See Johnson (1984) for a detailed description of differences between models and operation features.

6. Each method of analysis also has its inherent problems. Laboratory analysis requires that discrete samples be collected, bottled, labeled, stored in the field, and then transported to the laboratory; this introduces many opportunities for samples to be lost through mislabeling, misplacement, or breakage. Also, the frequency of sampling may be insufficient to clearly define the changes in dye concentration as a function of time.

7. In situ analysis, on the other hand, is usually performed under adverse environmental conditions--often a a fast pace, in a cramped, makeshift work space, or in less than ideal weather conditions. Thus, it is more likely that an error will occur during in situ analysis than during analysis in the controlled environment of a laboratory. It is also usually

necessary to compute and apply many more temperature correction factors to fluorescence values during in situ analysis than during a laboratory analysis, since the samples to be analyzed in situ have not had a chance to reach a common temperature. This also increases the chances for error during analysis. In addition, in situ analysis is usually final. That is, if questions are raised about the validity of a measurement after the analysis, no sample is available for verification. In situ analysis may not be used when turbidity interference occurs, as may be the case for the effluent of many DMCAs.

8. To minimize the risk involved in relying on either method alone, a combination of the two may be employed--a preliminary in situ analysis to help guide the sampling effort and a final laboratory analysis to ensure accurate results for quantitative analysis.

9. Regardless of when and where fluorometric analysis takes place, general precautionary measures should be taken to ensure that the analysis is reliable.

a. The fluorometer should be accurately calibrated.

b. Sample contamination should be avoided by rinsing or flushing the sample chamber between readings.

c. The fluorometer operator should have experience with the instrument that is used. Experience can be gained through practice with samples of known fluorescence prior to the analysis.

d. Sample temperatures should be observed and recorded during analysis to determine the necessary fluorescence correction factors.

e. All information used to determine concentration units should be recorded (i.e., scale and meter or dial deflection).

f. The calibration should be checked on a regular basis (every hour or so). This is especially important if the fluorometer is powered by a battery; when the battery is drained, readings are no longer accurate.

10. For flow-through analysis in particular, all connections between the sampling hose, fluorometer, and pump must be tight to prevent air bubbles from entering the sample chamber. Air bubbles may also be introduced by a leaky pump seal; thus, it is recommended that the pump be connected to the system so that water is drawn up through the fluorometer to the pump. A screen placed at the intake end of the sampling hose will prevent sand and pebbles from altering the optics of the system since they may scratch the glass in the sample chamber as they travel through the system.

11. When analyzing samples in cuvette mode, the optics of the system may be distorted by scratches or smudges on the cuvette, making it necessary to wipe the cuvette clean prior to its insertion in the sample chamber. Once the cuvette is inside the warm sample chamber, a reading must be made quickly to prevent warming of the sample or condensation forming on the cuvette. Warming of the sample would cause a reduction in fluorescence, whereas condensation would distort the system optics.

Sampling

Sampling equipment

12. The basic equipment needed to perform a dye tracer study includes the following:

a. Fluorometers and accessories (filters, spare lamps, recorders, cuvettes, and sample holders). A spare fluorometer should be included if available since the entire field study centers around its operation.

b. Standard dye solutions for the calibrating fluorometers.

c. Generators or 12-volt deep-cycle marine batteries (with charger) to power fluorometers and pumps, if the dye concentration is to be monitored continuously.

d. Sampling equipment--pump and hoses, automatic sampler or discrete sampler (e.g., a Van Dorn sampler), bottles, labels, waterproof markers.

e. Temperature-measuring device for measuring sample temperatures if the temperature of the samples being analyzed will vary significantly.

f. Dye, dilution vessels, and injection equipment (e.g., bucket, pump, and hoses).

g. Description and dimensions of the containment area and surveying equipment to measure dimensions of containment area.

h. Equipment and records to determine the flow rate of the effluent from the containment area (e.g., production records, dredge discharge rate, weir length, depth of flow over the weir, and head above the weir).

i. Miscellaneous equipment (e.g., life jackets, tool kits).

j. Data forms.

Additional equipment might include cameras, radios, rain gear, rope, and lights. All equipment should be checked for proper performance prior to transporting to the field.

Preparatory tasks

13. Prior to conducting the dye-tracer study, the average discharge rate at all points of discharge from the containment area should be measured or estimated. If significant unaccountable leakage is suspected, the inflow rate must also be measured to determine the leakage rate. Equipment should be prepared, calibrated, and installed to measure or estimate the discharge rate during the dye-tracer study. If dredge production records are to be used to estimate the discharge, the discharge should be correlated to production. The average discharge rate $\bar{q}$ is equal to the sum of the average discharge rate at each discharge point including leakage.

14. A survey of the containment area should be performed to determine the area, depth, and volume of ponding V at the site for determination of the theoretical residence time T. The volume can be estimated from as-built or design drawings of the site, but the depth of fill and ponding should be verified in the field if an accurate estimate of the hydraulic efficiency is to be determined from the dye-tracer study. The ponded volume is needed to estimate dye requirements. An accurate determination of the volume is not needed if only the mean residence time is to be determined.

15. Using the average discharge rate and the ponded volume, the theoretical residence time of the site should be computed to plan the duration of the dye-tracer study and to determine the hydraulic efficiency.

$$T = V/\bar{q} \qquad \text{(B-1)}$$

16. The background fluorescence should be measured at the site. Background fluorescence is the sum of all contributions to fluorescence by materials other than the fluorescent dye. The best method to determine the background fluorescence is to measure the fluorescence of the discharge from the site several times prior to the addition of dye at the inlet. If the background fluorescence is expected to be variable, the fluorescence of supernatant from the influent should be measured before and during the dye-tracer study. The fluorescence of the water at the dredging site should not be used as the background fluorescence since some of the sediment that is mixed with the site water may remain suspended and exhibit fluorescence. Similarly, the sediment may release or adsorb fluorescence materials that would alter the fluorescence of the site water.

17. The effect of turbidity on the measurement of fluorescence should be examined to determine whether the discharge samples should be filtered prior to measuring their fluorescence. Turbidity will reduce the fluorescence by absorbing and scattering the light from the fluorometer lamp. Filtering is necessary only when samples are highly turbid or when the turbidity varies significantly. The effect of turbidity can be tested very simply. A sample of the discharge is divided in half, and a small amount of dye is added to one of the portions. The fluorometer is blanked or zeroed on the portion without dye in it, and the fluorescence of the portion containing dye is measured. Next, both samples are filtered or centrifuged to remove the turbidity. The process is then repeated using the filtrates or supernatants--blanking the fluorometer on the portion without dye in it and measuring the fluorescence of the portion containing dye. If the measured fluorescence of the sample without turbidity differed from the measured fluorescence of the sample with turbidity, then it is evident that turbidity affected the analysis. Alternatively, distilled water could be used as the blank when the turbidity or the background fluorescence is expected to vary significantly during the study.

Dye dosage requirements

18. Dye is usually released instantaneously as a slug to measure the mean residence time or hydraulic efficiency of a basin. The dye marks a small parcel of water that disperses as the parcel passes through the basin. Ideally, the dispersion in a settling basin is kept very low, and the parcel moves as a slug through the basin by plug flow. In practice, the net flow-through velocity is very low, sufficiently low that in the absence of external forces the parcel would move by plug flow with some longitudinal dispersion. However, containment areas are subject to wind forces that transform the basins into partially mixed basins where the velocities induced by wind are much greater than the net flow-through velocity. Consequently, the flow through the basin more closely represents completely mixed conditions than plug flow conditions. Therefore, the dye requirements are determined assuming that the dye is completely mixed in the basin rather than longitudinally dispersed.

19. A typical dye-tracer curve for a dredged material containment area, shown in Figure B1, shows a residence time distribution that is characteristic of a partially mixed basin. Dye appears quickly at the discharge point at time t_1, and then shortly thereafter the peak concentration is discharged at

time t_p . After the peak concentration reaches the discharge point, the dye concentration quickly decreases to about 30 to 60 percent of the peak concentration depending on the wind and the theoretical residence time of the basin. The dye concentration then gradually decreases until all of the dye is finally discharged at time t_f . The mean residence time and theoretical residence time are shown in Figure B1 as $\bar{t}$ and T , respectively. The residence time distribution indicates that some of the water short-circuits to the discharge point before the dye is completely mixed throughout the containment area. However, the dye becomes well mixed soon after the peak concentration is discharged, and then the dye concentration decreases gradually (instead of rapidly as before being completely mixed) to zero.

20. Before determining the dye dosage requirements for a study, a standard calibration curve should be developed for the dye and fluorometers to be

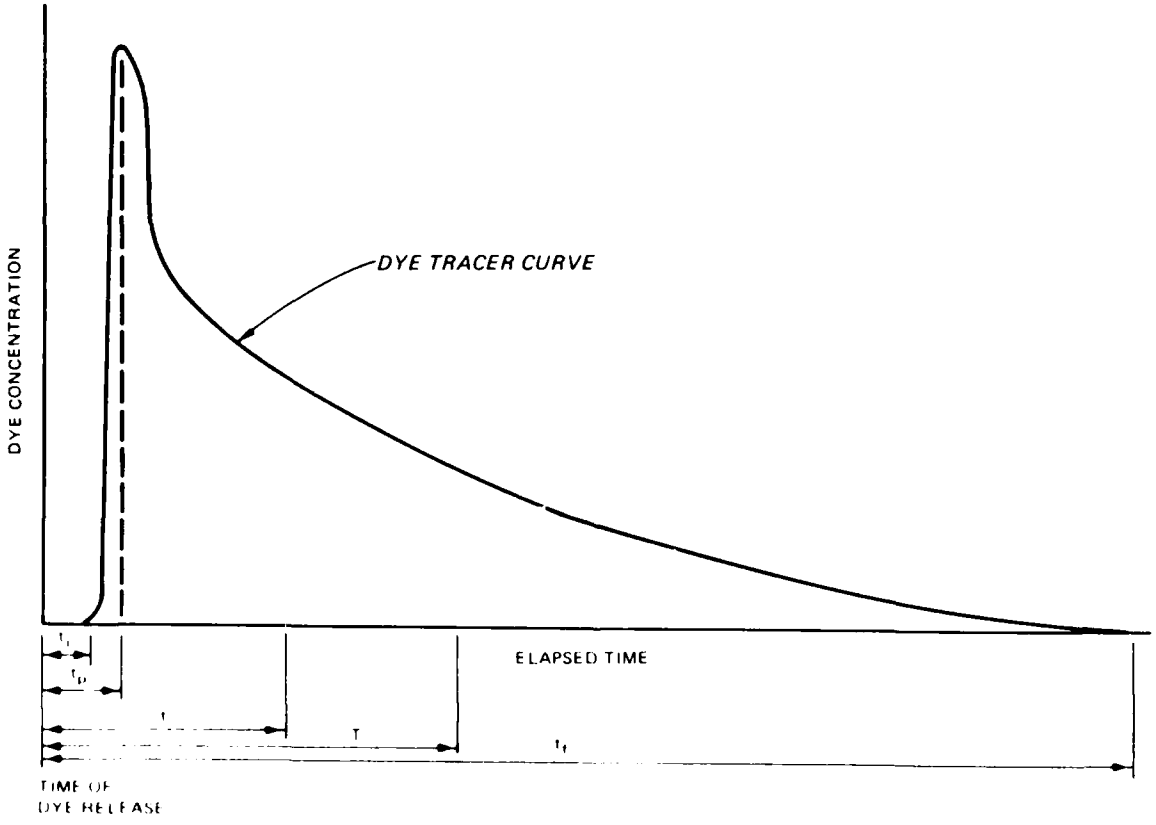

Figure B1. A typical plot of the residence time distribution for dredged material containment areas

used. This consists of plotting the fluorometer response for at least five known concentrations of dye. The design dye concentration is based on the requirement to produce accurately measurable concentrations of dye for the length of the study while not exceeding the maximum fluorometer response or excessively coloring the water.

21. The dye dosage requirements are based on achieving an initial concentration of 30 ppb in a completely mixed basin. This concentration of Rhodamine WT corresponds to 30 percent of the full scale deflection of many commonly used fluorometers. With this quantity of dye, the peak concentration will generally be less than 100 ppb (or 100 percent of the maximum fluorometer response) except for very small containment areas (<15 acres) or for areas with very bad channeling and short-circuiting. Since the peak concentration may exceed the capacity of the fluorometer, discrete samples should be taken during the period when the peak concentration is being discharged. These samples may be diluted to measure the peak concentration.

22. The dye dosage requirements are computed as follows:

$$\text{Dye Dosage, lb} = 0.00272\ (C_o, \text{ppb})\ (V_p, \text{acre-ft}) \qquad \text{(B-2a)}$$

$$= 6.24 \times 10^{-8}\ (C_o, \text{ppb})\ (V_p, \text{ft}^2) \qquad \text{(B-2b)}$$

$$= 2.21 \times 10^{-9}\ (C_o, \text{ppb})\ V_p, \ell) \qquad \text{(B-2c)}$$

where

C_o = desired dye concentration (generally 30 ppb for Rhodamine WT)

V_p = ponded volume

Dye Dosage = quantity in pounds of pure dye to be added to containment area

23. Fluorescent dyes are not generally produced at 100-percent strength. Rhodamine WT is typically distributed at 20-percent dye by weight. Consequently, the quantity of manufacturer stock dye would be five times as large as computed in Equation B-2.

$$\text{Stock Dye Dosage} = \frac{\text{Dye Dosage}}{\text{Stock Concentration}} \qquad \text{(B-3)}$$

where the stock concentration is the fractional dye content by weight. The volume of stock dye required can be computed as follows:

$$\text{Volume of Stock Dye} = \frac{\text{Stock Dye Dosage}}{\text{Specific Weight}} \qquad \text{(B-4)}$$

The specific gravity of liquid Rhodamine WT dye at a concentration of 20 percent by weight is about 1.19, corresponding to a specific weight of 1.19 kg/ℓ or 9.92 lb/gal.

Dye addition

24. The dye should added to the influent stream in liquid form in a quantity and manner that is easy to manage. If the dye comes in solid form, it should be dissolved prior to adding it. Solid dye is easier to transport, but it is often inconvenient to dissolve at field locations. The dye may be diluted to a volume that will ensure good mixing with the influent stream, but the quantity should not be so large that it takes more than about 5 or 10 minutes to add the dye. The dye may be pumped into the influent pipe or poured into the influent jet or pool. Greater dilutions should be used to ensure good mixing if the dye is to be poured into the influent. Care must be taken that the dye is distributed as it flows into the containment area in the same manner as the influent. Caution should be used to prevent concentrated dye from contaminating sampling and measuring equipment.

Sampling procedures

25. Sampling should be conducted at all points of discharge from the containment area. The dye concentration may be measured continuously at the discharge, or discrete samples may be collected throughout the test. Discrete samples must be taken when turbidity interference occurs since the samples must be filtered or centrifuged. Discrete samples should be taken when the dye is being measured continuously to provide a backup in the case of equipment malfunction and to verify the results of the continuous monitor.

26. The sampling frequency should be scheduled to observe any significant change in dye concentration (about 5 to 10 percent of the peak dye concentration). Sampling should be more frequent near the start of the test when dye starts to exit from the containment area and when the peak dye concentration passes the discharge points. About 40 carefully spaced samples should clearly define the residence time distribution or dye-tracer curve.

27. The sampling duration should be sufficiently long to permit the dye concentration to decrease to at least 10 percent of the peak concentration. For planning purposes, the duration should be two to three times the theoretical residence time.

28. The flow rate at all points of discharge from th containment area should be measured. If the flow rate varies significantly (more than 20 percent of average), it should be measured periodically throughout the test. Production records may be used to provide an indication of the variability of the flow rate. The rate for flow over weirs may be estimated by measuring the depth of flow over the weir and the length of the weir crest and then applying the weir formula for sharp-crested weirs:

$$Q = 3.3\ BH^{3/2} \qquad \text{(B-5)}$$

or

$$Q = 2.6\ Bh^{3/2} \qquad \text{(B-6)}$$

where:

Q = flow rate, cfs

B = weir crest length, ft

H = static head above weir crest, ft

h = depth of flow above weir crest, ft

Data analysis

29. Data reduction. The data should be tabulated in the following form:

Sample	Time from Dye Addition	Flow Rate	Dye Concentration Above Background	Time Interval
i	t_i	qi	C_i	Δt_i

Column 1 is the number of the sample i . If the dye concentration was monitored continuously, discrete points on the dye concentration curve may be used as samples. Column 2 is the time t_i that elapsed between the time that the dye was added to the influent and the sample was taken from the effluent. Column 3 is the flow rate q_i at the time that the sample was taken. The estimate of flow rate is needed only when this rate is not constant during the

test. Column 4 is the dye concentration of the sample discounted for the background fluorescence C_i ; that is:

$$C_i = C_{si} - C_{bi} \tag{B-7}$$

where

C_i = dye concentration discounted for background fluorescence of sample i

C_{si} = measured fluorescence of sample i

C_{bi} = background fluorescence at time t_i

If the background fluorescence does not vary, C_{bi} will be a constant and may be eliminated from the expression for calculating C_i if the fluorometer is blanked or zeroed with the site water. Column 5 is the interval of time Δt_i over which the sample is representative of the results. The value of this interval is one half of the interval between the times when the samples immediately preceding and following the sample of interest were taken.

$$\Delta t_i = \frac{t_{i+1} - t_{i-1}}{2} \tag{B-8}$$

where

Δt_i = time interval over which sample i is representative

t_{i+1} = time when the following sample was taken where t_{n+1} is time when the effluent fluorescence returns to the background level

t_{i-1} = time when the preceding sample was taken where $t_o = 0$

A data table is produced for each point of discharge.

30. Determination of mean residence time. After generating the data tables, the mean residence time is computed as follows:

$$\bar{t} = \frac{\sum_{i=0}^{n} t_i C_i q_i \Delta t_i}{\sum_{i=0}^{n} C_i q_i \Delta t_i} \tag{B-9}$$

where:

$\bar{t}$ = mean residence time

n = total number of samples (the sum of the samples from each sampling location)

If the flow rate is nearly constant throughout the test, the equation may be simplified to:

$$\bar{t} = \frac{\sum_{i=0}^{n} t_i C_i \Delta t_i}{\sum_{i=0}^{n} C_i \Delta t_i} \qquad \text{(B-10)}$$

If the sampling interval is constant (i.e., Δt_i = constant), but the flow rate is not constant, the equation may be simplified to:

$$\bar{t} = \frac{\sum_{i=0}^{n} t_i C_i q_i}{\sum_{i=0}^{n} C_i q_i} \qquad \text{(B-11)}$$

If both the sampling interval and flow rate are constant, the equation may be simplified to:

$$\bar{t} = \frac{\sum_{i=0}^{n} t_i C_i}{\sum_{i=0}^{n} C_i} \qquad \text{(B-12)}$$

31. An alternative method of computing $\bar{t}$ for constant flow with a variable sampling interval is presented in the main body of this report. The same method has been computerized in a program called DYECON, which is part of a family of programs named ADDAMS (Automated Dredging and Disposal Alternatives Management System) by Hayes et al. (1985).

32. Determination of hydraulic efficiency. The hydraulic efficiency is the ratio of the mean residence time to the theoretical residence time, where

$$\text{Hydraulic Efficiency} = \frac{\bar{t}}{T} \tag{B-13}$$

33. The correction factor for containment area volume requirements is equal to the inverse of the hydraulic efficiency. This correction is applied by multiplying the volume by the correction factor.

$$\text{Hydraulic Efficiency Correction Factor for Volume Requirements} = \frac{1}{\text{Hydraulic Efficiency}} \tag{B-14}$$

34. Other descriptions of residence time distribution. The despersion index, modal time, initial time, and Morrill index are other common descriptions of residence time distributions. The DYECON program can compute these values. The equation for computing the dispersion index (which may be the best indicator of residence time distribution) is presented in the main body of this report.

APPENDIX C: FIELD DATA

Field measurements for the twelve DMCA dye tracer tests described in Part III are shown in Tables C1 through C13. The tables are listings of data files that were input to the computer program DYECON to generate the statistics given in Table C7. These data files contain both measured values and predicted values for dye curve decay limbs (see Part IV). The three numbers at the top of each listing represent the number of data points, the background concentration, and the theoretical residence times in hours. Dummy theoretical residence times of 20 hr were used for Tests 9 and 11, since actual values were unknown. Dye concentrations are listed in the second column, and times are in the third column. Dye concentrations are in units of fluorescence, and times are in hours, except for Test 3, for which times are in minutes.

Table C1

DMCA Dye Tracer Test 1

31 1.00 51.80 THESIS YAZOO 1-A #5-1 TEST 1

1	0.	1.00
2	1.98	6.82
3	3.60	11.75
4	4.80	16.45
5	6.00	21.15
6	6.60	23.50
7	7.20	25.85
8	9.00	30.55
9	10.20	35.25
10	11.10	40.42
11	12.00	41.13
12	12.18	42.54
13	15.00	39.95
14	16.02	41.36
15	16.80	39.95
16	18.60	39.48
17	19.20	38.54
18	22.20	28.67
19	24.00	25.85
20	25.80	25.38
21	27.00	23.97
22	30.00	24.44
23	31.20	23.50
24	36.00	18.10
25	40.20	16.45
26	44.40	16.22
27	69.00	7.80
28	94.00	4.20
29	118.00	2.50
30	143.00	1.50
31	168.00	1.00

Table C2

DMCA Dye Tracer Test 2

52 12.00 138.64 FT EUSTIS TEST 2

1	0.	12.00
2	1.00	16.00
3	2.00	13.50
4	3.00	12.50
5	4.00	13.00
6	5.00	12.50
7	6.00	20.00
8	7.00	91.00
9	8.00	25.50
10	9.00	24.00
11	10.00	44.00
12	11.00	67.00
13	12.00	75.50
14	13.00	127.00
15	14.00	98.00
16	15.00	93.00
17	16.00	89.00
18	17.00	85.00
19	18.00	81.00
20	19.00	78.00
21	20.00	74.00
22	21.00	71.00
23	22.00	69.00
24	23.00	66.00
25	24.00	64.00
26	25.00	61.00
27	26.00	59.00
28	27.00	57.00
29	28.00	55.00
30	29.00	53.00
31	30.00	51.00
32	31.00	50.00
33	32.00	49.00
34	33.00	47.00
35	34.00	45.00
36	35.00	44.00
37	36.00	43.00
38	37.00	42.00
39	38.00	40.00
40	39.00	39.00
41	40.00	38.00
42	44.00	34.00
43	48.00	30.00
44	52.00	27.00
45	56.00	24.00
46	60.00	21.00
47	64.00	19.00

(Continued)

Table C2 (Concluded)

52	12.00	138.64	FT	EUSTIS TEST 2
	48	68.00		17.00
	49	72.00		14.00
	50	76.00		13.00
	51	80.00		12.00
	52	87.00		10.00

Table C3

DMCA Dye Tracer Test 3

42 0.10 3.52 BURNSVILLE TEST 3

1	0.	0.10
2	13.00	0.
3	14.00	1.35
4	16.00	1.20
5	20.00	1.24
6	24.00	2.06
7	28.00	2.88
8	32.00	2.68
9	36.00	3.72
10	40.00	5.72
11	44.00	5.46
12	48.00	9.56
13	52.00	21.50
14	54.00	12.50
15	56.00	5.80
16	60.00	3.90
17	64.00	4.06
18	68.00	4.06
19	74.00	4.26
20	80.00	3.10
21	86.00	2.20
22	92.00	1.60
23	98.00	1.70
24	104.00	1.50
25	110.00	1.35
26	118.00	1.62
27	126.00	1.80
28	134.00	1.90
29	142.00	1.90
30	150.00	1.80
31	158.00	1.76
32	166.00	1.58
33	174.00	1.26
34	186.00	1.20
35	198.00	1.38
36	210.00	1.16
37	222.00	1.08
38	264.00	0.47
39	307.00	0.31
40	349.00	0.21
41	391.00	0.14
42	434.00	0.10

Table C4

DMCA Dye Tracer Test 4

26 1.00 9.38 THESIS YAZOO 1-A #5-2 TEST 4

1	0.	1.00
2	1.05	2.59
3	1.92	9.87
4	2.04	18.57
5	2.28	18.57
6	2.40	24.44
7	2.76	22.33
8	3.00	83.43
9	3.54	53.35
10	3.78	64.16
11	4.26	59.93
12	4.74	54.05
13	4.80	26.32
14	5.34	40.42
15	5.46	33.14
16	5.76	45.83
17	6.00	17.63
18	7.86	28.67
19	10.08	10.11
20	12.00	6.35
21	13.80	4.70
22	15.00	2.93
23	16.00	2.22
24	17.00	1.69
25	18.00	1.29
26	19.00	1.00

Table C5

DMCA Dye Tracer Test 5

79 15.00 154.94 YAZOO I-B #5 TEST 5

1	0.	15.00
2	1.00	15.00
3	2.00	35.50
4	3.00	51.00
5	4.00	54.50
6	5.00	51.00
7	6.00	67.50
8	7.00	58.00
9	8.00	95.00
10	9.00	66.00
11	10.00	64.50
12	11.00	59.50
13	12.00	62.00
14	13.00	50.50
15	15.00	59.00
16	17.00	60.50
17	18.00	60.00
18	20.00	59.50
19	21.00	60.00
20	23.00	60.00
21	24.00	61.50
22	25.00	67.50
23	26.00	60.50
24	28.00	59.50
25	29.00	65.00
26	30.00	65.50
27	31.00	75.00
28	32.00	77.50
29	33.00	89.00
30	34.00	52.00
31	35.00	68.00
32	36.00	51.50
33	37.00	45.00
34	38.00	61.50
35	39.00	68.50
36	40.00	72.00
37	41.00	65.50
38	42.00	41.50
39	43.00	70.50
40	45.00	65.50
41	46.00	62.50
42	49.00	52.20
43	51.00	52.50
44	52.00	54.50
45	54.00	68.50

(Continued)

Table C5 (Concluded)

79 15.00 154.94 YAZOO 1-B #5 TEST 5

46	55.00	68.50
47	56.00	70.50
48	58.00	66.50
49	60.00	55.50
50	62.00	65.50
51	64.00	68.00
52	65.00	64.00
53	66.00	70.00
54	68.00	71.00
55	71.00	41.50
56	72.00	70.00
57	74.00	65.50
58	76.00	65.50
59	78.00	59.50
60	81.00	48.50
61	83.00	35.00
62	85.00	27.00
63	87.00	29.00
64	89.00	29.50
65	90.00	37.00
66	93.00	38.00
67	94.00	52.50
68	95.00	35.00
69	97.00	27.00
70	99.00	33.50
71	101.00	32.50
72	103.00	39.00
73	105.00	42.00
74	106.00	28.50
75	143.00	29.16
76	179.00	24.00
77	215.00	20.19
78	251.00	17.27
79	287.00	15.00

Table C6

DMCA Dye Tracer Test 6

77 1.50 225.26 MOBILE TEST 6

1	0.	1.50
2	2.00	1.50
3	4.00	2.00
4	6.50	2.00
5	8.00	20.00
6	10.00	11.00
7	12.00	46.00
8	16.00	34.00
9	18.00	34.00
10	20.00	29.50
11	22.00	20.50
12	24.00	21.00
13	26.00	25.50
14	28.00	23.50
15	30.00	25.50
16	32.00	23.50
17	34.00	25.00
18	36.00	24.00
19	38.00	28.50
20	40.00	21.00
21	42.00	31.00
22	44.00	28.00
23	46.00	40.50
24	48.00	21.00
25	50.00	21.00
26	52.00	19.00
27	54.00	26.50
28	56.00	19.00
29	58.00	20.00
30	60.00	24.50
31	62.00	27.50
32	64.00	31.50
33	66.00	37.00
34	68.00	29.00
35	70.00	29.00
36	72.00	26.00
37	74.00	21.50
38	76.00	37.50
39	78.00	19.50
40	80.00	19.50
41	82.00	15.50
42	86.00	15.50
43	90.00	20.50
44	94.00	27.00

(Continued)

Table C6 (Concluded)

77 1.50 225.26 MOBILE TEST 6

45	98.00	16.50
46	102.00	19.50
47	106.00	16.50
48	108.00	15.50
49	112.00	15.50
50	116.00	15.00
51	120.00	14.00
52	124.00	10.50
53	132.00	10.50
54	136.00	10.50
55	140.00	11.00
56	144.00	14.50
57	148.00	11.50
58	150.00	8.50
59	152.00	6.00
60	156.00	10.00
61	160.00	10.00
62	164.00	8.50
63	168.00	9.50
64	170.00	8.50
65	172.00	7.50
66	174.00	9.50
67	176.00	6.00
68	178.00	10.00
69	184.00	9.00
70	188.00	9.50
71	192.00	9.50
72	194.00	8.00
73	254.00	5.50
74	314.00	3.00
75	316.00	2.50
76	319.00	2.00
77	320.00	1.50

Table C7

DMCA Dye Tracer Test 7

28 1.00 41.41 YAZOO I-A #6 TEST 7

1	0.	1.00
2	2.00	1.00
3	4.00	2.00
4	6.00	3.50
5	8.00	5.00
6	10.00	7.00
7	12.00	9.20
8	14.00	12.00
9	16.00	16.00
10	17.00	18.50
11	18.00	17.70
12	20.00	15.60
13	22.00	15.20
14	24.00	15.00
15	26.00	14.00
16	28.00	12.00
17	30.00	9.50
18	32.00	9.30
19	34.00	9.20
20	36.00	9.00
21	38.00	8.50
22	40.00	8.00
23	42.00	7.30
24	44.00	6.50
25	67.00	5.04
26	89.00	3.23
27	112.00	2.10
28	124.20	1.72

Table C8

DMCA Dye Tracer Test 8

39 7.50 164.01 YAZOO 1-B #3 TEST 8

1	0.	7.50
2	1.00	7.50
3	2.00	7.00
4	3.00	6.50
5	4.00	6.50
6	4.50	7.00
7	8.50	6.50
8	13.50	15.00
9	17.50	21.00
10	19.50	34.00
11	21.50	20.00
12	23.50	29.50
13	25.50	45.00
14	27.50	57.50
15	28.50	53.00
16	32.50	45.00
17	38.50	32.00
18	41.50	32.50
19	44.00	32.00
20	45.50	32.00
21	46.50	31.50
22	49.00	33.00
23	51.50	31.00
24	56.50	36.00
25	61.50	35.00
26	66.50	29.50
27	68.50	21.50
28	70.50	28.00
29	71.00	26.50
30	73.50	25.50
31	95.50	19.70
32	121.00	19.70
33	145.10	26.60
34	169.00	24.30
35	193.60	19.90
36	216.80	14.00
37	238.50	13.40
38	400.00	13.50
39	492.00	10.30

Table C9

DMCA Dye Tracer Test 9

69	1.00	20.00 N	BLAKELY TEST 9
	1	0.	1.00
	2	1.50	0.
	3	3.75	44.00
	4	3.86	73.00
	5	4.00	30.00
	6	4.21	158.00
	7	4.38	209.00
	8	4.50	200.00
	9	4.66	180.00
	10	4.91	146.00
	11	5.00	95.00
	12	5.16	107.00
	13	5.33	120.00
	14	5.50	120.00
	15	5.80	120.00
	16	6.00	40.00
	17	6.16	30.00
	18	6.33	16.00
	19	6.50	18.00
	20	6.66	12.00
	21	7.00	10.00
	22	7.16	14.00
	23	7.33	14.00
	24	7.50	14.00
	25	7.66	14.00
	26	7.83	14.00
	27	8.00	13.00
	28	8.16	14.00
	29	8.33	15.00
	30	8.50	19.00
	31	8.66	28.00
	32	8.83	25.00
	33	9.00	29.00
	34	9.50	25.00
	35	10.00	2.00
	36	10.58	6.00
	37	11.50	13.00
	38	12.01	22.00
	39	12.58	11.00
	40	13.50	17.00
	41	14.50	11.00
	42	15.06	10.00
	43	15.55	10.00
	44	16.15	9.00

(Continued)

Table C9 (Concluded)

69	1.00	20.00	N BLAKELY TEST 9
45		16.60	9.00
46		17.18	8.00
47		17.68	8.00
48		18.25	6.00
49		18.76	12.00
50		20.25	15.00
51		20.50	14.00
52		20.76	18.00
53		21.00	21.00
54		21.50	23.00
55		22.00	15.00
56		22.50	25.00
57		23.00	27.00
58		23.50	21.00
59		24.00	15.00
60		25.00	1.00
61		26.00	0.
62		27.00	9.00
63		28.00	3.00
64		30.33	2.00
65		31.00	2.00
66		32.00	2.00
67		33.00	2.00
68		34.00	1.00
69		35.00	1.00

Table C11

DMCA Dye Tracer Test 11

74	0.04	20.00	CRANEY ISLAND TEST 11
1		0.	0.04
2		1.00	0.04
3		2.00	0.09
4		3.00	0.09
5		4.00	0.09
6		5.00	0.09
7		6.00	0.14
8		7.00	0.09
9		8.00	0.09
10		9.00	0.15
11		10.00	0.20
12		11.00	0.15
13		12.00	0.15
14		13.00	0.15
15		14.00	0.21
16		15.00	0.10
17		16.00	0.21
18		17.00	0.75
19		18.00	2.50
20		19.00	8.50
21		20.00	1.95
22		21.00	19.40
23		22.00	24.00
24		23.00	50.00
25		24.00	15.40
26		25.00	6.50
27		26.00	12.80
28		27.00	23.10
29		28.00	30.00
30		29.00	33.20
31		30.00	35.00
32		31.00	16.00
33		32.00	15.20
34		33.00	29.30
35		34.00	32.30
36		35.00	24.30
37		36.00	18.20
38		37.00	21.60
39		38.00	19.30
40		39.00	19.30
41		40.00	22.60
42		41.00	16.20
43		42.00	21.30
44		43.00	17.00

(Continued)

Table C11 (Concluded)

74	0.04	20.00	CRANEY ISLAND TEST 11
45		44.00	13.20
46		45.00	12.80
47		46.00	12.00
48		47.00	16.60
49		48.00	11.00
50		49.00	12.00
51		50.00	12.00
52		51.00	12.00
53		52.00	13.80
54		53.00	15.60
55		54.00	16.70
56		55.00	15.20
57		56.00	13.80
58		57.00	9.90
59		58.00	14.50
60		59.00	13.60
61		60.00	12.20
62		62.00	16.00
63		64.00	3.70
64		66.00	0.77
65		68.00	0.83
66		70.00	0.71
67		72.00	6.70
68		78.00	0.01
69		84.00	2.10
70		90.00	0.45
71		96.00	0.21
72		103.00	0.11
73		109.00	0.07
74		116.00	0.03

Table C12

DMCA Dye Tracer Test 12

75 0.05 20.00 BR1-R-F TEST 12

1	0.	0.05
2	0.03	0.05
3	0.17	0.05
4	0.33	53.50
5	0.42	11.50
6	0.50	20.00
7	0.53	1.50
8	0.58	1.10
9	0.67	0.20
10	0.75	1.15
11	0.83	16.50
12	1.00	2.25
13	1.17	13.00
14	1.33	7.00
15	1.50	17.00
16	1.67	15.00
17	1.83	2.20
18	2.00	4.20
19	2.17	11.10
20	2.33	5.00
21	2.50	8.30
22	2.67	8.10
23	2.83	8.30
24	3.00	8.00
25	3.17	7.50
26	3.67	7.00
27	4.17	7.50
28	4.67	4.60
29	5.17	5.80
30	5.67	7.00
31	6.17	4.60
32	6.67	4.40
33	7.17	2.10
34	7.67	4.60
35	8.17	4.60
36	8.67	1.00
37	9.17	3.20
38	9.67	2.80
39	10.17	0.50
40	10.67	2.75
41	11.17	2.05
42	11.67	2.75
43	12.17	2.05
44	12.67	2.00

(Continued)

Table C12 (Concluded)

75 0.05 20.00 BR1-R-F TEST 12

45	13.17	1.85
46	13.67	2.05
47	14.17	2.00
48	14.67	2.15
49	15.17	2.10
50	15.67	2.20
51	16.17	2.20
52	16.67	2.35
53	17.17	2.35
54	17.67	2.35
55	18.17	1.35
56	18.67	1.60
57	19.17	2.05
58	19.67	1.55
59	20.17	1.75
60	20.67	1.45
61	21.17	1.40
62	21.67	0.25
63	22.17	1.50
64	22.67	1.40
65	23.17	1.40
66	23.67	0.85
67	24.17	1.20
68	24.67	1.15
69	25.17	0.65
70	25.67	0.75
71	26.17	0.60
72	26.67	0.75
73	27.17	1.05
74	27.67	0.80
75	28.17	1.00

Table C13

DMCA Dye Tracer Test 13

19 4.00 13.52 FOWLRIV TEST 13

1	0.	4.00
2	1.00	4.00
3	2.00	4.00
4	3.00	4.00
5	4.00	6.00
6	4.50	57.00
7	5.00	80.00
8	5.50	42.00
9	6.00	45.00
10	6.50	67.00
11	7.00	55.00
12	7.50	37.00
13	8.00	35.00
14	8.50	40.00
15	9.00	34.00
16	10.00	19.74
17	11.00	12.19
18	12.00	7.25
19	13.00	4.20

END

DATE

FILMED

FEB.

1988